

Chemical Evolution of Monoterpenes in *Mentha*

Zur Erlangung des akademischen Grades einer

DOKTORIN DER NATURWISSENSCHAFTEN

(Dr. rer. nat.)

von der KIT-Fakultät für Chemie und Biowissenschaften

des Karlsruher Instituts für Technologie (KIT)

genehmigte

DISSERTATION

von

M.Sc. Nathalie Hering

1. Referent: Prof. Dr. Peter Nick

2. Referent: Prof. Dr. Tilman Lamparter

Tag der mündlichen Prüfung: 24. Oktober 2023

Die vorliegende Dissertation wurde am Joseph Gottlieb Kölreuter Institut für Pflanzenwissenschaften (JKIP) des Karlsruher Instituts für Technologie (KIT), Lehrstuhl I für molekulare Zellbiologie, im Zeitraum von Oktober 2019 bis September 2023 angefertigt.

I. Statement

I. Statement

Hiermit erkläre ich, Nathalie Hering, dass ich die vorliegende Dissertation, abgesehen von der Benutzung der angegebenen Hilfsmittel, selbstständig verfasst habe.

Alle Stellen, die gemäß Wortlaut oder Inhalt aus anderen Arbeiten entnommen sind, wurden durch Angabe der Quelle als Entlehnungen kenntlich gemacht.

Diese Dissertation liegt in gleicher oder ähnlicher Form keiner anderen Prüfungsbehörde vor.

Zudem erkläre ich, dass ich mich beim Anfertigen dieser Arbeit an die Regeln zur Sicherung guter wissenschaftlicher Praxis des KIT gehalten habe, einschließlich der Abgabe und Archivierung der Primärdaten, und dass die elektronische Version mit der schriftlichen übereinstimmt.

Tiefenbronn, den 13. September 2023

Nathalie Hering

II. Acknowledgements

It will be difficult to find words for my thanks, but it is worth a try.

First of all, I would like to express my deepest gratitude to Prof. Dr. Peter Nick. He paved my way into plant science since my bachelor studies. Through stimulating discussions, helpful advice, and teaching me to build a frustration tolerance, I never lost my passion for biology. Many, many thanks.

In addition, I would like to thank Prof. Dr. Tilman Lamparter for taking on the second correction as well as the committee.

I am also grateful for my dear colleagues, who have really sweetened my daily laboratory life. They were not only contemporaries for the one or other fun but helped me to learn new methods and stimulated the flow of thoughts by helpful discussions. I can sincerely say: colleagues became friends. I especially thank my inspiring roommates Wengjing, Noemie, Chris, Kai, Nasim, but also my other colleagues who have accompanied me on my journey. In particular I would like to mention Dr. Sascha Wetters, Dr. Vaidurya Pratap Sahi, Dr. Manish Raorane, Dr. Michael Riemann, Manuel, Madeleine, Seyma, Daniela, Gero, Nitin, Toranj, Eman, Tizian and Nina.

Sabine Purpur, Dr. Gabriele Jürges, Ernst Heene, Nadja Wunsch, Nora Weber, and Joachim Krüger were at my side for all administrative questions, technical support and the one or other daily chat. Thank you.

Thanks to the whole team of the JKIP Experimental Station of the KIT who took care of my mint plants day in and day out.

I would also like to thank the trainees, whom I could (hopefully) teach a lot during my study time, but who also taught me a lot. Thank you for your active support: Sophie, Mara, Moses, and Lena!

I sincerely thank the Graduate Funding from the German States Program ("Landesgraduierertenförderung") for financial support.

Now would be the time to thank my beloved family as well as my supportive friends, but for this, words are definitely not enough...

So, let's move on to the scientific part.

III. Abstract

Monoterpenes are important secondary compounds that give plants a kind of chemical language that is still poorly understood today. Plants are sessile organisms and therefore depend on these signals to survive in their environment. The immense secondary metabolism of plants enables them to synthesize a variety of signaling substances to deal with competitors and adapt to their environment. The background of the project is to apply a new strategy for biocontrol by mimicking this chemical language for the development of a sustainable and specific bioherbicide based on the natural effect of allelopathy. Bioherbicides are urgently needed from an ecological perspective because chemical herbicides often affect non-target organisms due to their low specificity, resulting in biodiversity reduction, environmental damage, and countless human diseases.

Monoterpenes belong to the secondary compound class of terpenes and occur within the *Mentha* genus, whose species are chemically diverse. Therefore, three closely related but chemically very distinct *Mentha* species were selected, namely watermint (*Mentha aquatica* L.), a variety of spearmint (*Mentha spicata* var. *crispa* Ridd.), and their hybrid peppermint (*Mentha x piperita* L.). These species will be used to investigate how and why such chemical diversity occurs within a genus in order to provide the basic knowledge required for the development of a bioherbicide.

In this study, it was shown that the hybrid *Mentha x piperita* has not inherited the compounds in an additive manner but has evolved a new, unique chemical profile, raising the question of how. To gain insight into the regulation of monoterpene synthases, comparative studies of gene expression, promoters, and phylogeny were conducted among the three *Mentha* species. In general, monoterpene synthases have been shown to be transcriptionally regulated with a temporal pattern that may differ among species, implying heterochrony. They are primarily active at an early leaf developmental stage, but competitive enzymes may also be expressed at different stages of leaf development within a species. The gene expression pattern of the monoterpene synthases correlates with the metabolite level. In addition, promoter analyses showed that monoterpene synthases are dependent on abiotic factors such as drought, light, and low temperatures, as well as on phytohormones such as methyl jasmonate, salicylic acid, abscisic acid, and gibberellic acid.

III. Abstract

Motifs may differ between species and between competing enzymes, allowing specific regulation of gene expression of the monoterpene synthases, which can contribute to the diverse chemistry of a species. Using the example of a key monoterpene synthase called menthofuran synthase (MFS), a close phylogenetic relationship, a similar amino acid sequence, and a nearly identical protein structure of the MFS of *Mentha aquatica* and *Mentha x piperita* could be elucidated. This explains why both mints contain the compound menthofuran in their essential oil, which is produced by MFS. However, it does not explain why the relative content of menthofuran differs by about 55 % in the essential oils of the two species. Further regulatory mechanisms must play a role here. The MFS of *Mentha spicata* var. *crispa* exhibited distant phylogeny as well as slightly altered protein structure, suggesting that the diversity of the many known monoterpene synthases results from gene diversification and lineage-specific independent evolution, which may be another mechanism for establishing chemical diversity.

In addition, the question of why such a chemical diversity is necessary for the plant was explored. It was shown that carvone, the main compound of *Mentha spicata* var. *crispa*, specifically inhibits the germination of weeds such as cress or poppy by degrading microtubules as well as bundling actin filaments, leading to cell death and consequently high cytotoxicity in BY-2 transgenic tobacco cells. This response is dose-dependent and specific, as the germination of poppy was more strongly inhibited by carvone than that of cress. Moreover, menthofuran, the main compound of *Mentha aquatica* and *Mentha x piperita*, did not elicit the same strong and persistent effect, indicating that the various monoterpenes have different target plants.

Taken together, important insights into the regulation and phylogeny of monoterpene synthases were provided. In addition, carvone was identified as a promising compound showing potential for the development of a sustainable, specific bioherbicide based on the natural effect of allelopathy.

Zusammenfassung

Monoterpene sind bedeutende Sekundärstoffe, die den Pflanzen eine Art chemische Sprache verleihen, die bis heute nur wenig verstanden wird. Pflanzen sind sessile Organismen und daher auf diese Signale angewiesen, um in ihrer Umwelt zu überleben. Der immense Sekundärstoffwechsel der Pflanzen ermöglicht es ihnen, eine Vielzahl von Signalstoffen zu synthetisieren, um sich mit Konkurrenten auseinanderzusetzen und sich an ihre Umwelt anzupassen. Hintergrund des Projekts ist die Anwendung einer neuen Strategie zur Biokontrolle durch Nachahmung dieser chemischen Sprache zur Entwicklung eines nachhaltigen und spezifischen Bioherbizids auf der Grundlage des natürlichen Effekts der Allelopathie. Bioherbizide werden aus ökologischer Sicht dringend benötigt, da chemische Herbizide durch ihre geringe Spezifität oft Nicht-Zielorganismen beeinträchtigen, was zur Verringerung der Artenvielfalt, Umweltschäden und zahllosen Krankheiten beim Menschen führt.

Monoterpene gehören zur Sekundärstoffklasse der Terpene und kommen innerhalb der Gattung *Mentha* vor, deren Arten chemisch vielfältig sind. Daher wurden drei eng verwandte, aber chemisch sehr unterschiedliche Minz-Arten ausgewählt, nämlich die Wasserminze (*Mentha aquatica* L.), eine Varietät der Grünen Minze (*Mentha spicata* var. *crispa* Ridd.) und deren Hybrid die Pfefferminze (*Mentha x piperita* L.). Anhand dieser Arten soll untersucht werden, wie und warum eine solche chemische Vielfalt innerhalb einer Gattung auftritt, um das erforderliche Grundlagenwissen für die Entwicklung eines Bioherbizids zu schaffen.

In dieser Studie wurde gezeigt, dass der Hybrid *Mentha x piperita* die Komponenten nicht additiv vererbt hat, sondern ein neues, einzigartiges chemisches Profil entwickelt hat, was die Frage nach dem Wie aufwirft. Um einen Einblick in die Regulierung der Monoterpen-Synthasen zu erhalten, wurden vergleichende Studien zur Genexpression, zu Promotoren und zur Phylogenie zwischen den drei *Mentha* Arten durchgeführt. Im Allgemeinen hat sich gezeigt, dass Monoterpen-Synthasen transkriptionell reguliert werden, und zwar mit einem zeitlichen Muster, das von Art zu Art unterschiedlich sein kann, was auf Heterochronie schließen lässt. Sie sind in erster Linie in einem frühen Stadium der Blattentwicklung aktiv, aber konkurrierende Enzyme können auch in verschiedenen Stadien der Blattentwicklung innerhalb einer Art exprimiert werden. Das Genexpressionsmuster der Monoterpen-Synthasen korreliert mit dem Metabolitengehalt.

Zusammenfassung

Darüber hinaus zeigten Promotoranalysen, dass Monoterpen-Synthasen von abiotischen Faktoren wie Trockenheit, Licht und niedrigen Temperaturen sowie von Phytohormonen wie Methyljasmonat, Salicylsäure, Abscisinsäure und Gibberellinsäure abhängig sind. Die Motive können sich zwischen den Arten und zwischen konkurrierenden Enzymen unterscheiden, was eine spezifische Regulierung der Genexpression von Monoterpen-Synthasen ermöglicht, die zur vielfältigen Chemie einer Art beitragen kann. Am Beispiel einer wichtigen Monoterpen-Synthase, der Menthofuran-Synthase (MFS), konnten eine enge phylogenetische Verwandtschaft, eine ähnliche Aminosäuresequenz und eine nahezu identische Proteinstruktur der MFS von *Mentha aquatica* und *Mentha x piperita* aufgeklärt werden. Dies erklärt, warum beide Minzen die Komponente Menthofuran in ihrem ätherischen Öl enthalten, das von MFS produziert wird. Es erklärt jedoch nicht, warum sich der relative Gehalt an Menthofuran in den ätherischen Ölen der beiden Arten um ca. 55 % unterscheidet. Hier müssen weitere Regulationsmechanismen eine Rolle spielen. Die MFS von *Mentha spicata* var. *crispa* wies eine entfernte Phylogenie sowie eine leicht veränderte Proteinstruktur auf, was darauf hindeutet, dass die Vielfalt der vielen bekannten Monoterpen-Synthasen auf eine Gendiversifizierung und abstammungsspezifische unabhängige Evolution zurückzuführen ist, was ein weiterer Mechanismus für die Entstehung der chemischen Vielfalt sein könnte.

Darüber hinaus wurde der Frage nachgegangen, warum eine solche chemische Vielfalt für die Pflanze notwendig ist. Es wurde gezeigt, dass Carvon, die Hauptkomponente von *Mentha spicata* var. *crispa*, spezifisch die Keimung von Unkräutern wie Kresse oder Mohn hemmt, indem es Mikrotubuli degradiert und Aktinfilamente bündelt, was zum Zelltod und damit auch zu hoher Zytotoxizität in transgenen BY-2 Tabakzellen führt. Diese Reaktion ist dosisabhängig und spezifisch, da die Keimung von Mohn durch Carvon stärker gehemmt wurde als die von Kresse. Zudem löste Menthofuran, der Hauptbestandteil von *Mentha aquatica* und *Mentha x piperita*, nicht dieselbe starke und anhaltende Wirkung aus, was darauf hindeutet, dass die verschiedenen Monoterpene unterschiedliche Zielpflanzen haben.

Insgesamt wurden wichtige Erkenntnisse über die Regulierung und die Phylogenie der Monoterpen-Synthasen gewonnen. Zudem wurde Carvon als vielversprechende Komponente identifiziert, die das Potenzial für die Entwicklung eines nachhaltigen, spezifischen Bioherbizids auf der Grundlage des natürlichen Effekts der Allelopathie besitzt.

Contents

I. Statement	II
II. Acknowledgements	III
III. Abstract	IV
Zusammenfassung	VI
Contents	VIII
Abbreviations	XI
1. Introduction	1
1.1 Secondary compounds: an overview	1
1.2 Glandular trichomes: the biofactories of secondary compounds	1
1.3 Monoterpene synthases: function, regulation, phylogeny	3
1.4 Allelopathy: are terpenes more than just systemic signals?	8
1.5 The chemically diverse genus <i>Mentha</i>	13
1.6 Scope of this study	15
2. Material	18
2.1 Reference plant material	18
2.2 List of primers	19
3. Methods	22
3.1 Species authentication and phylogenetic studies	22
3.1.1 Species authentication by floral traits	22
3.1.2 DNA extraction, PCR, and purification.....	22
3.1.3 TA-cloning	23
3.1.4 Sequencing and evaluation of the sequencing results	24
3.1.5 Relative substitution rates	25
3.1.6 3D protein structures of PR and MFS via AlphaFold and PyMOL	25
3.2 Chemical profile analysis of <i>Mentha</i> essential oils	26
3.2.1 Hydro distillation	26
3.2.2 Gas chromatography (GC)	26

Contents

3.2.3 Gas chromatography with mass spectrometry (GC-MS).....	26
3.3 Bioactivity studies.....	27
3.3.1 Germination assays.....	27
3.3.2 Cell cultures.....	27
3.3.3 Cell mortality assay with Evans Blue.....	28
3.3.4 Live cell imaging.....	29
3.4 Gene expression analysis and correlation to the metabolite level.....	29
3.4.1 Sampling.....	29
3.4.2 RNA extraction and RT-PCR.....	30
3.4.3 semi-qPCR and qPCR.....	30
3.4.4 Solid phase microextraction (SPME) with GC-MS.....	31
3.5 <i>In silico</i> promoter analysis via PLANTCare.....	32
3.6 Localization study of the MFS.....	32
3.6.1 Gateway cloning.....	32
3.6.2 Transformation of <i>Agrobacterium</i>	34
3.6.3 BY-2 cell transformation.....	35
3.6.4 Verifying the overexpression of MFS.....	36
3.6.5 Localization and colocalization study of MFS.....	36
4. Results.....	37
4.1 Phylogenetic studies.....	37
4.1.1 Authentication study and “maternal test” of <i>Mentha</i> species.....	37
4.1.2 Phylogeny of the monoterpene synthases PR and MFS within <i>Mentha</i>	42
4.1.3 Predicted protein structures of PR are quite similar in contrast to MFS....	48
4.2 Species-specific chemical profiles in a non-additive manner.....	52
4.3 Bioactivity studies.....	54
4.3.1 Dose-dependent germination inhibition of cress and poppy by carvone... 54	
4.3.2 Strong cytotoxicity in transgenic BY-2 lines caused by carvone.....	57
4.3.3 Microtubules and actin filaments as cellular target of carvone.....	59

Contents

4.4 Regulation of the monoterpene biosynthesis pathway.....	68
4.4.1 Predominant expression of key monoterpene synthases in young leaves and cases of heterochrony	68
4.4.2 Temporal expression pattern correlates with the metabolite level	71
4.4.3 Predicted promoter motifs suggest interaction with abiotic factors and various phytohormones.....	72
4.5 Localization of MFS of all three <i>Mentha</i> species in the ER.....	77
4.6 Summary of results	80
5. Discussion	82
5.1 Is the species being examined the one it claims to be?	82
5.2 How could such a chemical diversity arise within a single genus?	85
5.3 How is the monoterpene biosynthesis pathway regulated?	88
5.4 Do mints have potent bioactive compounds with herbicidal character?	95
6. Conclusion and Outlook.....	101
7. References	103
Appendix.....	113

Abbreviations

Abbreviations

ABA = abscisic acid

GA = gibberellic acid

ITS = internal transcribed spacer

L3H = limonene-3-hydroxylase

L6H = limonene-6-hydroxylase

MA = *Mentha aquatica*

MeJA = methyl jasmonate

MFS = menthofuran synthase

MP = *Mentha x piperita*

MSC = *Mentha spicata* var. *crispa*

PR = pulegone reductase

RMSD = root-mean-square deviation

SA = salicylic acid

TF = transcription factor

TPL = TOPLESS-like protein

1. Introduction

1.1 Secondary compounds: an overview

Plants are able to produce structurally diverse secondary compounds that derive biosynthetically from primary metabolism such as the glycolysis or shikimic acid pathway (Patra *et al.*, 2013). These small molecules can vary in their total abundance between different plants. There is no precise data about the number of secondary compounds occurring in a plant species, but a rough estimation varies from 5,000 to 25,000 compounds of 100,000 known chemical structures in the plant kingdom, which may be less than 10 % of the total amount (Trethewey 2004).

In plants, secondary compounds can be divided into three main classes: terpenoids, alkaloids, and phenylpropanoids / phenolic compounds. In addition to these three main classes, there are other minor groups. These include amines, cyanogens, glycosides, glucosinolates, acetylenes, and psoralens (Fang *et al.*, 2011). Secondary compounds were once considered redundant to plant growth and development but are now recognized as essential for sessile organisms such as plants as they are involved in adaptive and defensive responses. For example, several alkaloids have been found to protect the plant against biotic stress as well as UV radiation. UV protection is also achieved by some flavonoids, which could additionally attract pollinators for seed dispersal. Furthermore, terpenes have been shown to be precursors of important phytohormones that regulate growth and development. Other terpenes are involved in defense responses against herbivores, such as the monoterpenes limonene and menthol (Patra *et al.*, 2013). This brief overview should give a first impression of the importance of knowledge about secondary compounds and how important they are for plants. Furthermore, it should be mentioned that secondary compounds could exert disruptive effects on cells, which is why their biosynthesis and storage must take place in specialized structures.

1.2 Glandular trichomes: the biofactories of secondary compounds

In the late 20th century, Abraham Fahn (1988) claimed that lipophilic material is produced in the specialized secretory structures of vascular plants. Moreover, he proposed an evolutionary model for the development of glandular trichomes. Namely, these secretory structures are derived from idioblasts that have migrated from the mesophyll to the leaf surface (Fahn 1988).

1. Introduction

Developmental process of glandular trichomes

Cryofixation and conventional chemical fixation methods were used to follow the development of glandular trichomes of peppermint (*Mentha x piperita*). In a presecretory phase prior to the onset of gland filling, a protruding epidermal cell undergoes two periclinal cell divisions, giving rise to an initial apical cell, a stalk cell, and a basal cell. This is followed by three anticlinal cell divisions in the initial apical cell, resulting in an eight-cell apical disc, which is later the biofactory for the production of terpenes. In the secretory phase, leucoplasts and the smooth endoplasmic reticulum of the glandular disc cells become larger and are in close proximity to each other. In addition, the cuticle is detached, creating a subcuticular space for oil storage. In the post-secretory phase, this subcuticular space is completely filled with essential oil, resulting in high pressure and the appearance of glandular trichomes as ovoid “domes”. The entire developmental and oil-filling process of glands is quite rapid and takes about 60 hours (Turner *et al.*, 2000).

Secretion of the essential oil into the ovoid “dome”

The mechanisms of lipid secretion into the subcuticular space are not yet fully understood. Recently, a study showed that heterologous overexpression of a lipid transfer protein (NtLTP1) from tobacco in orange mint (*Mentha x piperita* f. *citrata*) resulted in elevated secretion and enhanced emission of monoterpenes, as well as an increased diameter of the glandular trichome heads. This suggests that these proteins facilitate the secretion of lipids into the subcuticular space (Hwang *et al.*, 2020). Furthermore, plasma membrane-localized transporters, such as ATP-binding cassette (ABC) and / or multidrug and toxic compound extrusion (MATE) transporters, could be required, but for volatile organic compounds (VOCs) no trichome transporter has been identified so far (Tissier *et al.*, 2017). However, in the flowers of *Petunia hybrida*, the ABC transporter PhABCG1 was found to allow VOCs such as methyl benzoate and benzyl alcohol to cross the plasma membrane. If this transporter is silenced by RNA interference, toxic levels of volatiles accumulate in the plasma membrane, leading to membrane damage (Adebesin *et al.*, 2017). This suggests, on the one hand, that ABC transporters may also be involved in the secretion of monoterpenes and, on the other hand, why toxic compounds like VOCs are immediately stored in specialized structures such as glandular trichomes after synthesis.

1. Introduction

1.3 Monoterpene synthases: function, regulation, phylogeny

Biosynthesis of monoterpenes

The glandular trichomes are small biofactories in which monoterpene biosynthesis takes place (Gershenzon *et al.*, 1989). Pyruvate and glyceraldehyde 3-phosphate synthesized in primary metabolism, the glycolysis, are metabolized in the plastidic methylerythritol phosphate (MEP) pathway to the C₅ precursors isopentenyl diphosphate (IPP) and dimethylallyl diphosphate (DMAPP) (McCaskill and Croteau, 1995; Eisenreich *et al.*, 1997; Turner and Croteau, 2004). IPP and DMAPP are then condensed in leucoplasts by a specific short-chain prenyltransferase, geranyl diphosphate synthase (GPPS), to synthesize the overall precursor of monoterpenes, geranyl diphosphate (Turner and Croteau, 2004).

Croteau *et al.* (2005) elucidated the enzymatic steps of menthol biosynthesis. The first committed step is the cyclization of the acyclic geranyl diphosphate to the parent olefin (–)-(4S)-limonene, which is catalyzed by the (–)-(4S)-limonene synthase. This is followed by a O₂- and NADPH-dependent hydroxylation of (–)-(4S)-limonene in the endoplasmic reticulum (ER) by the regioselective cytochrome P450 enzyme (–)-(4S)-limonene-3-hydroxylase (L3H). Here a change in stereochemistry at the C4 atom is induced producing (–)-(3S,4R)-trans-isopiperitenol. Subsequently, an allylic oxidation is conducted in the mitochondria to form (–)-isopiperitenone catalyzed by the NAD-dependent (–)-trans-isopiperitenol dehydrogenase (IPDH). All following steps of menthol biosynthesis are localized in the cytosol beginning with the stereospecific NADPH-dependent reduction of (–)-trans-isopiperitenone to (+)-cis-isopulegone by the soluble (–)-isopiperitenone reductase (IPR). This is followed by an isomerization of (+)-cis-isopulegone without the need of cofactors to produce (+)-pulegone catalyzed by (+)-cis-isopulegone isomerase (IPGI). Thereafter, (+)-pulegone is either NADPH-dependently reduced to (–)-menthone and (+)-isomenthone by the (+)-pulegone reductase (PR) in the cytosol or transported to the ER for the production of (+)-menthofuran mediated by the (+)-menthofuran synthase (MFS). The final step of menthol biosynthesis includes the reduction of (–)-menthone and (+)-isomenthone to (–)-menthol and its stereoisomers by two stereoselective and NADPH-dependent ketoreductases, namely (–)-menthone:(–)-(3R)-menthol reductase (MMR) and (–)-menthone:(+)-(3S)-neomenthol reductase (MNMR).

1. Introduction

In spearmint, the monoterpene biosynthesis branches off early, at the olefin (–)-(4S)-limonene. Instead of hydroxylating the C3 atom mediated by L3H in peppermint, a hydroxy group is added to the C6 atom by a very similar, regioselective cytochrome P450 enzyme called (–)-(4S)-limonene-6-hydroxylase (L6H). L6H produces (–)-trans-carveol, which is further metabolized to (–)-carvone by the NAD-dependent (–)-trans-carveol dehydrogenase (Turner and Croteau, 2004; Croteau *et al.*, 2005; Lange and Srividya, 2019). In **Figure 1** the monoterpene biosynthesis pathway and the subcellular localization of the different monoterpene synthases is illustrated according to Fuchs *et al.* (2022).

It is not known how monoterpenes enter and leave the different organelles. However, lipid transfer proteins are thought to be involved in intracellular trafficking between the leucoplast, mitochondria, ER, and cytosol, as it has already been suggested for the secretion of monoterpenes into the subcuticular space (see above) (Lange *et al.*, 2000).

1. Introduction

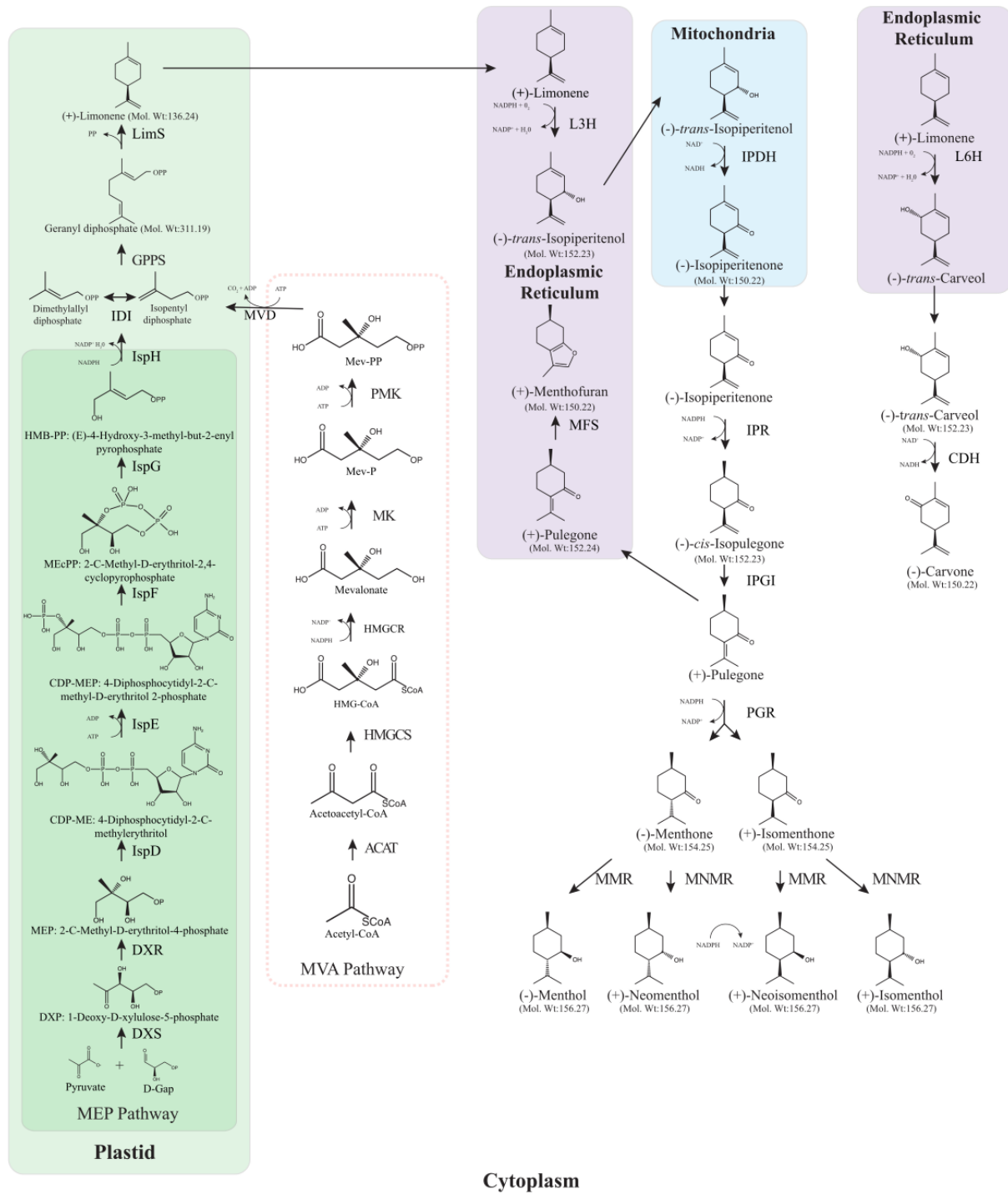


Figure 1: Monoterpene biosynthesis pathway and the subcellular localization of terpene synthases. Both the methylerythritol phosphate (MEP) and the mevalonate (MVA) pathway are demonstrated. However, only the MEP pathway provides precursors for monoterpenes in the glandular trichomes of *Mentha* species. Abbreviations adopted from Fuchs *et al.* (2022).

1. Introduction

Regulatory mechanisms of monoterpene biosynthesis

The regulation of the monoterpene biosynthesis pathway appears to be quite complex and is not fully understood. Monoterpene content increases between 12 and 20 days of leaf age, which correlates with the peak period of monoterpene biosynthesis. When the leaf reaches full expansion, biosynthesis decreases and the essential oil content remains stable for the rest of the leaf's life, as there is no evidence for monoterpene loss through catabolism or significant volatilization. This implies that the chemical composition of essential oils is based solely on altered rates of monoterpene biosynthesis (Gershenzon *et al.*, 2000).

A correlation was determined between the *in vitro* activities of monoterpene synthases in cell-free peppermint leaf extracts of different ages, paralleling transcript and protein levels, and *in vivo* monoterpene biosynthesis rates from leaves of different ages. This suggests that the pathway may be developmentally regulated at the transcript level. For most monoterpene synthases, except (–)-menthone reductase, which is active in a later developmental stage, the highest enzyme activity was shown at day 15 of leaf development. Nevertheless, the enzyme activity level, and therefore, the correlating transcript and protein levels can also vary between different monoterpene synthases. For example, (–)-trans-isopiperitenol dehydrogenase, (–)-isopiperitenone reductase, and (+)-cis-isopulegone isomerase, which produce intermediates, have higher enzyme activities and therefore higher transcript levels compared to those of final steps such as (+)-pulegone reductase and (–)-menthone reductase. This results in (–)-menthone as an early product and (–)-menthol as the later, very abundant product, and only trace amounts of the intermediates. It confirms the assumed regulation at the transcript level dependent on leaf development (McConkey *et al.*, 2000). A further study with transgenic peppermint plants overexpressing a homologous anti-sense version of the (+)-menthofuran synthase (MFS) cDNA verified that this synthase appears to be transcriptionally regulated. Transgenic downregulation resulted in a decrease in (+)-menthofuran content without loss of oil yield. Unexpectedly, the (+)-pulegone content did not increase but decreased, suggesting that other regulatory mechanisms are involved at the branch point of (+)-pulegone (Mahmoud and Croteau, 2001). Therefore, Mahmoud and Croteau extended their study in 2003, where they cosuppressed and overexpressed *mfs* in peppermint plants.

1. Introduction

Cosuppression of *mfs* caused a decrease in (+)-menthofuran production and an increase in *pr* transcript levels, resulting in increased catabolism of (+)-pulegone to (–)-menthone and further to (–)-menthol. In contrast, the overexpression of *mfs* led to an increase in (+)-menthofuran content and a decrease in *pr* transcript, resulting in the accumulation of (+)-pulegone. This indicates that the metabolite (+)-menthofuran is a negative regulator of *pr* gene expression, which was confirmed by stem-feeding experiments on wild-type peppermint plants (Mahmoud and Croteau, 2003).

Moreover, the involvement of two trichome-specific transcription factors has been elucidated. By metabolic engineering of wild-type spearmint plants, subsequent essential oil analysis, and further ectopic expression, it was found that MsYABBY5 from spearmint could be a possible negative regulator of monoterpene biosynthesis. It can bind to the MsWRKY75 promoter and influences its expression, suggesting that MsWRKY75 is a downstream signaling target (Wang *et al.*, 2016). In addition, another trichome-specific transcription factor from the R2R3-MYB subgroup 7, namely MsMYB from spearmint, was found. With MsMYB-overexpressing and MsMYB-RNAi lines, it could be demonstrated, that MsMYB is also a negative regulator of monoterpene biosynthesis like MsYABBY5. Here, the large subunit of geranyl diphosphate synthase (GPPS.LSU), the enzyme that produces the precursor of monoterpenes, is a downstream target of MsMYB. It binds to the promoter of *gpps.lsu* and represses its gene expression (Reddy *et al.*, 2017). Nevertheless, further intensive research is needed to identify additional transcription factors involved in monoterpene biosynthesis and their downstream targets to obtain a comprehensive view of the regulation of this secondary metabolism.

In addition to transcriptional regulation and the involvement of transcription factors, pre-transcriptional gene silencing could be another mechanism for the regulation of monoterpene biosynthesis. De novo DNA methylation via RNA-directed DNA methylation is a major epigenetic mechanism in plants (Zhang *et al.*, 2018). It has been shown that spearmint had a significantly higher total cytosine methylation rate of 41 % in the (–)-trans-isopiperitenone reductase (*ipr*) gene isolated from glandular trichomes compared to those of watermint and peppermint (11 % and 16 %, respectively). The high DNA methylation rate in spearmint was accompanied by a loss of the *ipr* transcript and the resulting compound, in contrast to the other two *Mentha* species, where the opposite was true (Ahkami *et al.*, 2015). Thus, methylation patterns in coding regions could play a role in regulating monoterpene biosynthesis as well.

1. Introduction

Evolution as driver for chemical diversity?

Furthermore, the DNA methylation pattern is often altered in a non-additive manner in hybrids compared to their parents (Wu *et al.*, 2021). This leads to the assumption that it is a possible evolutionary mechanism for the great chemical diversity within the mint genus. Moreover, this chemical diversity could be established by the diversification of ancestral genes in different evolutionary directions, giving rise to new monoterpene synthases based on pre-existing genes. An example would be L3H of peppermint, which shares 70 % sequence identity with L6H of spearmint. A single amino acid change (F363I) in the p450 domain of the L6H resulted in a shift in regioselectivity from the C6- to the C3-atom (Schalk and Croteau, 2000). This indicates that these enzymes are closely related and could be traced back to a common precursor gene. The Mint Evolutionary Genomics Consortium also postulated that the chemical diversity of monoterpenes rather developed from gene family expansion than from promiscuous enzymes (Mint Evolutionary Genomics Consortium, 2018). Moreover, there is evidence that syntenic relationships among the core genes of a diterpene biosynthetic gene cluster are present all over the Lamiaceae family. It is claimed that this cluster evolved in an early ancestor of the Lamiaceae family and has undergone some lineage-specific independent evolution to create such chemical diversity (Bryson *et al.*, 2023). This is probably also true for a monoterpene biosynthetic gene cluster in the mints. But why there is such chemical diversity within a single genus has not yet been clarified. However, it could be related to distinct functions of the various monoterpenes.

1.4 Allelopathy: are terpenes more than just systemic signals?

The term “allelopathy” is derived from the Greek language. The first root “allelon” means ‘to each other’ and the second root “pathos” means ‘to suffer’. Hans Molisch (1937) coined the term allelopathy for chemical interactions between plants mediated by small organic molecules, so called allelochemicals. By producing such allelochemicals, plants can either inhibit or stimulate processes in other organisms.

The donor plant can release self-produced allelochemicals through various routes, such as root exudates, plant residues, leaching by rain, or volatiles (Zhang *et al.*, 2021). The different routes are shown in **Figure 2**.

1. Introduction

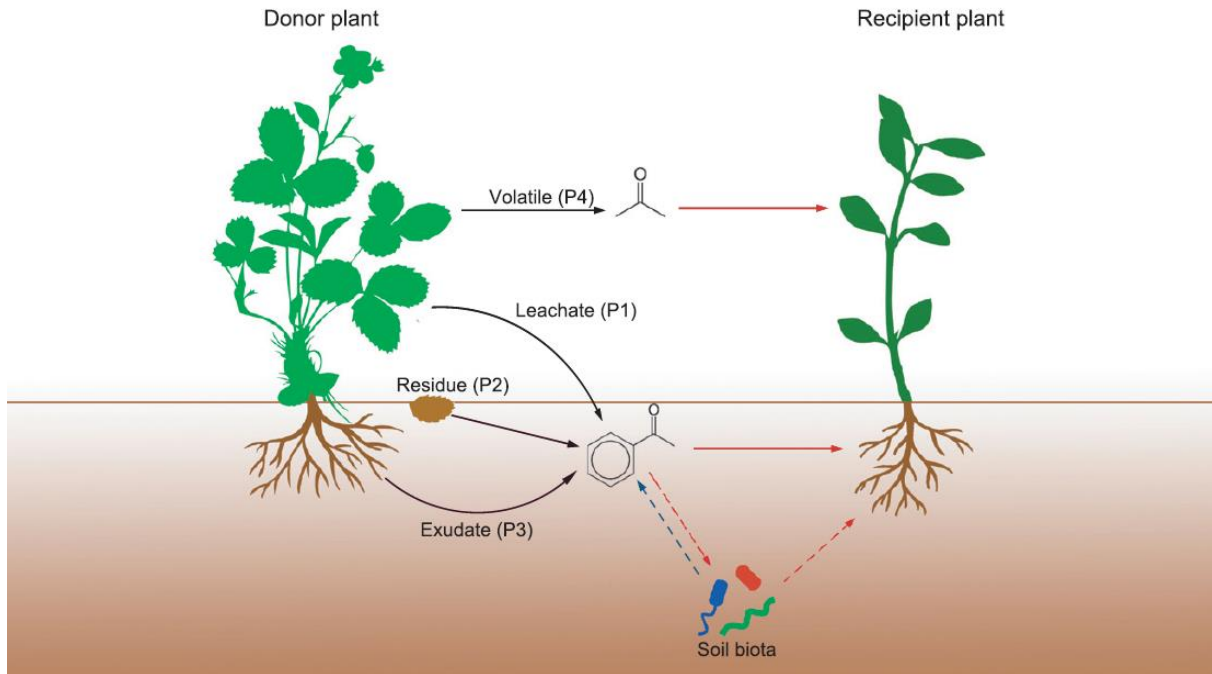


Figure 2: Diverse ways how allelochemicals can be released and mediated by the donor plant to affect the recipient plant. This can occur through leaching by rain (P1), decomposition of plant residues (P2), exudation from roots (P3), and volatilization (P4). The released allelochemicals (black arrows) can exert their effect either directly (red arrows) or indirectly via soil microbes (dashed red arrows) on the recipient plant. Moreover, the allelochemicals can also be degraded by soil microbes (dashed blue arrow) (Zhang *et al.*, 2021).

The natural production of allelochemicals is closely related to environmental factors such as abiotic stress, e.g., temperature extremes, drought, or oxidative stress, but also to biotic stress as a defense strategy against microorganisms and herbivores. These several types of stress can lead to increased levels of allelochemicals in the donor plant (Wink 1988; Einhellig 1995). Sharkey and Singaas (1995) used a photosystem II chlorophyll fluorescence assay to show that leaves fumigated with isoprene, the building block of terpenes, cope better with heat stress, resulting in less damage to the photosystem than unfumigated leaves. Additionally, isoprene can mitigate damage caused by reactive oxygen species (ROS). However, the mechanism by which isoprene is able to do so, remains unclear. It is hypothesized that isoprene stabilizes membranes, which protects against heat damage and leads to a reduction in ROS (Sharkey *et al.*, 2008). Furthermore, high emissions of (S)-limonene have been detected in response to oxidative stress caused by hydrogen peroxide, UV-B, and γ -irradiation in rice seedlings. This suggests that (S)-limonene could be an antioxidant that facilitates the management of oxidative stress (Lee *et al.*, 2015). This proves that terpenes act as systemic signals within the individual plant itself.

1. Introduction

Terpenes as the chemical language of plants?

However, terpenes are also able to perform a second function, they are chemical messengers. Because of their chemical nature as highly volatile, small lipophilic molecules, they can convey messages over a certain distance, which allows the establishment of a system (Gershenzon and Dudareva, 2007).

One must distinguish between terpenes as cues and terpenes as signals. Cues are not emitted for a specific purpose. They can be released permanently and provide information about the genetic identity of the emitter. Parasitic plants, for instance, can find their hosts using these cues. Beyond this, plants can also emit terpenes for specific communication as an adaptive defense strategy due to changes in their environment (Ninkovic *et al.*, 2021). An example of a naturally evolved defense system can be found in maize. In maize roots, β -caryophyllene is released as a belowground signal in response to insect infestation by the beetle *Diabrotica virgifera virgifera*, a well-known pest. The sesquiterpene then attracts nematodes that feed on the insect larvae. Thus, maize has developed its own biological pest control system (Rasmann *et al.*, 2005), but how the attraction is achieved is not yet clear.

What is the cellular target of terpenes?

The mode of action of most terpenes is barely understood. In addition, it has to be considered that if a mode of action is found for a particular compound, this does not necessarily mean that the essential oil from which it is derived will exert the same function. In essential oil blends, compounds may have synergistic or antagonistic effects. This could be advantageous because of the higher information content and thus higher specificity. Therefore, the combination of compounds could address different targets simultaneously, which could help to fight various competitors at the same time or outwit enemies that have already adapted to a certain compound (Gershenzon and Dudareva, 2007). Nevertheless, for some terpenes, the mode of action has already been elucidated. Sarheed *et al.* (2020) have shown that the monoterpene menthone strongly disrupts microtubules in a BY-2 tobacco cell line overexpressing α -tubulin fused to the green fluorescent protein (GFP). In contrast, a derivative of menthone, namely menthol, which has a hydroxyl group instead of a keto group, needed a tenfold concentration to reach such an effect (Sarheed *et al.*, 2020). Furthermore, Chaimovitsh *et al.* (2010) described the mode of action of the monoterpene citral.

1. Introduction

They demonstrated that citral leads to plant growth inhibition due to a time- and dose-dependent disruption of microtubules in *Arabidopsis* seedlings, whereas the citral derivative nerol did not (Chaimovitsh *et al.*, 2010). This study was continued in 2012, where they further investigated the effect of citral on young wheat seedlings and BY-2 cells. They showed that depending on the concentration of citral, it attacks either mitotic or cortical microtubules, leading to interference with cell division and cytokinesis or inhibition of cell elongation (Chaimovitsh *et al.*, 2012). Overall, microtubules appear to be a downstream target of several monoterpenes that act in a dose-dependent and specific manner, indicating that they are signals rather than toxins.

Chemical diversity that generates specific signals?

There is a wide variety of different volatiles that enable specificity (Gershenson and Dudareva, 2007). In biology, specificity is often associated with specific signaling. However, the molecular basis of how terpenes could be perceived is largely unknown in plants. Nevertheless, some evidence about monoterpene perception can be found in animals. There exists a receptor called TRPM8, which is a mammalian ion channel specifically expressed in temperature-sensing neurons, responding to cold stimuli and to the commonly known monoterpene menthol (Peier *et al.*, 2002). This suggests that terpene perception in plants might also be mediated by membrane receptors, although no homologous membrane receptor has yet been described. However, in 2019, an intracellular receptor was identified. It was revealed that volatile caryophyllene analogs can bind to TOPLESS-like proteins (TPLs) to induce expression of stress-related genes (Nagashima *et al.*, 2019).

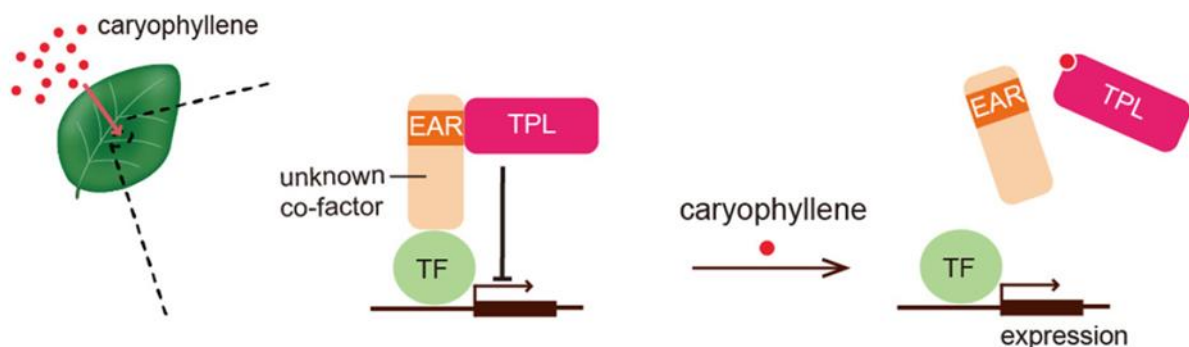


Figure 3: Hypothetical model for activating gene expression via caryophyllene by releasing TPL.

In the absence of caryophyllene, TPL acts as a transcriptional co-repressor linked via its EAR domain to an adapter protein, which in turn interacts with a transcription factor (TF). Once caryophyllene is present, it triggers the release of TPL and the adapter protein, allowing the TF to activate gene expression (Nagashima *et al.*, 2019).

1. Introduction

TPLs are transcriptional co-repressors and are known to be involved in other important stress- and growth-related signaling processes, such as jasmonate signaling. In the absence of jasmonoyl-isoleucine, the active form of jasmonate, TPL is associated with the adaptor protein NINJA. NINJA in turn physically interacts with the repressor JAZ, which binds the transcriptional activator protein MYC2 of jasmonate-induced genes (Pauwels *et al.*, 2010). In addition, TPLs were shown to bind effector proteins of the poplar leaf rust fungus, suggesting that TPLs function not only as transcriptional regulators but also as sensor molecules for external signals (Petre *et al.*, 2015). Thus, the use of specific adapter proteins could facilitate TPLs to perceive different signal molecules and regulate multiple signaling pathways with the same molecular mechanisms (Pauwels *et al.*, 2010). Overall, this is an indication that plants have evolved a different perception strategy compared to animals that use olfactory receptors (Nagashima *et al.*, 2019).

Moreover, other mechanisms of early responses in terpene perception were proposed by Maffei *et al.* (2001). They did research on changes in membrane potential in cucumber roots in response to peppermint essential oil and various monoterpenes. They showed that peppermint essential oil and, e.g., menthol can depolarize membranes, probably through disruption of membrane integrity, resulting in altered ion flux across the plasma membrane (Maffei *et al.*, 2001). A subsequent study in *Physcomitrella patens* elucidated which mechanisms are responsible for the menthol-evoked membrane depolarization, namely inhibition of proton pump activity, and opening of chloride ion channels, which leads to an efflux of Cl⁻ ions into the extracellular space (Koselski *et al.*, 2019). Therefore, membrane depolarization could activate voltage-gated ion channels that enable signal transduction pathways within the plant, or even open the gate for terpenes to enter the cell.

It is not clearly understood how the signals are transmitted through the cell to alter gene expression. However, in a study, caryophyllene and isoprene were shown to use different defense pathways to elicit plant resistance against a pathogen. In addition to jasmonate signaling associated with induced systemic resistance, another phytohormone, salicylic acid (SA), causes systemic acquired resistance. While caryophyllene depends on the abundance of proteins involved in jasmonate signaling, isoprene has been shown to induce resistance via the SA pathway (Frank *et al.*, 2021). All this suggests that chemical diversity has become established for specific communication between plants and other organisms, such as in the genus *Mentha*.

1. Introduction

1.5 The chemically diverse genus *Mentha*

The mints belong to the Lamiaceae family. This family is famous for its richness in species and its immense variety of secondary compounds. Such great chemical diversity can be found, for example, within the genus *Mentha*. The mints are aromatic perennial herbs that comprise about 30 species and are distributed mainly in the temperate regions of Eurasia, Australia, and South Africa. The mints are economically especially important because they contain aromatic and medical compounds in their essential oils, which have been used by people for a long time (Shaiq Ali *et al.*, 2002; Dorman *et al.*, 2003).

The significance is evident when considering the demand for the global mint essential oil market, which was estimated about USD 194.2 million in 2019. It is expected to grow at a compound annual growth rate (CAGR) of 9.2 % during the forecast period to 2025. The various application areas driving demand in the mint essential oil market are wellness and relaxation including aromatherapy, massage oils, and care products including cosmetics, toiletries, and fragrances; food and beverages with mint aroma and taste; medical products; and cleaning products (Grand View Research 2019).

The focus of this study was on three closely related but chemically very distinct *Mentha* species, namely watermint (*Mentha aquatica*), a variety of spearmint (*Mentha spicata* var. *crispa*) and their hybrid peppermint (*Mentha x piperita*).



Figure 4: Phenotypes of the three *Mentha* species growing in the greenhouse at the JKIP Experimental Station of the KIT. From left to right: watermint (8680 *M. aquatica*), variety of spearmint (5391 *M. spicata* var. *crispa*), and their hybrid peppermint (5393 *M. x piperita*).

1. Introduction

M. aquatica typically contains high concentrations of (+)-menthofuran of about 40 - 80 % in its essential oil. Other highly abundant compounds include 1,8-cineole at 8 - 18 % and β -caryophyllene at 6 - 12 %. In contrast, *M. spicata* essential oil has highly abundant carvone of about 60 - 70 %, followed by (-)-limonene with an abundance of about 13 - 20 %. The hybrid *M. x piperita* is chemically more closely related to *M. aquatica*, as it also contains (+)-menthofuran in its essential oil, but in a smaller amount of only 5 - 8 %. Here, (-)-menthol and (-)-menthone are the main compounds found for this species, with abundances of 37 - 47 % and 15 - 21 %, respectively (Lange Laboratory, 2014 - 2021). The concentration of compounds can vary within a species due to many environmental factors, resulting in different chemotypes (Fuchs *et al.*, 2022). Because of this variation, one should always elucidate the chemical profile of the species under study before making generalized statements.

Interactions with mammals, insects, microbes, and plants have been investigated for some of these various compounds or the essential oil blends from which they are derived. Peppermint oil and its main compound menthol exert some beneficial functions on mammals, e.g., it has been shown to prevent vomiting by interacting with a serotonin receptor subtype in rodents (Heimes *et al.*, 2011). Due to their low toxicity to warm-blooded animals and their chemical nature to be highly volatile, essential oils and their compounds have been used as fumigants against storage pests or as repellents for certain mosquitoes (Kumar *et al.*, 2011). Furthermore, antimicrobial and antioxidant activities have been reported (Mimica-Dukić *et al.*, 2003; Boni *et al.*, 2016). The effects on plants have also been extensively researched. It has been found that the germination of common weeds such as *Amaranthus retroflexus* or *Sinapis arvensis* is inhibited by the essential oil of *M. spicata*, while the ornamental plant *Alcea pallida* seems to be less affected, indicating specific responses of the recipient plant (Azirak and Karaman, 2008). In *Arabidopsis thaliana*, another common weed, exposure to peppermint oil results in larger and strongly opened stomata but without severe damage, whereas pure menthol induces the collapse of guard cell protoplasts, leading to desiccation. This confirms that essential oil blends might have a different mode of action compared to a single compound (Schulz *et al.*, 2007). It is therefore necessary to investigate the mode of action of individual compounds and essential oil blends so that they can be deployed selectively for different applications.

1. Introduction

Nevertheless, all this demonstrates that *Mentha*, which is a chemically diverse genus, could provide many different bioactive compounds that can be targeted against specific weeds, e.g., in cereal or crop fields, to inhibit weed growth without harming off-target organisms.

1.6 Scope of this study

Chemical herbicides toxify weeds and crops to varying degrees, so that the weaker one dies. However, due to the long exposure to these chemical herbicides, a strong selection pressure was generated, which led to resistances through evolutionary adaptation mechanisms, rendering the chemical herbicide useless (Gaines *et al.*, 2020). Nevertheless, there is still a large market for chemical herbicides. The global expenditure on herbicides at producer level was estimated at approximately USD 24.7 million of the world market in 2012 (Atwood and Paisley-Jones, 2017). However, these chemical pesticides cause a lot of problems due to their unfavorable ecotoxicology, as mostly non-target organisms are also affected. For example, the overall decline in insects was about 41 % in 2019, including Hymenoptera, where the decline was estimated to be about 46 %. Bumblebees, wild bees, and honeybees, which belong to this order, have been found to be declining in species richness and abundance, mainly due to intensive agriculture and chemical pesticides. From an ecological point of view, their extinction would be catastrophic, as they are valuable pollinators (Sánchez-Bayo and Wyckhuys, 2019). If they become extinct, we will have yield losses and thus a major problem in the food supply. Therefore, alternatives to chemical pesticides are urgently needed to preserve our biodiversity. Additionally, health problems such as neural and respiratory diseases have been reported for manufacturers or farmers exposed to chemical pesticides. Furthermore, chemical pesticides can cause residues in soil or groundwater that are taken up by food plants, aquatic organisms, or the consumers themselves, which can lead to health problems as well (Aktar *et al.*, 2009). Concisely, there is every reason to develop a sustainable bioherbicide that controls the unwanted weeds in the field without harming off-target organisms, thus preserving our precious biodiversity, and preventing human disease and further environmental pollution.

Here we aim to apply a new strategy from communication theory, based on signals that can convey different information depending on the context between sender and receiver. This is described in Karl Bühler's Organon model from 1934 (Bühler, 1965).

1. Introduction

Therefore, we want to use natural compounds to mimic biological signaling pathways and thus manipulate communication between organisms, allowing for higher specificity and thus a higher level of ecological safety than simply toxifying plants, as chemical herbicides do.

As described above, several *Mentha* species contain bioactive compounds that are very efficient in outcompeting other plants. Therefore, three closely related but chemically very distinct *Mentha* species were chosen as model organisms to have a deeper look at the chemical evolution of monoterpenes, namely *M. aquatica*, *M. spicata* var. *crispa*, and their hybrid *M. x piperita*.

Several research questions should be followed:

- **Is the species being examined the one it claims to be?**

An authentication study should be conducted using both a morphological approach with determination keys and a phylogenetic approach with various DNA barcoding markers to determine the phylogenetic relationships among the mints as well as the parental origin of hybrids.

- **How could such a chemical diversity arise within a single genus?**

The chemical profile of the individual *Mentha* species should be elucidated to verify the different chemistry. Phylogenetic studies should be performed to gain insight into the phylogenetic relationship of two competing monoterpene synthases and to make assumptions about whether each enzyme within the different *Mentha* species is derived from a common ancestral gene through gene diversification or whether the chemical diversity arises from promiscuity. Moreover, the protein structures of these enzymes and their localization should be examined for differences.

- **How is the monoterpene biosynthesis pathway regulated?**

Key enzymes of the monoterpene biosynthesis pathway, which control the metabolic flux to different main compounds, should be investigated for their temporal expression pattern and their correlation to the metabolite level within the different *Mentha* species. In addition, promoter studies for two enzymes should be exemplarily performed to detect possible transcription factor binding sites or abiotic factors that might influence expression patterns.

1. Introduction

- **Do mints have potent bioactive compounds with herbicidal character?**

The main compounds should serve as a basis for screening possible bioactivity in terms of weed germination inhibition. The selection of highly bioactive compounds and the elucidation of their cellular mode of action will be the focus of this research part.

2. Material

2. Material

2.1 Reference plant material

The three *Mentha* species of main interest used in this study, *M. aquatica*, *M. spicata* var. *crispa*, and *M. x piperita*, were grown in separate pots in the greenhouse at the JKIP Experimental Station of the KIT. Plants of other *Mentha* species and close relatives used for the phylogenetic analysis were grown outside in separate pots at the JKIP Experimental Station of the KIT (**Table 1**).

Table 1: Accessions used in this investigation.

KIT ID	species	common name	origin
45	<i>Mentha canadensis</i> L.	Canada or Chinese mint	JKIP KIT
45.2	<i>Mentha canadensis</i> L.	Canada or Chinese mint	JKIP KIT
83	<i>Salvia officinalis</i> L.	real sage	JKIP KIT
3638	<i>Mentha suaveolens</i> Ehrh.	apple mint	Botanical Garden Vácrátót
5391	<i>Mentha spicata</i> var. <i>crispa</i> Ridd.	variety of spearmint	WEL-Project; JKIP KIT
5393	<i>Mentha x piperita</i> L.	peppermint	JKIP KIT
7576	<i>Agastache rugosa</i> Kuntze	Korean mint	JKIP KIT
7579	<i>Mentha spicata</i> L.	spearmint	JKIP KIT
7580	<i>Mentha suaveolens</i> Ehrh.	apple mint	Fa. Ruehlemanns, MEN22
7583	<i>Mentha</i> spec.	-	Fa. Ruehlemanns, MEN80
7602	<i>Mentha rotundifolia</i> cv. <i>variegata</i>	cultivar of round leaf mint	JKIP KIT
8680	<i>Mentha aquatica</i> L.	watermint	WEL-Project 3/451; JKIP KIT
8681	<i>Mentha arvensis</i> L.	corn mint	WEL-Project 3/437; JKIP KIT
8682	<i>Mentha longifolia</i> L.	horse mint	WEL-Project 3/72; JKIP KIT
8682.2	<i>Mentha longifolia</i> L.	horse mint	WEL-Project 3/72; JKIP KIT
9133	<i>Salvia pratensis</i> L.	meadow sage	Saatgut-Vielfalt, Walter Wolf
9603	<i>Nepeta nuda</i> L.	hairless cat mint	JKIP KIT
9617	<i>Mentha arvensis</i> L.	corn mint	JKIP KIT

2. Material

2.2 List of primers

Table 2–5 lists the primers used in this study.

Table 2: Primers used for DNA barcoding and phylogenetic analysis of the monoterpene synthases PR and MFS.

primer name	purpose	sequence 5' - 3'	annealing temp.	source
ITS A	barcoding	GGAAGGAGAAGTCGTAACAAGG	55 °C	Blattner 1999
ITS B		CTTTTCCTCCGCTTATTGATATG		
ycf1b fw		TCTCGACGAAAATCAGATTGTTGTGAAT	52 °C	Dong <i>et al.</i> , 2015
ycf1b rv		ATACATGTCAAAGTGATGGAAAA		
psbA		GTTATGCATGAACGTAATGCTC	56 °C	Sang <i>et al.</i> , 1997
trnH		CGCGCATGGTGGATTCACAATCC		
rbcLa fw		ATGTCACCACAAACAGAGACTAAAGC	55 °C	Kress <i>et al.</i> , 2009
rbcLa rv		GTA AAAATCAAGTCCACCACG		
Whole_MFS fw	phylogeny and sequence analysis	ATGGCCGCTCTTCTAGTATTTTTTC	54 °C	AF346833.1
Whole_MFS rv		TCAAGATTGACGTGGAGTAGC		
Whole_PR fw		ATGGTGATGAACAAGCAAATTGTA CTC	54 °C	AY300163.1
Whole_PR rv		TTACTCGCGAGAAACGGC		
M13 uni 21	colony PCR / sequencing	CGCCAGGGTTTTCCCAGTCACGAC	59 °C	Promega GmbH, Mannheim, Germany
M13 rv 29		CAGGAAACAGCTATGAC		

2. Material

Table 3: Primers used for gene expression analysis.

primer name	purpose	sequence 5' - 3'	annealing temp.	source
18 S fw	gene expression analysis	ATGATAACTCGACGGATCGC	56 °C	Nazari <i>et al.</i> , 2017
18 S rv		CTTGGATGTGGTAGCCGTTT		
actin fw		CCCTTTATGCCAGTGGTCGT	56 °C	KR082011
actin rv		GCGGTGGTGGTGAATGAGTA		
L3H fw		TCGGGTTGGCAAATGTTGAG	58 °C	AF124816.1
L3H rv		GGGTGTGGGAACGAGTAGAA		
L6H fw		GGTTCCTGGAGGAGCATAGGG	58 °C	KM051107.1
L6H rv		CCCTTGATGCCATTGGAAGTAATGG		
MFS fw		GATGACGTGGACAAGATGCC	58 °C	AF346833.1
MFS rv		GTCTCTCGATATGGCCCAGT		
PR fw		CTCCCAGTACAGCCTGAAGC	58 °C	AY300163.1
PR rv		ATTGCCAACGTTACGACCGA		

Table 4: Primers used for *in silico* promoter analysis.

primer name	purpose	sequence 5' - 3'	annealing temp.	source
MFS_upstream_fw	promoter analysis	GGCTATTTTGGTCGCTCTCGT	54 °C	PRJNA310613
MFS_upstream_rv		CACATGCCCTATTATGTCCTCCTAGC		
PR_upstream_fw		GCTACTTTGCCTATTGCTTGGGTG	54 °C	
PR_upstream_rv		CGTGGCTGAAGTTATGTTCTTCTAG		

2. Material

Table 5: Primers used for the establishment of transgenic BY-2 cell lines.

primer name	purpose	sequence 5' - 3'	annealing temp.	source
attb_MFS_CT_fw	attB primers for gateway cloning	GGGGACAAGTTTGTACAAAAA GCAGGCTATGGCCGCTCTTCT AGTA	58 °C	this thesis
attb_MFS_CT_rv		GGGGACCACTTTGTACAAGAA AGCTGGGTAAGATTGACGTGG AGTAGCAA		
attb_MFS_MS_C_CT_fw		GGGGACAAGTTTGTACAAAAA GCAGGCTATGGCCGCTCTTCT AGTATT	58 °C	this thesis
attb_MFS_MS_C_CT_rv		GGGGACCACTTTGTACAAGAA AGCTGGGTAAGATTGACGTGG AGTAGCGA		
C-PCR GW-V12_fw	colony PCR / sequencing	GCCGTCGTCTTGAAGAAGA	56 °C	this thesis
C-PCR GW-V12_rv		ACCTACAAATGCCATCATTGCG		
NtL25 fw	verifying overexpression of the established transgenic cell lines	GTTGCCAAGGCTGTCAAGTCA GG	58 °C	L18908.1
NtL25 rv		GCACTAATACGAGGGTACTTG GGG		
NtEF1α fw		TGAGATGCACCACGAAGCTCT TC	58 °C	AF120093. 1
NtEF1α rv		GCTGAAGCACCCATTGCTGGG		

3. Methods

3.1 Species authentication and phylogenetic studies

3.1.1 Species authentication by floral traits

The authentication of the *Mentha* plants growing at JKIP Experimental Station of the KIT was carried out using different morphology-based determination keys, namely "Die Flora Deutschlands und angrenzender Länder" (Parolly and Rohwer, 2019), the Flora of China (Brach and Song, 2006), and "Pflanzensoziologische Exkursionsflora - für Deutschland und angrenzende Gebiete" by Oberdorfer *et al.* (2001). In addition, the flowers of each *Mentha* species were collected, and pictures were taken using the Keyence VHX digital microscope (Keyence Deutschland GmbH, Neu-Isenburg, Germany).

3.1.2 DNA extraction, PCR, and purification

3.1.2.1 DNA extraction

The genomic DNA was extracted from up to 50 mg of fresh leaf material from plants of the JKIP Experimental Station of the KIT (**Table 1**) using the Invisorb® Spin Plant Mini Kit (Invitek Molecular GmbH, Berlin, Germany) according to the manufacturer's instructions. This kit is based on adsorption chromatography. The quality and quantity of isolated genomic DNA were evaluated using a NanoDrop® ND-1000 spectrophotometer (PeqLab Biotechnologie GmbH, Erlangen, Germany). The genomic DNA was diluted to a concentration of 50 ng / μ L to be used as a template in PCR or stored at -20 °C for further downstream experiments.

3.1.2.2 PCR and purification of the amplified fragment

A PCR makes it possible to amplify any gene or region of interest. For one approach, a 30 μ L reaction volume containing 20.4 μ L nuclease-free H₂O (Biozym, Hessisch Oldendorf, Germany), 1-fold Thermopol Buffer (New England Biolabs, Frankfurt, Germany), 1 mg / mL bovine serum albumin (Carl Roth GmbH + Co. KG, Karlsruhe, Germany) as enhancer, 200 μ M dNTPs (New England Biolabs, Frankfurt, Germany), 0.2 μ M of forward and reverse primers (**Table 2**), one unit of *Taq* DNA polymerase (New England Biolabs, Frankfurt, Germany), and 50 ng / μ L gDNA or 1:50 diluted cDNA template (synthesis is described in **Chapter 3.4.2**) was used.

3. Methods

With this approach, the entire monoterpene synthase gene with exons and introns, the open reading frame, and the barcoding region of interest were amplified. The program of the thermal cycler (FlexCycler, Analytik Jena AG, Jena, Germany) was set as follows: initial denaturation at 95 °C for 2 min; followed by 35 cycles at 94 °C for 30 s, 52 °C - 59 °C depending on the primers used (**Table 2**) for 30 s, and 68 °C for 1 min; final elongation at 68 °C for 5 min. PCR was then evaluated by agarose gel electrophoresis. Loading dye (50 % glycerol / H₂O (Carl Roth GmbH + Co. KG, Karlsruhe, Germany) and 0.05 % bromophenol blue (AppliChem GmbH, Darmstadt, Germany)) was added in a 1:5 ratio to the samples. Afterwards, the samples were loaded into a 1.5 % agarose (Carl Roth GmbH + Co. KG, Karlsruhe, Germany) gel prepared in 0.5 x TAE buffer (20 mM Tris (Carl Roth GmbH + Co. KG, Karlsruhe, Germany), 10 mM acetic acid (Carl Roth GmbH + Co. KG, Karlsruhe, Germany), and 1 mM EDTA (Carl Roth GmbH + Co. KG, Karlsruhe, Germany), pH 8.3). The gel ran at 100 V for 25 min in an electrophoresis chamber (Mupid® One, Advance, Mupid CO., Tokyo, Japan). The intercalating dye Midori green Xtra (Nippon Genetics Europe GmbH, Düren, Germany) was used to visualize the amplified fragments under blue light excitation. Fragment size was determined using a 100 bp or 1 kb size marker (New England Biolabs, Frankfurt, Germany). If more than one allelic variant was present, further cloning steps were required. Therefore, the amplified fragment was either directly purified using the MSB® Spin PCRapace (Invitex Molecular GmbH, Berlin, Germany) or, if double bands were present, purified from the gel using the Invisorb® Spin DNA Extraction Kit (Invitex Molecular GmbH, Berlin, Germany) according to the manufacturer's instructions. The purified PCR product was stored at -20 °C for further analysis.

3.1.3 TA-cloning

The amplified PCR product has adenine overhangs at its 3' ends resulting from amplification with *Taq* DNA polymerase (New England Biolabs, Frankfurt, Germany), which are required for correct insertion into the pGEM-T Easy Vector (Promega GmbH, Mannheim, Germany). Ligation was performed as described in the manufacturer's instructions using 2 µL of purified PCR product and overnight incubation at 4 °C. Transformation was performed with competent *E. coli* strain DH5α cells (Invitrogen, Carlsbad, CA, USA), mixing 10 µL of the ligation product with 50 µL of competent cells. The mixture was placed on ice for 30 min. Heat-shock was applied at 42 °C for 50 s. The cells were immediately transferred to ice for 2 min.

3. Methods

950 μ L of sterile LB medium (Lennox, Carl Roth GmbH + Co. KG, Karlsruhe, Germany) was added, and the cells were incubated at 37 °C for 2 h at 150 rpm. Subsequently, the cells were centrifuged at 3000 rpm for 2 min and 700 μ L of the LB medium was removed. The remaining 300 μ L of cells were resuspended, and 150 μ L cells were plated on LB agar plates (LB medium containing 15 g / L agar-agar (Carl Roth GmbH + Co. KG, Karlsruhe, Germany) including 100 μ g / mL ampicillin (Carl Roth GmbH + Co. KG, Karlsruhe, Germany) as antibiotic, 500 μ M IPTG (Carl Roth GmbH + Co. KG, Karlsruhe, Germany) as inducer of the lac-operon, and 80 μ g / mL X-Gal (Biomol GmbH, Hamburg, Germany) as substrate for the β -galactosidase). Incubation took place overnight at 37 °C. A blue-white screening was performed the next day. White colonies were most likely to carry the desired insert. To exclude false-positive results, colony PCR was conducted as described in **Chapter 3.1.2.2**, except that a 10 μ L approach was done with 6.3 μ L nuclease-free H₂O (Biozym, Hessisch Oldendorf, Germany), universal M13 primers (**Table 2**), and 1 μ L of culture filtrate as a template. For this purpose, colonies were collected and incubated in liquid LB medium containing 100 μ g / mL ampicillin (Carl Roth GmbH + Co. KG, Karlsruhe, Germany) at 37 °C for 2 h at 150 rpm. Colonies that showed the expected fragment size in colony PCR were further incubated overnight at 37 °C at 150 rpm. The next day, plasmids carrying the desired insert were isolated from bacteria using the peqGOLD Plasmid Miniprep Kit I (VWR, Leuven, Belgium) according to the manufacturer's instructions. The quality and quantity of isolated plasmid DNA were determined using a NanoDrop® ND-1000 spectrophotometer (PeqLab Biotechnologie GmbH, Erlangen, Germany). Plasmids were sent for sequencing or stored at -20 °C for further downstream experiments.

3.1.4 Sequencing and evaluation of the sequencing results

Sanger sequencing was conducted by Eurofins Genomics (Ebersberg, Germany). Sequencing was performed with the universal primers M13 (**Table 2**) for the cloned fragments of the monoterpene synthase genes or with the respective primers for each barcoding region (**Table 2**), to obtain the sequences of the leading and complementary strands. The chromatogram was visualized, and the quality of the sequences was checked using FinchTV version 1.4 software (Geospiza, Inc.). MEGA7 (Kumar *et al.*, 2016) was applied to generate a consensus sequence of the forward and reverse sequences of each monoterpene synthase gene or barcoding marker of interest. An alignment was then calculated from the consensus sequences using the MUSCLE algorithm (Edgar 2004).

3. Methods

Sequences from the NCBI database (<https://www.ncbi.nlm.nih.gov/>) were included in some alignments. Phylogenetic analysis was performed using the corresponding alignment for the respective monoterpene synthase gene or barcoding marker of interest. The evolutionary history was inferred using the Neighbor-Joining method. Evolutionary distances were calculated using the Tamura-Nei method (Tamura and Nei, 1993). The bootstrap method with 1000 replicates was used to determine the significance of each branch in the tree. Trees were drawn in MEGA7 (Kumar et al., 2016).

3.1.5 Relative substitution rates

The substitution rates were determined to illustrate the resolution strength of the different barcoding markers and to show the differences in exon, intron, amino acid, and DNA sequences of the key monoterpene synthases. Always two sequences were compared. First, the differences were counted. A difference is identified as a single nucleotide polymorphism (SNP) or a complete insertion or deletion. Then, the percent substitution rate was calculated as the relative value of the differences to the average fragment length in base pairs of the two compared sequences.

3.1.6 3D protein structures of PR and MFS via AlphaFold and PyMOL

The 3D protein structure of pulegone reductase (PR) and menthofuran synthase (MFS) of *M. x piperita* predicted by AlphaFold was received from the database hosted by the European Bioinformatics Institute (<http://alphafold.ebi.ac.uk>). For *M. aquatica* and *M. spicata* var. *crispa*, the cloned cDNA sequences of PR and MFS (see **Chapter 3.1.3**) were translated into amino acid sequences using MEGA7 (Kumar *et al.*, 2016). These sequences were then used to predict 3D protein structures via AlphaFold 1.3 (DeepMind, London, UK). The generated file was uploaded to PyMOL 2.5.4 (Schrödinger LLC, New York, USA) to visualize the predicted 3D protein structures. The per-residue confidence score (pLDDT) between 0 and 100 was calculated. An alignment of two individual protein structures was also demonstrated. The root-mean-square deviation (RMSD) value of each alignment was reported.

3. Methods

3.2 Chemical profile analysis of *Mentha* essential oils

3.2.1 Hydro distillation

To extract the essential oils of *M. aquatica*, *M. x piperita*, and *M. spicata* var. *crispa* 50 g of fresh leaf material was taken from a living plant. It was slightly crushed with liquid nitrogen to break up the oil cavities of the glandular hairs and scales. To obtain maximum surface area, the frozen powder was placed in a round-bottomed flask and filled to half its height with distilled water. The distillation apparatus was also filled with distilled water to enable reflux. A water-cooling system was turned on, and then hydro distillation took place. After heating the material to 100 °C for 1.5 h, the extracted oil was quantified with a glass burette, harvested in small glass vials, and stored at 4 °C for further analysis.

3.2.2 Gas chromatography (GC)

To get a rough overview of the qualitative differences in the composition of the essential oils of the three *Mentha* species, gas chromatography was conducted. The Agilent 7890B device (Agilent technologies, Waldbronn, Germany), equipped with a HP-5 capillary column (30 m × 0.32 mm I.D. × 0.25 µm film thickness) in combination with a flame ionization detector, was used. Injection was performed with a syringe and a volume of 1 µL of essential oil. The GC injector (split 12.5:1, pressure 9.2 psi) was set at 300 °C. The thermal program was executed as follows: 40 °C (1 min isotherm), followed by heating by 5 °C/min to 60 °C, held for 4 min, further heating by 3 °C/min to 170 °C, and a final heating ramp by 30 °C/min to 270 °C, held for 10 min. Helium (2 mL / min) was used as a carrier gas. Reference substances, namely (+)-menthofuran, (–)-carvone, (–)-limonene, (–)-menthol, and (–)-menthone (all from Sigma-Aldrich, Steinheim, Germany), were injected to estimate their retention time.

3.2.3 Gas chromatography with mass spectrometry (GC-MS)

To completely elucidate and quantify the individual essential oil compounds of the three *Mentha* species, a GC-MS was performed. An Agilent instrument with a HP-5 column (30 m × 0.25 mm I.D. × 0.25 µm film thickness) was utilized. The GC injector (splitless, pressure 16.7 psi) was set to 280 °C.

3. Methods

The thermal program was run under the following conditions: 40 °C (2 min isotherm), followed by a first heating ramp of 10 °C/min to 220 °C and a second heating ramp of 30 °C/min to 300 °C, using helium (1.6 mL / min) as carrier gas. Mass spectra were collected in electron impact (EI) mode at 70 eV, 33 - 450 m/z.

3.3 Bioactivity studies

3.3.1 Germination assays

In order to verify whether some compounds of the essential oils exert a specific bioactive potential, several germination assays were performed. First, a screening of the main compounds was conducted in a standard cress germination test according to the protocol proposed by the International Seed Testing Association (www.seedtest.org) to select possible candidates with high bioactivity. For this purpose, 50 cress seeds (*Lepidium sativum*) purchased from Rapunzel Naturkost GmbH (Legau, Germany) were sown equidistantly on a Whatman filter paper (85 mm in diameter) wetted with 2 mL of distilled water in a Petri dish (100 mm x 15 mm). A cover slip (18 mm x 18 mm) was placed in the center of the Petri dish with different volumes (0.1, 1, 10 µL corresponding to 1, 10, and 100 ppm) of the pure compounds or the respective solvent control *n*-hexane (Merck KGaA, Darmstadt, Germany) to allow the compounds to interfere with the seeds only in the gas phase, as it occurs in nature. Petri dishes were sealed with parafilm to prevent water loss as well as cross-reactions of the gas phase between Petri dishes, and they were incubated in darkness at 25 °C for 3 or 5 days. The same experimental setup was performed for the germination test with poppy seeds (5194 *Papaver rhoeas*, JKIP KIT, Germany), except that the seeds were incubated on a 12 h light / 12 h dark cycle at 20 °C for 2 or 6 days. The ratio of ungerminated seeds to the total number of seeds gives the inhibition rate.

3.3.2 Cell cultures

In this investigation, different cell lines of tobacco BY-2 (*Nicotiana tabacum* L. cv. Bright Yellow-2) (Nagata *et al.*, 1992) were used as suspension cultures: a non-transformed cell line (BY-2 WT) and two transgenic cell lines. One of the transgenic cell lines, namely TuA3, expresses tobacco tubulin α 3 with a N-terminal fusion of GFP under control of a constitutive 35S promoter of cauliflower mosaic virus (CaMV), which enables the visualization of microtubules *in vivo* (Kumagai *et al.*, 2001).

3. Methods

The other transgenic cell line, GF11, expresses the second actin-binding domain of fimbrin (AtFim1) fused to GFP, also under the control of the cauliflower mosaic virus (CaMV) 35S promoter, allowing actin filament tracking *in vivo* (Sano *et al.*, 2005). Cells were weakly subcultured by inoculating 1.5 mL of mother cell culture into 30 mL of freshly prepared and modified Murashige-Skoog medium (Maisch and Nick, 2007). Transgenic cell lines were complemented with the appropriate antibiotics to maintain selective stringency (TuA3: 50 µg / mL kanamycin (Carl Roth GmbH + Co. KG, Karlsruhe, Germany); GF11: 30 µg / mL hygromycin (Carl Roth GmbH + Co. KG, Karlsruhe, Germany)). Cells were cultivated at 26 °C in darkness under constant shaking at 150 rpm, as described previously (Maisch and Nick, 2007).

3.3.3 Cell mortality assay with Evans Blue

To test the allelopathic effect of the essential oils of *M. aquatica* and *M. spicata* var. *crispa* as well as their main compounds (–)-carvone (Sigma-Aldrich, Steinheim, Germany) and (+)-menthofuran (Sigma-Aldrich, Steinheim, Germany) on the different cell lines BY-2 WT, TuA3, and GF11, the Evans Blue Dye Exclusion Assay according to Gaff and Okong’o-Ogola (1971) was performed. This impermeable dye can only penetrate dead cells with membrane leakage and therefore stains dead cells blue, which can be evaluated. For an approach, 200 µL of a 3-day-old, mitotically highly active cell culture was transferred to a tube and incubated with 0.5 % (v/v) of the essential oil, the respective compound, or the solvent control *n*-hexane (Merck KGaA, Darmstadt, Germany) in the dark culture room for 30 min at 150 rpm. The suspension was put on a self-made cell filter tube and stained with 2.5 % Evans Blue (Sigma-Aldrich, Steinheim, Germany) for 5 min. Subsequently, the cells were washed three times in distilled water for 5 min each. Then, 20 µL of the suspension was transferred to a slide and observed under the Axio Imager.Z1 ApoTome (Carl Zeiss AG, Jena, Germany) equipped with a digital CCD camera (AxioCam 503 mono, Carl Zeiss AG, Jena, Germany) operated by the ZEN Blue software (Carl Zeiss AG, Jena, Germany). The relative number of dead cells is represented by the cell mortality percentage. Three independent replicates were performed with a population of 2500 individual cells per replicate. A one-tailed paired Student’s t-test was conducted to test significance, with significance values visualized by asterisks (*: p-value<0.05, **: p-value<0.01, ***: p-value<0.001).

3. Methods

3.3.4 Live cell imaging

Live cell imaging was performed to follow the cellular effect of the essential oils of *M. aquatica* and *M. spicata* var. *crispa* as well as their main compounds (–)-carvone (Sigma-Aldrich, Steinheim, Germany) and (+)-menthofuran (Sigma-Aldrich, Steinheim, Germany) on the microtubule-marker cell line TuA3 and the actin-marker cell line GF11 *in vivo*. For this purpose, the essential oils or compounds were applied and could only interfere with the cells through the gas phase, as described in Sarheed *et al.* (2020). Briefly, 200 µL of a 3-day-old, mitotically highly active cell culture was transferred to a sterile tube under the clean bench and diluted with Murashige-Skoog medium to an appropriate density that allowed observation of individual cells. 20 µL of suspension were put on a slide. In close proximity to but not touching the cells, 0.5 µL the essential oil, compound, or solvent control *n*-hexane (Merck KGaA, Darmstadt, Germany) was added to both sides before a 40 x 24 mm coverslip was placed on the slide. Cells were visualized with the Axio Observer.Z1 Spinning Disc microscope (Carl Zeiss AG, Jena, Germany) operated by the ZEN Blue software (Carl Zeiss AG, Jena, Germany). The device was equipped with a digital CCD camera (AxioCam MRm, Carl Zeiss AG, Jena, Germany) and a laser dual spinning disc device (CSU-X1, Yokogawa, Tokyo, Japan). Cells were observed with a 63x oil immersion objective under excitation with blue light (488 nm) from an argon-krypton-laser (Carl Zeiss AG, Jena, Germany) to detect the GFP signal. Individual cells with high fluorescence were randomly chosen and observed for 35 minutes. Geometric projections were processed from confocal z-stacks.

3.4 Gene expression analysis and correlation to the metabolite level

3.4.1 Sampling

To analyze the transcript level of key monoterpene synthases of *M. aquatica*, *M. x piperita*, and *M. spicata* var. *crispa*, namely limonene-3-hydroxylase (L3H), limonene-6-hydroxylase (L6H), pulegone reductase (PR), and menthofuran synthase (MFS), as well as the metabolite level in leaves of different ages, samples were collected as follows: A single leaf of the same position from three individual plants was put together. The plant material was immediately frozen in liquid nitrogen and stored at -80 °C to prevent RNA degradation. The sample number indicates the position of the leaf: 1st, 2nd, 3rd, 4th, 5th, and 6th leaf from apical to basal.

3. Methods

3.4.2 RNA extraction and RT-PCR

Plant material was grounded in liquid nitrogen using a mortar and pestle. RNA was extracted using the Spectrum™ Plant Total RNA Kit (Sigma-Aldrich, Steinheim, Germany) following the manufacturer's instructions for protocol A with some exceptions: the volume of the added lysis solution was doubled, precipitation of cell debris was done at 4 °C for 15 min, an additional washing step was included to maximize RNA purity, and a treatment with RNase free DNase I (QIAGEN GmbH, Hilden, Germany) was conducted to remove DNA. The quality and quantity of isolated RNA were evaluated using a NanoDrop® ND-1000 spectrophotometer (PeqLab Biotechnologie GmbH, Erlangen, Germany). Reverse transcription-PCR (RT-PCR) was performed to synthesize cDNA. Therefore, 1 µg of RNA was mixed with 1 µL of 10 mM dNTPs (New England Biolabs, Frankfurt, Germany) and 0.4 µL of 100 µM Oligo d(T)18 mRNA primers (New England Biolabs, Frankfurt, Germany). This reaction was incubated in a Primus 96 advanced® thermal cycler (PEQLAB, Erlangen, Germany) at 65 °C for 5 min and immediately placed on ice before adding 4 µL of the second master mix, which consists of 2 µL of 10x reverse transcriptase buffer (New England Biolabs, Frankfurt, Germany), 1.25 µL nuclease-free H₂O (Biozym, Hessisch Oldendorf, Germany), 0.5 µL RNase inhibitor (New England Biolabs, Frankfurt, Germany), and 0.25 µL of the reverse transcriptase MuLV (New England Biolabs, Frankfurt, Germany). This reaction was continued at 42 °C for 60 min to synthesize the cDNA, followed by inactivation of the enzyme at 90 °C for 10 min and a final storage step at 12 °C. The cDNA was then diluted 1:50 for semi-qPCR and 1:10 for qPCR and stored at -20 °C for downstream experiments.

3.4.3 semi-qPCR and qPCR

For qualitative analysis of gene expression, semi-qPCR was performed as described for PCR in **Chapter 3.1.2.2**, except that a 10 µL approach was conducted and the elongation step took place at 68 °C for only 30 s instead of 1 min, because the expected fragment size was smaller. Primers used in this investigation are listed in **Table 3**.

3. Methods

Subsequently, transcript levels were determined by quantitative real time PCR (qPCR) using a reaction volume of 20 μL containing 11.75 μL nuclease-free H_2O (Biozym, Hessisch Oldendorf, Germany), 1-fold GoTaq® Buffer (Promega GmbH, Mannheim, Germany), 200 μM dNTPs (New England Biolabs, Frankfurt, Germany), 0.2 μM of forward and reverse primers (**Table 3**), 2.5 mM MgCl_2 (USB Corporation, Cleveland Ohio, USA), 0.5-fold SYBR™ Green (Thermo Fisher Scientific Inc., Waltham, Massachusetts, USA), 0.5 units of GoTaq® polymerase (Promega GmbH, Mannheim, Germany), and 1 μL of 1:10 diluted cDNA. The reaction was performed with the CFX96 Touch™ Real-Time PCR Detection System (Bio-Rad Laboratories GmbH, Munich, Germany) under the following thermal conditions: initial denaturation at 95 °C for 3 min; following 39 cycles at 95 °C for 15 s, 58 °C for 40 s, and a plate reading step; followed by a denaturation step at 95 °C for 10 s; ensued by a melting curve step of 5 s with an increase rate of 0.5 °C and a plate reading step from 65 °C to 95 °C. The $2^{-\Delta\text{ct}}$ method, according to Livak and Schmittgen (2001), was used to analyze the real-time data obtained. The ct values (cycle threshold; number of cycles at which the defined threshold of fluorescence intensity is reached) of the individual samples as well as the melting curve were displayed in Bio-Rad CFX Manager™ 3.1 (Bio-Rad Laboratories GmbH, Munich, Germany). Only those samples were used for analysis whose ct values differed by a maximum of 0.5 within the technical replicates and which have a correct melting point temperature. The relative expression of each key monoterpene synthase to the two housekeeping genes 18 S and actin was calculated by taking the difference (Δct) of the ct values of the target gene to the geometric mean of the two housekeeping genes and then applying the formula $2^{-\Delta\text{ct}}$. The standard error is based on three biological replicates. For significance testing, ANOVA analysis was performed using IBM SPSS Statistics 28.0 (IBM, Armonk, USA).

3.4.4 Solid phase microextraction (SPME) with GC-MS

Prior to analysis, the frozen leaf samples 1 and 6 (sampling described in detail in **Chapter 3.4.1**) of *M. aquatica*, *M. x piperita*, and *M. spicata* var. *crispa* were crushed in liquid nitrogen using micropestles in microcentrifuge tubes. For qualitative analysis of monoterpenes in *Mentha* leaves of different ages, the homogenized freeze-dried sample was collected in a 1.5 mL solid phase microextraction (SPME) vial. A 100 μm polydimethylsiloxane SPME fiber (Sigma-Aldrich, Steinheim, Germany) was exposed to the headspace of the sample for 2 min at room temperature.

3. Methods

Samples were analyzed using a GC-MS Agilent 7890B / 5977B Inert Plus (Agilent Technologies, Waldbronn, Germany). The discharge of the SPME fiber was performed in splitless mode. Analytical separation was performed in a Supreme-5ms column (30 m × 0.25 mm I.D. × 0.25 µm film thickness) using helium as carrier gas at a flow rate of 1 mL / min. The oven temperature was held at 40 °C for 3 min, then increased to 200 °C at a rate of 7 °C/min, followed by a rate of 100 °C/min up to 300 °C, which was held for 3 min. The injector and interface temperatures were set at 220 °C and 250 °C, respectively, with an ionization potential of 70 eV and a scan range of 50 - 350 amu. Chromatographic peak identification was validated using the NIST 14 (National Institute of Standards and Technology) mass spectra library and the Adams mass spectra library for essential oil compounds.

3.5 *In silico* promoter analysis via PLANTCare

To obtain the promoter sequence of the monoterpene key synthases PR and MFS of *M. aquatica*, *M. x piperita*, and *M. spicata* var. *crispa*, the coding sequences were aligned to the reference genome of *M. longifolia* (NCBI accession: PRJNA310613). Sequences 1200 bp upstream of the transcription start were used as templates for the design of specific primers (**Table 4**). Regions were cloned using the TA cloning protocol (see **Chapter 3.1.3**). The sequences obtained were used to predict possible promoter motifs. For this purpose, the sequences were analyzed *in silico* with PLANTCare (Lescot *et al.*, 2002), a database of cis-acting regulatory elements in plants. All predicted promoter motifs that were abundant in the promoter considered were shown with their sequence motif and position to scale. For clarity, the many predicted binding sites for MYC- and MYB-transcription factors with unknown downstream functions and other light responsive elements were omitted.

3.6 Localization study of the MFS

3.6.1 Gateway cloning

To construct a fusion protein of each MFS of the three different *Mentha* species of interest and the green fluorescence protein (GFP), the respective coding sequence of each MFS was cloned into an expression vector carrying the coding sequence for GFP via Gateway® Technology using the Clonase™ II system (Invitrogen, Carlsbad, CA, USA) according to the manufacturer's instructions.

3. Methods

This system is based on site-specific recombination *in vitro* (Hartley *et al.*, 2000). Therefore, primers containing attB sites were designed (**Table 5**) and used to amplify the entire coding region of each MFS using the PCR protocol mentioned in **Chapter 3.1.2.2**. The purified attB PCR product was cloned into a donor vector (Gateway™ pDONR™ / Zeo Vector) in a BP recombination reaction. The vector was transformed into competent *E. coli* strain DH5α cells (Invitrogen, Carlsbad, CA, USA) using the heat-shock protocol mentioned in **Chapter 3.1.3**, except that only 1 μL of BP product was added to the bacterial cells and Zeocin (Alfa Aesar, Candel, Germany) was used as a selective antibiotic in LB agar plates. Colonies were screened by colony PCR and Sanger sequencing by Eurofins Genomics (Ebersberg, Germany) using the universal M13 primers to determine whether the gene of interest was present in the right orientation. If yes, plasmids were extracted (see **Chapter 3.1.3**). The BP plasmid was used in the LR reaction, in which the gene of interest was cloned into the destination vector pK7FWG2 (**Figure 5**), which contains a C-terminal coding sequence for GFP (Karimi *et al.*, 2002). The vector was then transformed into competent *E. coli* strain DH5α cells (Invitrogen, Carlsbad, CA, USA) using spectinomycin (Sigma-Aldrich, Steinheim, Germany) as a selective antibiotic in LB agar plates. Colonies were verified by colony PCR, and plasmids were extracted, followed by sequencing (see **Chapters 3.1.3 and 3.1.4**) using the self-designed C-PCR GW-V12 fw and rv primers (**Table 5**).

3. Methods

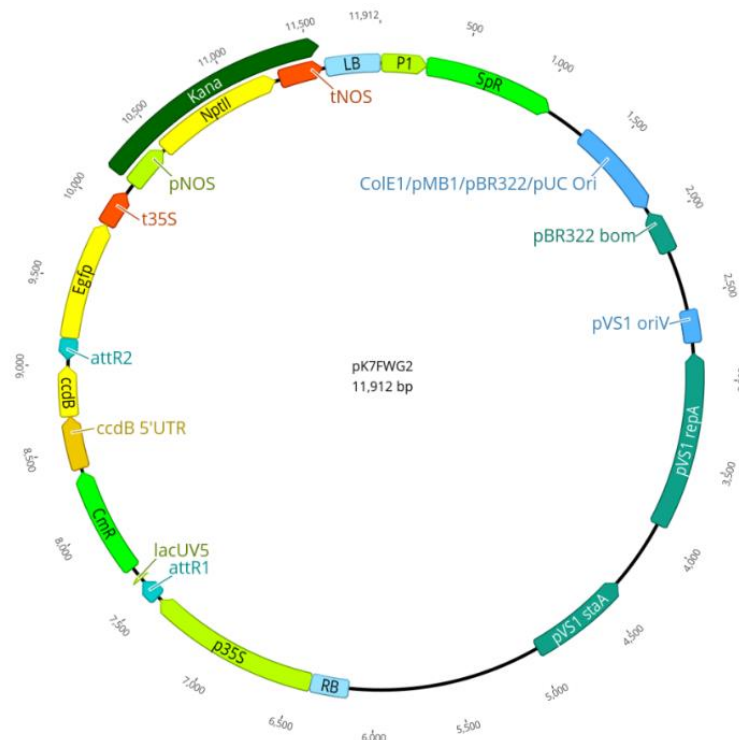


Figure 5: Schematic representation of the pK7FWG2 destination vector used for *Agrobacterium*-mediated transformation of plant cells. The vector carries the attR sites required for site-specific recombination, the cauliflower mosaic virus (CaMV) 35S promoter, the ccdB gene that is excised and into which the gene of interest is inserted, GFP for subcellular localization, and spectinomycin and kanamycin resistance for prokaryotic and eukaryotic cells (Karimi *et al.*, 2002).

3.6.2 Transformation of *Agrobacterium*

A freeze-thaw transformation protocol for *Agrobacterium tumefaciens* was established in the KIT JKIP-MZB laboratory. Briefly, 500 ng of the purified expression vector was gently mixed with 100 μ L of *Agrobacterium* cells and immediately frozen in liquid nitrogen for 5 min. The mixture was thawed in a heating block (TSC ThermoShaker, Biometra, Göttingen, Germany) at 37 °C for 10 min and liquid LB medium was added to a total volume of 1 mL. *Agrobacterium* cells were incubated at 28 °C for 3 h at 150 rpm. Afterwards, the cells were centrifuged at 3000 rpm for 2 min, and 900 μ L of LB medium was removed. The remaining 100 μ L of cells were carefully resuspended and plated on LB agar plates containing 100 μ g / mL rifampicin (Carl Roth GmbH + Co. KG, Karlsruhe, Germany), 300 μ g / mL streptomycin (Sigma-Aldrich, Steinheim, Germany), and 100 μ g / mL spectinomycin (Sigma-Aldrich, Steinheim, Germany). Incubation was at 28 °C. After three days, colonies were selected and grown in 5 mL of liquid LB medium containing rifampicin, streptomycin, and spectinomycin at the above concentrations for 2 h.

3. Methods

Each bacterial suspension culture was checked by colony PCR (see **Chapter 3.1.3**) using the self-designed C-PCR GW-V12 fw and rv primers (**Table 5**) to see if it contained the expression vector with the desired insert. If yes, incubation was extended overnight at 28 °C. The following day, the *Agrobacterium* cells were used for BY-2 plant cell transformation.

3.6.3 BY-2 cell transformation

A stable transformation protocol for *Nicotiana tabacum* L. cv. Bright Yellow-2 (Nagata *et al.*, 1992) cells with *A. tumefaciens* was established in the KIT JKIP-MZB laboratory. First, 1.5 mL of the overnight bacterial suspension culture (see **Chapter 3.6.2**) was transferred to 6 mL fresh liquid LB medium without antibiotics. *Agrobacterium* cells were grown at 28 °C for 4 - 6 h at 150 rpm until an OD₆₀₀ of 0.8 – 1 was achieved. The bacterial cells were centrifuged at 8000 g for 8 min. The supernatant was discarded, and the bacterial cells were gently resuspended in 180 µL of Paul's medium (4.3 g / L MS salts (Duchefa, Haarlem, The Netherlands) and 1 % sucrose (Carl Roth GmbH + Co. KG, Karlsruhe, Germany), pH 5.8). Subsequently, 60 mL of a 3-day-old, mitotically highly active wild-type BY-2 cell culture was washed with 700 mL Paul's medium on a Nalgene™ BottleTop filter made of polysulfone device (Thermo Fisher Scientific Inc., Waltham, Massachusetts, USA) under sterile conditions. Afterwards, 6 mL of BY-2 cells were added to the resuspended *Agrobacterium* cells and mixed with Paul's medium until a slightly viscous mixture was obtained. This mixture was rotated overhead for 15 min at 50 rpm and plated out as spots on Paul's agar plates with sterile Whatman filter paper (85 mm in diameter). The infection occurred at 22 °C for 4 days. After this time, the filter paper containing the transformed BY-2 cells was transferred to MS agar plates supplemented with 50 µg / mL kanamycin (Carl Roth GmbH + Co. KG, Karlsruhe, Germany) to select transformed cells and 300 µg / mL cefotaxime to eliminate *A. tumefaciens*. MS agar plates were incubated at 26 °C in darkness for three weeks. Then, calli were finely sectioned and transferred to liquid Murashige-Skoog medium supplemented with 25 µg / mL kanamycin (Carl Roth GmbH + Co. KG, Karlsruhe, Germany) to maintain selective stringency. Henceforth, cells were subcultured weekly by inoculating 1.5 mL of mother cell culture into 30 mL of freshly prepared Murashige-Skoog medium complemented with 25 µg / mL kanamycin (Carl Roth GmbH + Co. KG, Karlsruhe, Germany) and 5 µM indole-3-acetic acid (Carl Roth GmbH + Co. KG, Karlsruhe, Germany) to maintain fluorescence. Cells were cultivated at 26 °C in darkness under constant shaking at 150 rpm.

3. Methods

3.6.4 Verifying the overexpression of MFS

In order to verify the overexpression of MFS in the transgenic cell lines, RNA was extracted using the Universal RNA Purification Kit (Roboklon GmbH, Berlin, Germany) following the manufacturer's instructions with the optional treatment with RNase-free DNase I (QIAGEN GmbH, Hilden, Germany) to remove DNA. The quality and quantity of isolated RNA were evaluated using a NanoDrop® ND-1000 spectrophotometer (PeqLab Biotechnologie GmbH, Erlangen, Germany). Synthesis of cDNA, semi-qPCR, and qPCR were performed as previously described in **Chapters 3.4.2 and 3.4.3**, except that housekeeping genes specific for tobacco, namely NtL25 and NtEF1 α , were used (**Table 5**).

3.6.5 Localization and colocalization study of MFS

The localization study of MFS in the three different *Mentha* species was performed by spinning disc confocal microscopy with a 3-day-old, mitotically highly active cell culture. Visualization of the cells was done with the Axio Observer.Z1 Spinning Disc microscope (Carl Zeiss AG, Jena, Germany), operated by the ZEN Blue software (Carl Zeiss AG, Jena, Germany). The device was equipped with a digital CCD camera (AxioCam MRm, Carl Zeiss AG, Jena, Germany) and a laser dual spinning disc device (CSU-X1, Yokogawa, Tokyo, Japan). Cells were observed with a 63x oil immersion objective under differential interference contrast (DIC) and under blue light excitation (488 nm) of an argon-krypton-laser (Carl Zeiss AG, Jena, Germany) to detect the GFP signal. For the colocalization study, 1 μ M ER-Tracker™ Red (BODIPY™ TR Glibenclamid) (Thermo Fisher Scientific Inc., Waltham, Massachusetts, USA) was used. The tracker was excited at 587 nm. Glibenclamide binds to the sulfonylurea receptors of the ATP-sensitive potassium channels (Hambrock *et al.*, 2002), which are abundant on the endoplasmic reticulum (ER).

4. Results

4.1 Phylogenetic studies

4.1.1 Authentication study and “maternal test” of *Mentha* species

To make reliable statements about the three *Mentha* species of interest, namely *M. aquatica*, *M. x piperita*, and *M. spicata* var. *crispa*, an authentication study with the other available *Mentha* accessions of the JKIP Experimental Station of the KIT was conducted using different morphology-based determination keys to verify their declared species. All species were confirmed except 7580 *M. suaveolens*, which could not be assigned to this species because its morphological characteristics belong to another species, *M. arvensis*. Additionally, there were other limitations, e.g., cultivars or varieties were often missing in the determination keys. Therefore, an additional phylogenetic authentication approach was performed using the nuclear barcoding marker internal transcribed spacer (ITS) AB and the plastid marker *ycf1b*. Furthermore, assumptions about hybrids and their parental species, even if it is the mother or the father, could be made because of the comparative approach of plastid and nuclear barcoding markers.

4. Results

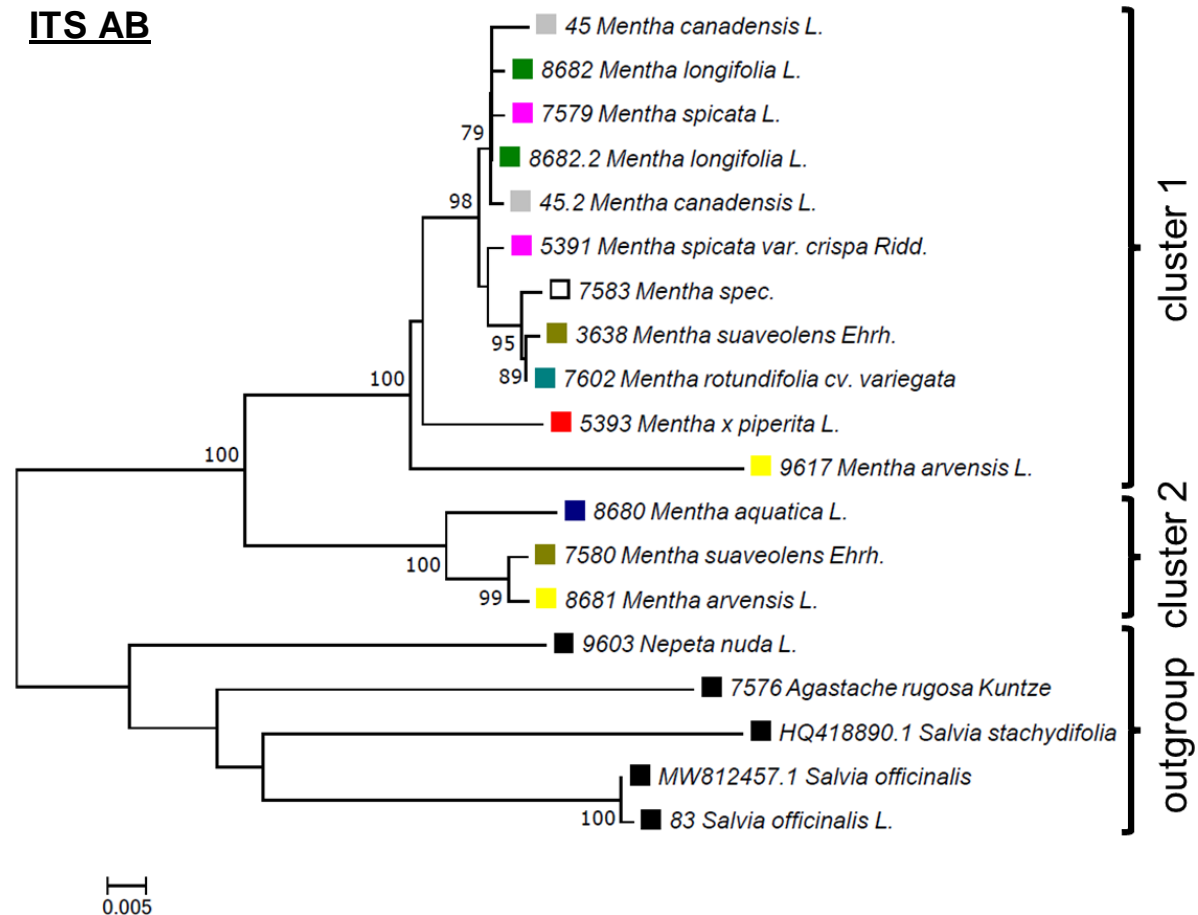


Figure 6: Phylogenetic tree based on the nuclear barcoding marker ITS AB. Neighbor-joining was used to infer the evolutionary history. Bootstrap values are given in percent next to the branches. The tree is drawn to scale, with branch lengths in the same units as the evolutionary distances used for phylogenetic inference. Evolutionary distances were calculated using the Tamura-Nei method in units of the number of base substitutions per site. Analyses were performed in MEGA7. Individuals of one *Mentha* species are represented by the same color, other genera are indicated by black squares. Sequences from NCBI (<https://www.ncbi.nlm.nih.gov/>) were included and could be remarked by their accession ID.

In **Figure 6** the phylogenetic relationship of different *Mentha* species and close relatives of the Lamiaceae family based on the trait-unrelated barcoding marker ITS AB is shown. Significant bootstrap values above 70 % are indicated next to the branches. The outgroup, consisting of two species commonly known as mint but belonging to different genera, namely *Agastache* and *Nepeta*, and three *Salvia* species, was included to root the tree and is demonstrated by black squares. The *Mentha* species are in general a monophyletic group that is divided into two clusters. Cluster one contains *M. canadensis*, *M. longifolia*, *M. spicata* and its variety, *M. x piperita*, *M. rotundifolia* cv. *variegata*, *M. spec.*, and one individual each of *M. arvensis* and *M. suaveolens*, with another individual also present in cluster two.

4. Results

In addition to *M. arvensis* and *M. suaveolens*, *M. aquatica* belongs to cluster two. Cluster one shows other smaller groups, e.g., one group containing all individuals of *M. canadensis* and *M. longifolia* as well as 7579 *M. spicata*, with small evolutionary distances, i.e., a small number of base substitutions per site. There is also a group with 7602 *M. rotundifolia* cv. *variegata* and 3638 *M. suaveolens*, suggesting a close phylogenetic relationship. The hybrid 5393 *M. x piperita* is part of cluster one and shows a smaller evolutionary distance to *M. spicata* var. *crispa* than to *M. aquatica*.

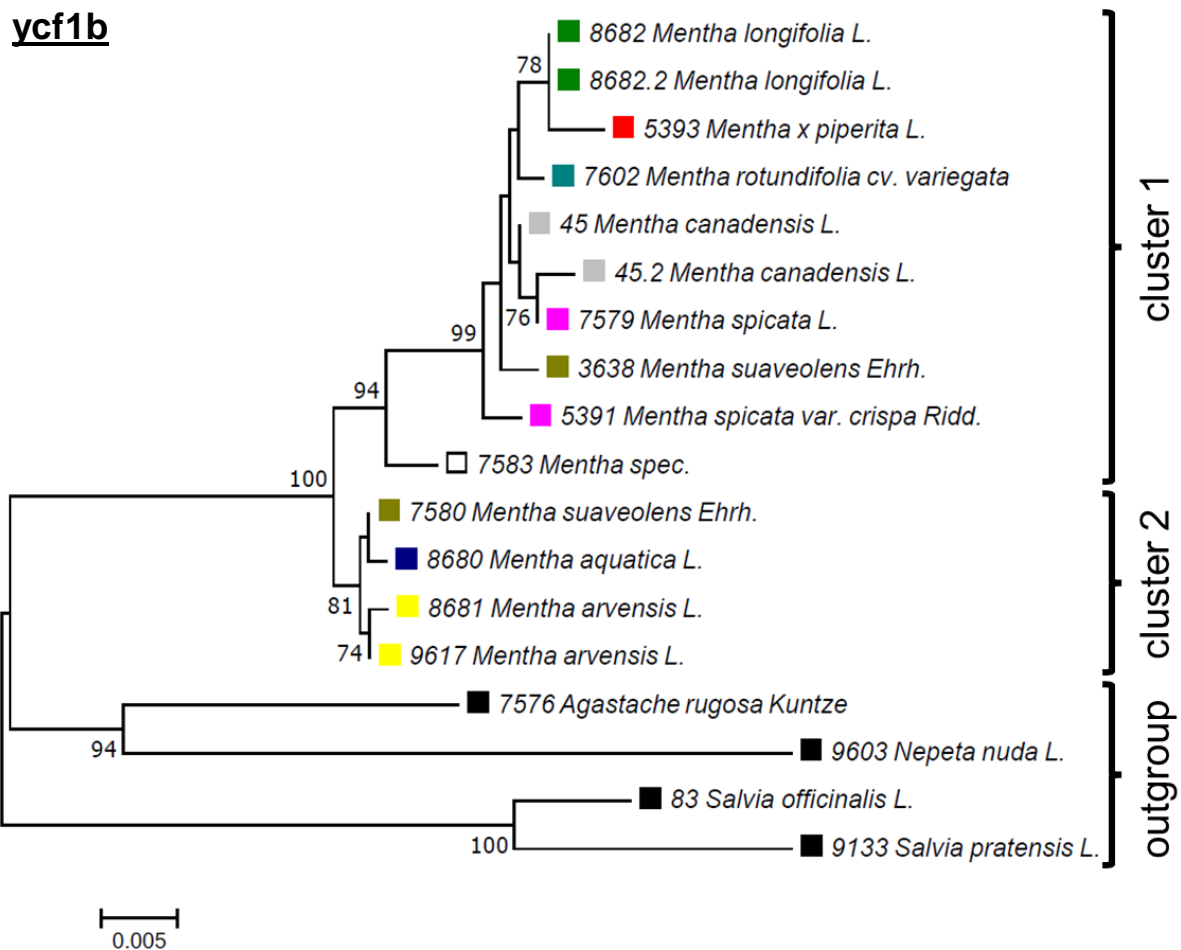


Figure 7: Phylogenetic tree based on the plastid barcoding marker ycf1b. Neighbor-joining was used to infer the evolutionary history. Bootstrap values are given in percent next to the branches. The tree is drawn to scale, with branch lengths in the same units as the evolutionary distances used for phylogenetic inference. Evolutionary distances were calculated using the Tamura-Nei method in units of the number of base substitutions per site. Analyses were performed in MEGA7. Individuals of one *Mentha* species are represented by the same color, other genera are indicated by black squares.

4. Results

The phylogenetic relationship of different *Mentha* species and close relatives of the Lamiaceae family based on the plastid barcoding marker *ycf1b* is demonstrated in **Figure 7**. Next to the branches, significant bootstrap values over 70 % are shown. Again, the two species commonly known as mint but from different genera, *Agastache* and *Nepeta*, as well as two different *Salvia* species served as an outgroup. Here, the *Salvia* accessions form the root of the tree. The other two genera, *Agastache* and *Nepeta*, build their own cluster next to the *Mentha* accessions, which are also monophyletic here. The *Mentha* species are again divided into two clusters. Cluster one contains *M. canadensis*, *M. longifolia*, *M. spicata* and its variety, *M. x piperita*, *M. rotundifolia* cv. *variegata*, *M. spec.* and one individual of *M. suaveolens*, with another individual also present in cluster two, like for the other barcoding marker ITS AB. Here, the individuals of *M. arvensis* are not separated. They are both present in cluster two with *M. aquatica* and one individual of *M. suaveolens*. Cluster one shows further separation. A small evolutionary distance of *M. longifolia* to *M. x piperita* is demonstrated. Additionally, the evolutionary distance of *M. x piperita* to *M. spicata* var. *crispa* is again smaller than to *M. aquatica*, suggesting a maternal relationship.

In general, individuals belonging to the same species show a lower number of base substitutions per site for the plastid barcoding marker *ycf1b* than for the nuclear marker ITS AB, suggesting different resolution strengths. To investigate this further, the relative base substitution rates of the barcoding markers were quantified for the three *Mentha* species of interest and are presented in the following **Figure 8**.

4. Results

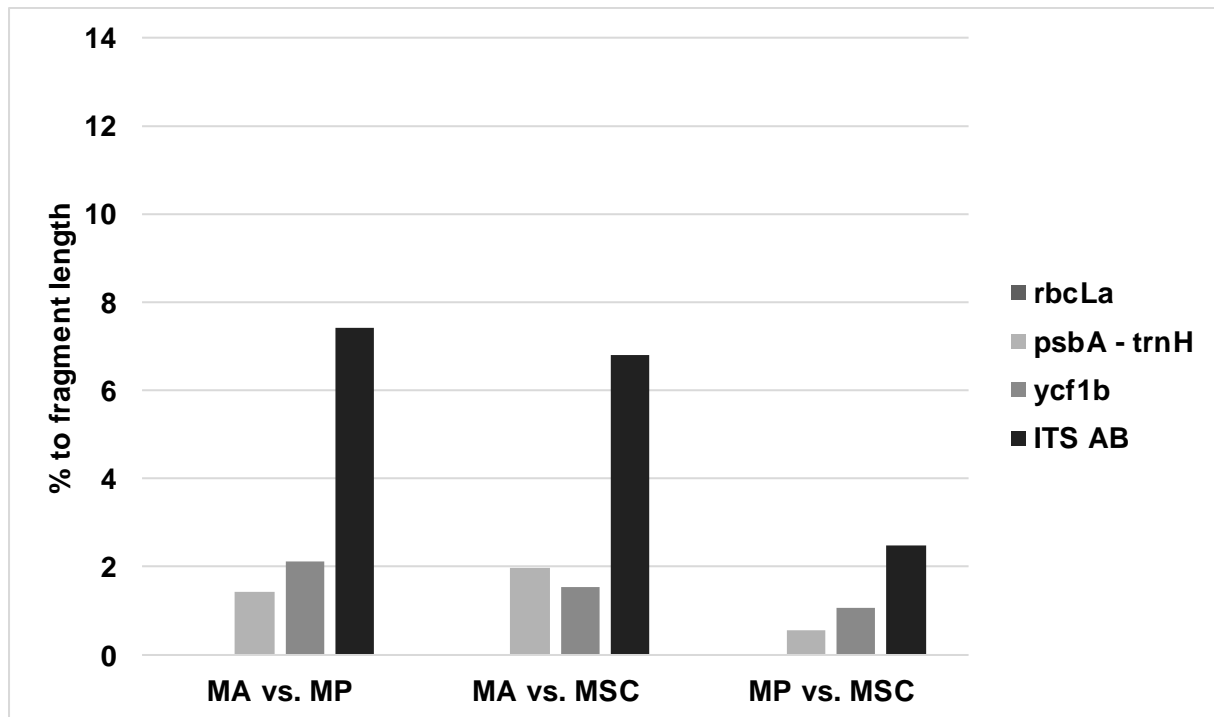


Figure 8: Relative base substitution rates of the barcoding markers *rbcLa*, *psbA - trnH*, *ycf1b* and ITS AB of the three different *Mentha* species. Base substitution rates are given in percent relative to fragment length. Always two sequences were compared. One difference was identified as one single nucleotide polymorphism (SNP). MA = *M. aquatica*; MP = *M. x piperita*; MSC = *M. spicata* var. *crispa*. The base substitution rate is given in percent relative to the average fragment length of the barcoding marker region of the two compared species. It indicates whether a barcoding marker is suitable for differentiation on interspecies or even on population level. To demonstrate the different resolution, i.e., the amount of sequence differences, of various barcoding markers, another two plastid markers were included, *rbcLa* and *psbA - trnH* (appendix, **Figure 41** and **Figure 42**). The plastid barcoding marker *rbcLa* showed no SNPs at all, no matter which species were compared. The sequences were completely identical. For the plastid barcoding marker *psbA - trnH* a lower base substitution rate was demonstrated for MP and MSC (0.57 %) than for MP and MA (1.41 %). This was also shown for the plastid barcoding marker *ycf1b* (1.06 % vs. 2.12 %) and the nuclear barcoding marker ITS AB (2.48 % vs. 7.43 %), inferring a smaller phylogenetic distance between MP and MSC compared to that between MP and MA.

In general, ITS AB showed the highest relative base substitution rates for the compared *Mentha* species, indicating high resolution and being a suitable barcoding marker for the differentiation of *Mentha* species, even at the population level.

4. Results

4.1.2 Phylogeny of the monoterpene synthases PR and MFS within *Mentha*

Phylogenetic studies on the two branching key monoterpene synthases pulegone reductase (PR) and menthofuran synthase (MFS) of *M. aquatica*, *M. x piperita*, and *M. spicata* var. *crispa* were conducted to detect differences between species in a trait-related marker that could provide evidence for gene diversification.

pulegone reductase

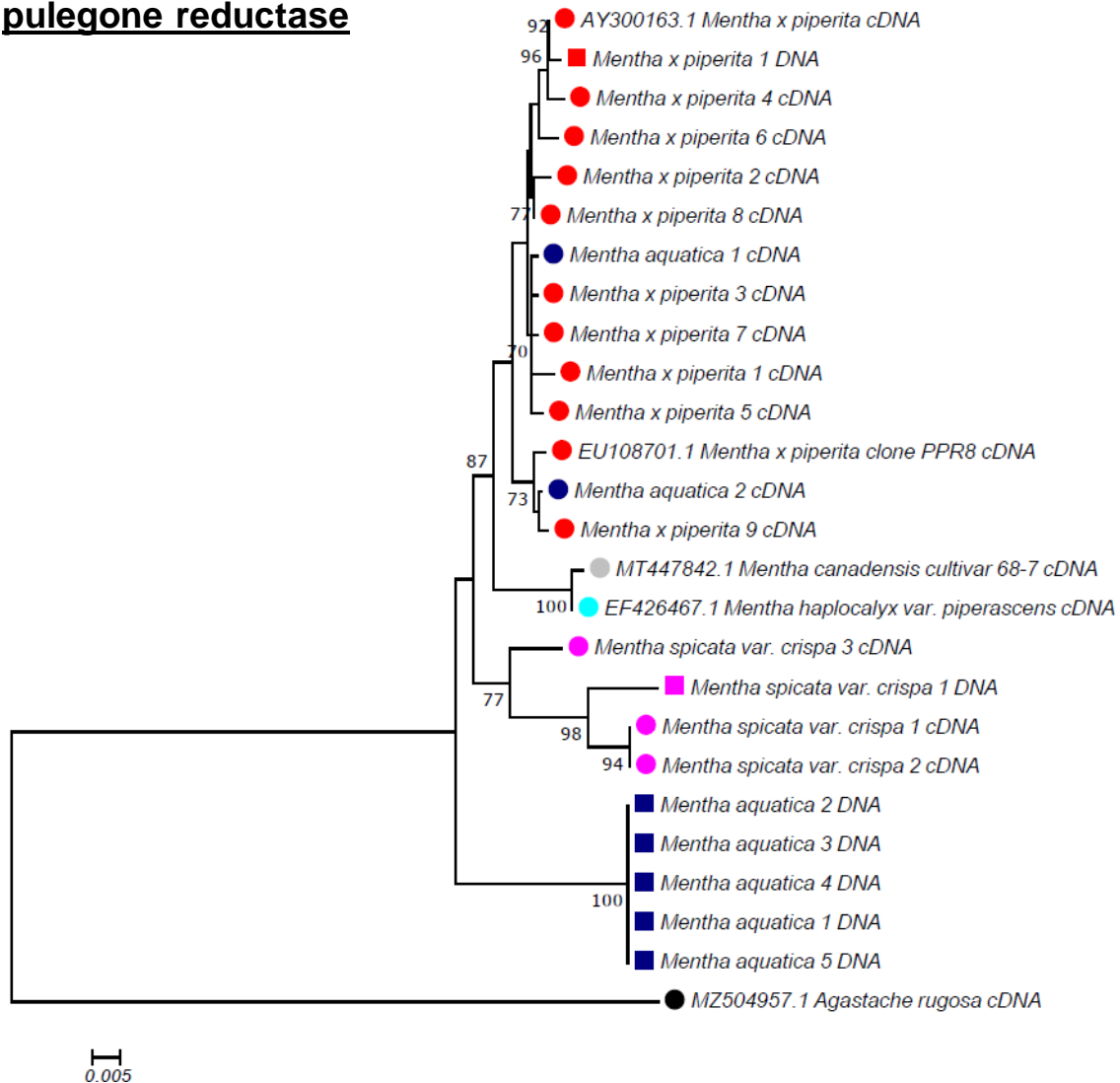


Figure 9: Phylogenetic tree based on PR sequences of different *Mentha* species. Neighbor-joining was used to infer the evolutionary history. Bootstrap values are given in percent next to the branches. The tree is drawn to scale, with branch lengths in the same units as the evolutionary distances used for phylogenetic inference. Evolutionary distances were calculated using the Tamura-Nei method in units of the number of base substitutions per site. Analyses were performed in MEGA7. Circles indicate cDNA sequences (MA, MP, and MSC 1029 bp in length), while squares represent DNA sequences (MA 1861 bp, MP 1647 bp, and MSC 1611 bp in length). Individuals of one *Mentha* species are represented by the same color, outgroup is black. Sequences from NCBI (<https://www.ncbi.nlm.nih.gov/>) were included and could be remarked by their Accession ID.

4. Results

The phylogenetic tree of the PR is demonstrated in **Figure 9**. Significant bootstrap values above 70 % are indicated next to the branches. As an outgroup *Agastache rugosa* (NCBI accession: MZ504957.1) was included to root the phylogenetic tree. It can be clearly seen that all sequences of *M. spicata* var. *crispa* build a monophyletic group, whereas all sequences of *M. x piperita* and cDNA sequences of *M. aquatica* cluster together. The DNA sequences of *M. aquatica* differed a lot from their cDNA sequences, indicating the occurrence of introns, leading to the establishment of their own cluster in the phylogenetic tree. If only the PR cDNA sequences of *M. aquatica* were considered, there would be a small evolutionary distance to *M. x piperita*. Another two coding sequences of *M. canadensis* (NCBI accession: MT447842.1) and *M. haplocalyx* var. *piperascens* (NCBI accession: EF426467.1) were included. They form their own cluster that is supported by a bootstrap value of 100%, indicating that they have remarkably similar coding sequences.

introns of PR

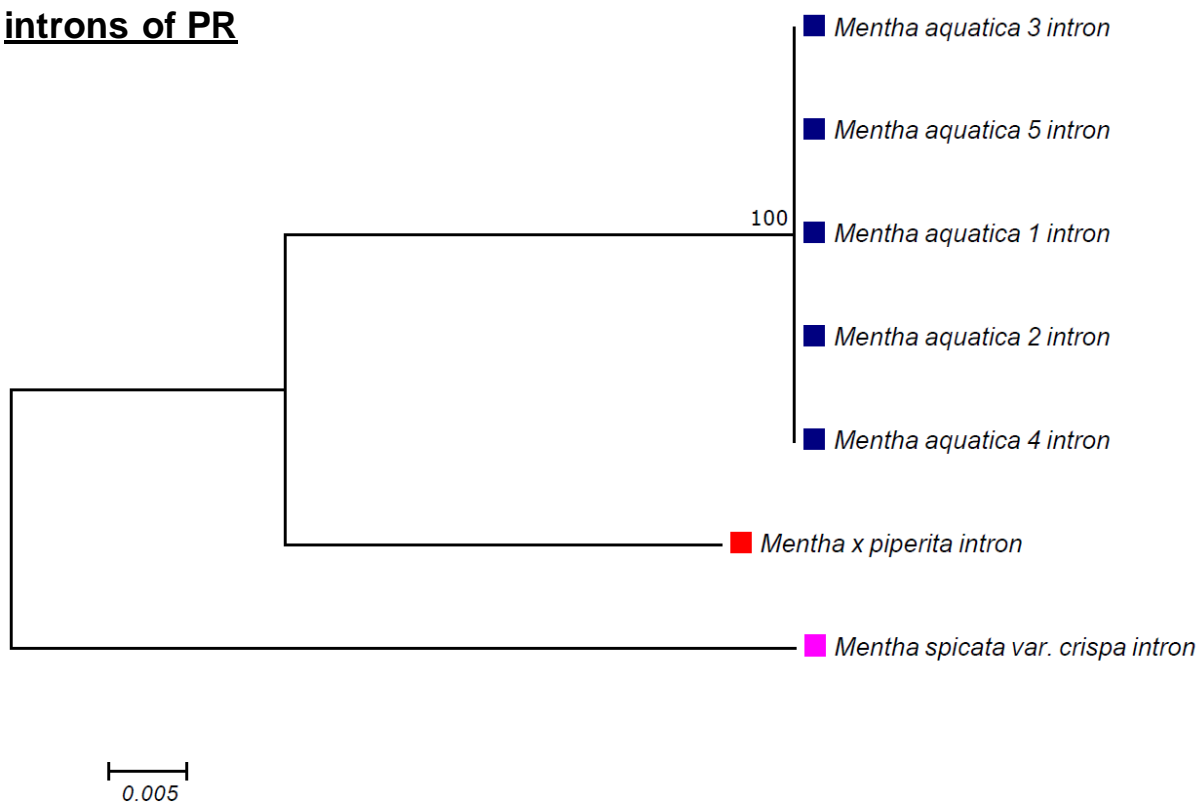


Figure 10: Phylogenetic tree based on intron sequences of PR. Neighbor-joining was used to infer the evolutionary history. Bootstrap values are given in percent next to the branches. The tree is drawn to scale, with branch lengths in the same units as the evolutionary distances used for phylogenetic inference. Evolutionary distances were calculated using the Tamura-Nei method in units of the number of base substitutions per site. Analyses were performed in MEGA7. Individuals of one *Mentha* species are represented by the same color. The intron length of MA was 832 bp, of MP 618 bp, and of MSC 582 bp.

4. Results

The phylogenetic relationship of highly variable regions, namely introns, occurring in PR DNA sequences of the three *Mentha* species is shown in **Figure 10**. A smaller evolutionary distance based on this region of *M. aquatica* to *M. x piperita* than to *M. spicata* var. *crispa* is demonstrated, even if a moderate evolutionary distance of *M. aquatica* to *M. x piperita* is present.

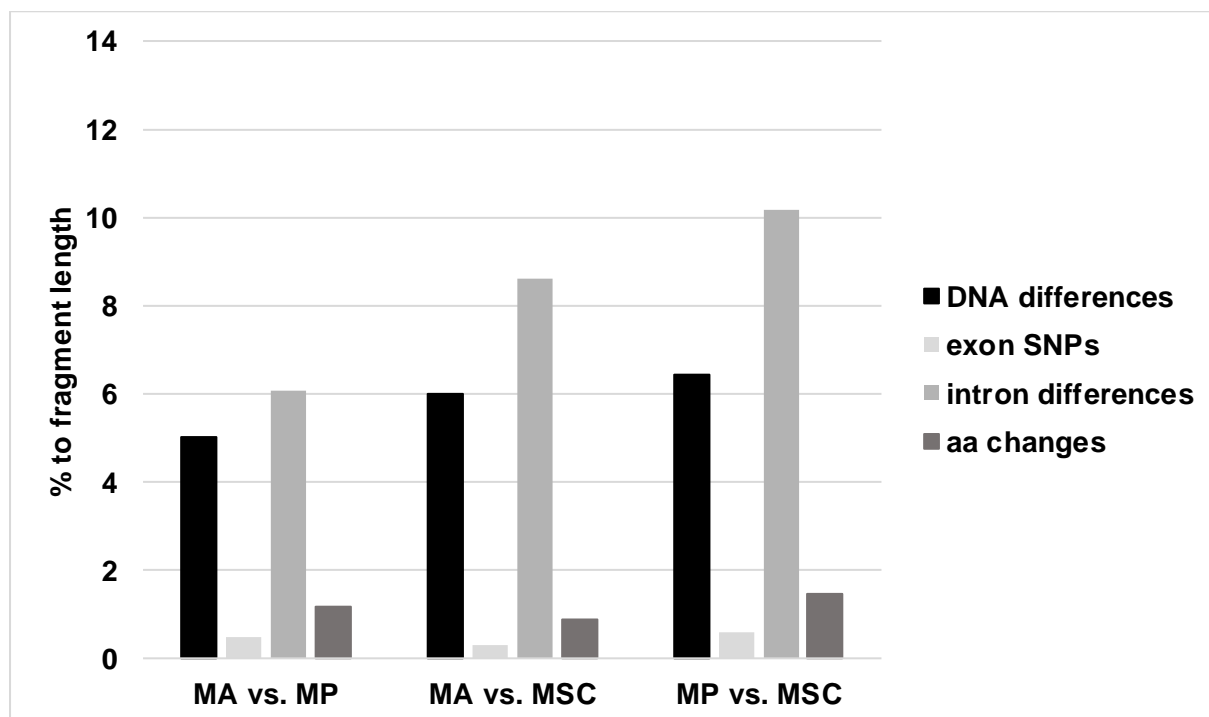


Figure 11: Relative substitution rates of PR sequences of the three different *Mentha* species. Substitution rates are given in percent relative to fragment length. Always two sequences were compared. One difference was identified as one single nucleotide polymorphism (SNP) or a complete insertion / deletion. MA = *M. aquatica*; MP = *M. x piperita*; MSC = *M. spicata* var. *crispa*.

Figure 11 shows the substitution rates of PR sequences of the three *Mentha* species relative to fragment length in percent. It provides evidence about the variability of the PR sequences on the DNA, exon, intron, and amino acid levels, which infers possible phylogenetic relationships of this monoterpene synthase between species. Even if the relative substitution rates did not differ greatly between the *Mentha* pairs, minor differences could be detected. The graph shows that *M. aquatica* and *M. x piperita* had a lower relative substitution rate on DNA and intron levels (5.02 % and 6.07 %) compared to *M. aquatica* and *M. spicata* var. *crispa* (5.99 % and 8.63), as well as to *M. x piperita* and *M. spicata* var. *crispa* (6.45 % and 10.12 %). If only the exons, i.e., the coding sequence, were considered, *M. aquatica* and *M. spicata* var. *crispa* showed the lowest relative substitution rate with 0.29 % compared to *M. aquatica* and *M. x piperita* with 0.49 % and to *M. x piperita* and *M. spicata* var. *crispa* with 0.58 %.

4. Results

This was confirmed by relative substitution rates on amino acid level (*M. aquatica* and *M. spicata* var. *crispa* = 0.87 %, *M. aquatica* and *M. x piperita* = 1.12 %, *M. x piperita* and *M. spicata* var. *crispa* = 1.46 %). In general, higher variability could be determined in DNA sequences and introns than in exons and amino acid sequences.

menthofuran synthase

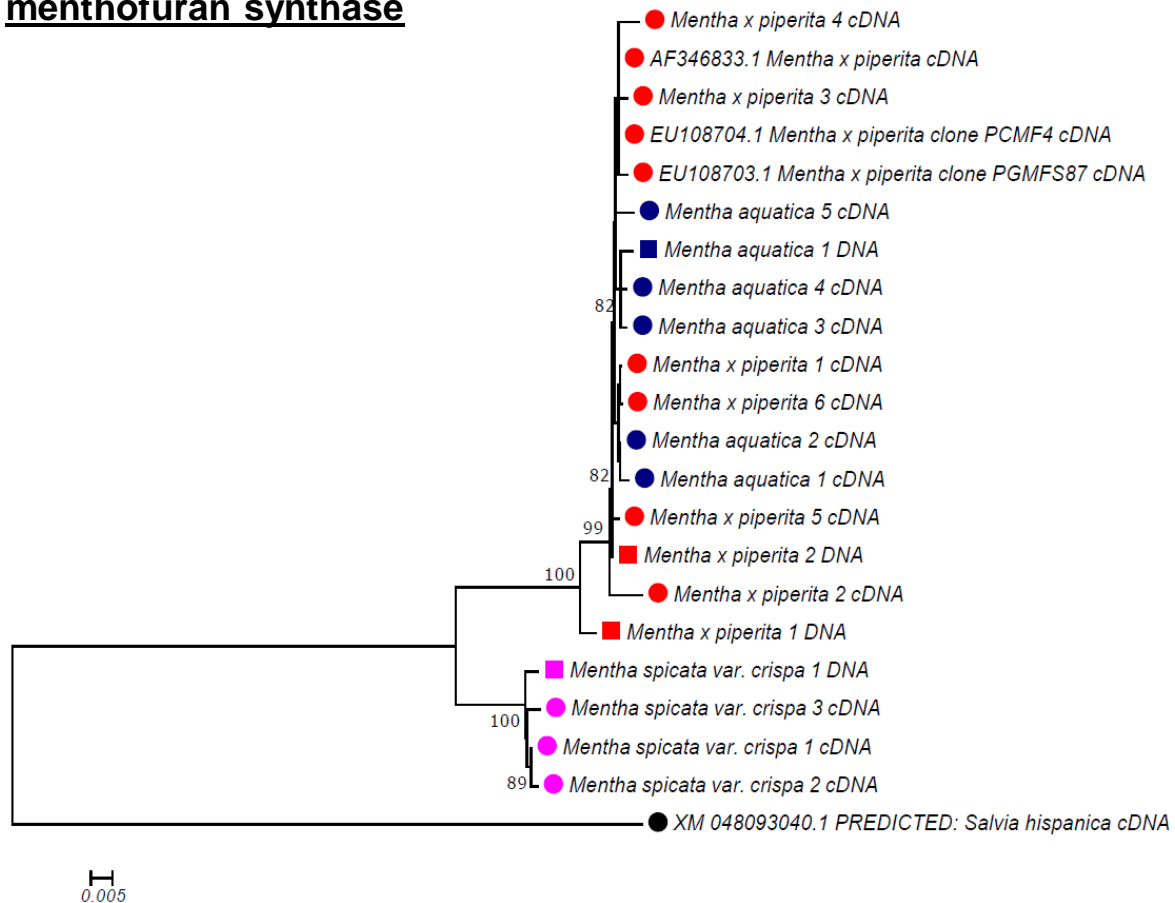


Figure 12: Phylogenetic tree based on MFS sequences of different *Mentha* species. Neighbor-joining was used to infer the evolutionary history. Bootstrap values are given in percent next to the branches. The tree is drawn to scale, with branch lengths in the same units as the evolutionary distances used for phylogenetic inference. Evolutionary distances were calculated using the Tamura-Nei method in units of the number of base substitutions per site. Analyses were performed in MEGA7. Circles indicate cDNA sequences (MA and MP 1482 bp, MSC 1494 bp in length), while squares represent DNA sequences (MA and MP 1564 bp, MSC 1576 bp in length). Individuals of one *Mentha* species are represented by the same color, outgroup is black. Sequences from NCBI (<https://www.ncbi.nlm.nih.gov/>) were included and can be remarked by their Accession ID.

The phylogenetic tree of the MFS is demonstrated **Figure 12**. Significant bootstrap values above 70 % are indicated next to the branches. As an outgroup and root of the phylogenetic tree, a predicted sequence of *Salvia hispanica* (NCBI accession: XM_048093040.1) was included.

4. Results

The phylogenetic tree of MFS is quite the same as the one of PR, except that all sequences of *M. aquatica* form a cluster together with *M. x piperita*, indicating an exceedingly small evolutionary distance in this trait. The sequences of *M. spicata* var. *crispa* build a monophyletic group and therefore have a high evolutionary distance to *M. aquatica* and *M. x piperita*.

introns of MFS

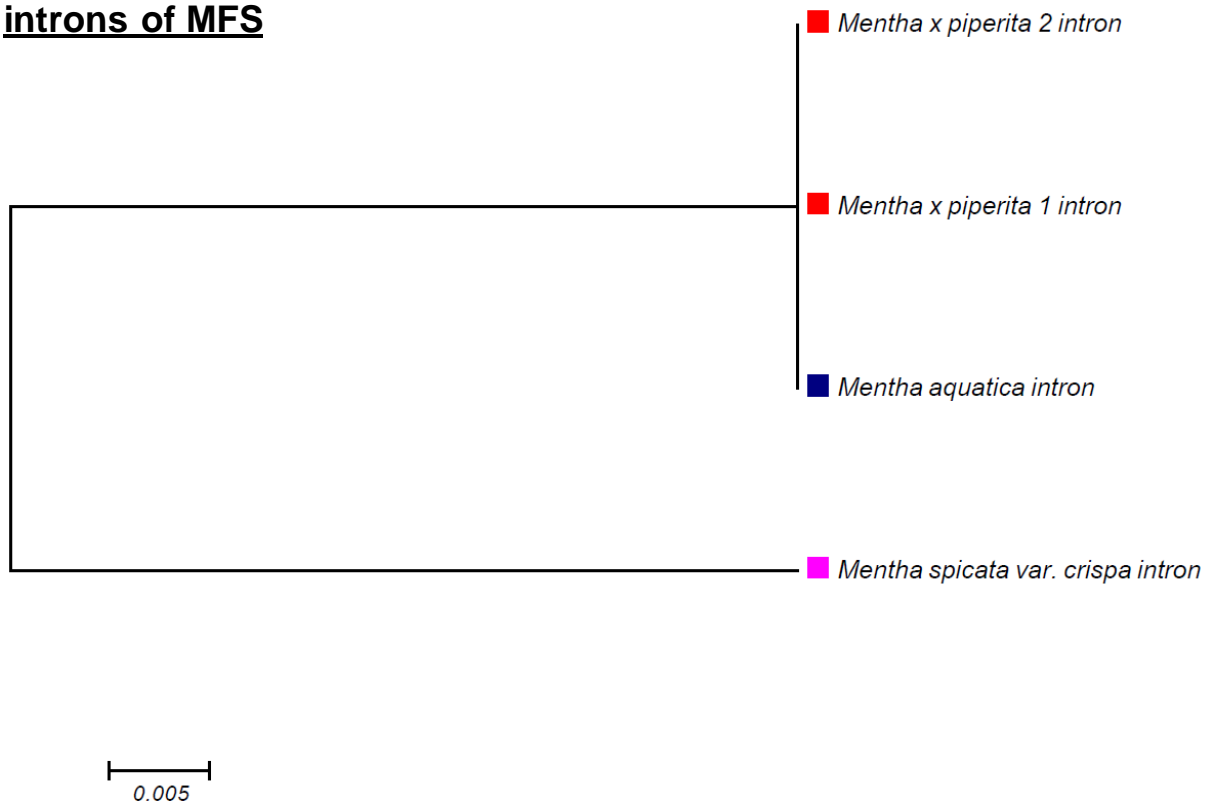


Figure 13: Phylogenetic tree based on intron sequences of MFS. Neighbor-joining was used to infer the evolutionary history. Bootstrap values are given in percent next to the branches. The tree is drawn to scale, with branch lengths in the same units as the evolutionary distances used for phylogenetic inference. Evolutionary distances were calculated using the Tamura-Nei method in units of the number of base substitutions per site. Analyses were performed in MEGA7. Individuals of one *Mentha* species are represented by the same color. The intron length of MA, MP, and MSC was 82 bp.

Figure 13 shows the phylogenetic relationship of introns originating from MFS DNA sequences of the three *Mentha* species. No sequence differences were detected in the introns of *M. aquatica* and *M. x piperita*, suggesting a remarkably close evolutionary relationship. For the intron of *M. spicata* var. *crispa*, a big evolutionary distance to the ones of *M. aquatica* and *M. x piperita* was found.

4. Results

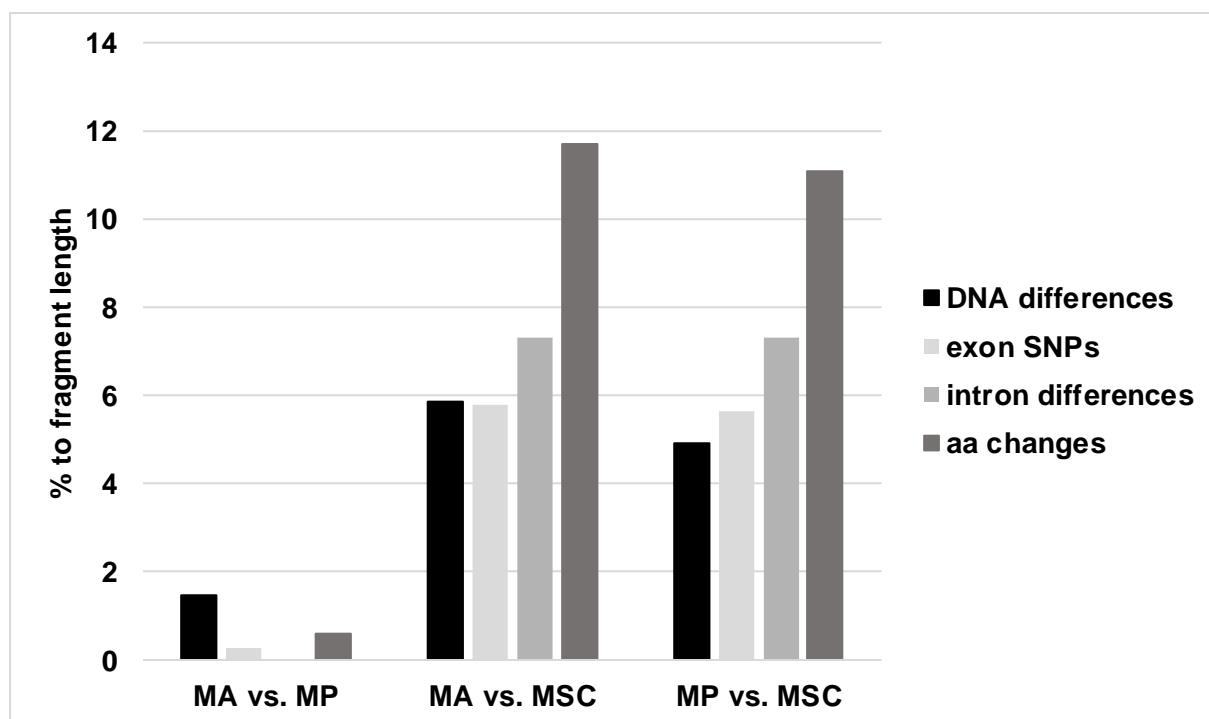


Figure 14: Relative substitution rates of MFS sequences of the three different *Mentha* species. Substitution rates are given in percent relative to fragment length. Always two sequences were compared. One difference was identified as one single nucleotide polymorphism (SNP) or a complete insertion / deletion. MA = *M. aquatica*; MP = *M. x piperita*; MSC = *M. spicata* var. *crispa*.

The variability of MFS sequences on DNA, exon, intron, and amino acid levels between species is demonstrated in **Figure 14**. Relative substitution rates are given in percent. For *M. aquatica* and *M. x piperita*, an extremely low relative substitution rate on DNA (1.47 %), exon (0.27 %), intron (0.00 %) and amino acid level (0.61 %) was demonstrated. In comparison, *M. aquatica* and *M. spicata* var. *crispa*, as well as *M. x piperita* and *M. spicata* var. *crispa* showed a similar, remarkably high, relative substitution rate on DNA (5.86 %; 4.90 %), exon (5.78 %; 5.65 %), intron (7.32 %; 7.32 %), and amino acid level (11.69 %; 11.09 %). In general, the MFS of *M. spicata* var. *crispa* differed a lot from those of *M. aquatica* and *M. x piperita*.

In summary, the phylogenetic analysis of the key monoterpene synthases, PR and MFS, of *M. aquatica*, *M. x piperita*, and *M. spicata* var. *crispa* indicated that the hybrid *M. x piperita* is phylogenetically more closely related to *M. aquatica* in these traits than to *M. spicata* var. *crispa*. Nevertheless, there were some discrepancies found for the relative substitution rates of PR, where the lowest rates on exon and amino acid levels were found for *M. aquatica* and *M. spicata* var. *crispa*, but with a very small distance to the other pairs. In addition, there is evidence for gene diversification due to sequence divergence of the MFS of *M. spicata* var. *crispa* rather than promiscuous enzymes.

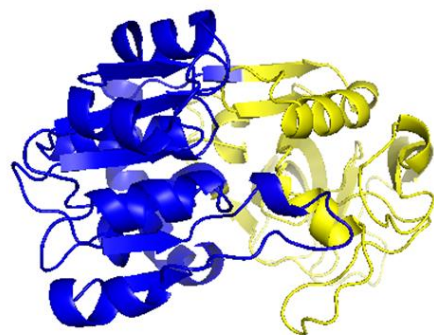
4. Results

4.1.3 Predicted protein structures of PR are quite similar in contrast to MFS

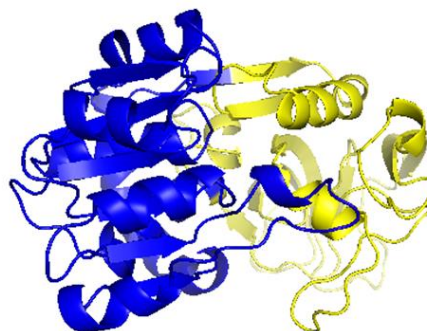
A close phylogeny of enzyme sequences suggests similar protein structures. To assess this hypothesis, the 3D protein structures of PR and MFS were analyzed. To obtain the 3D protein structures of PR and MFS of *M. aquatica* and *M. spicata* var. *crispa*, the cloned cDNA sequences were first translated into amino acid sequences that were then used to predict a 3D protein structure by AlphaFold 1.3. For *M. x piperita*, the 3D protein structure was already available and received from the database hosted by the European Bioinformatics Institute (<http://alphafold.ebi.ac.uk>). PyMOL 2.5.4 was applied to visualize the predicted 3D protein structures.

4. Results

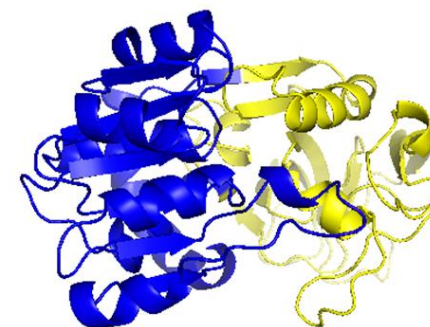
A



M. aquatica

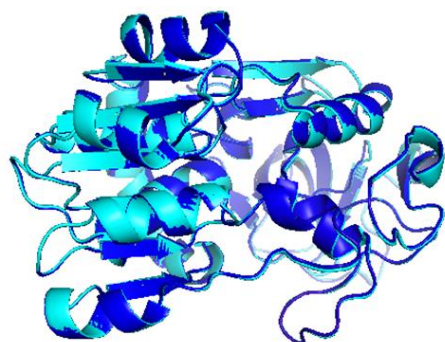


M. x piperita
Q6WAU0

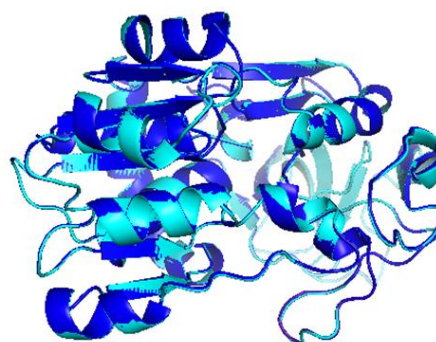


M. spicata var. crispa

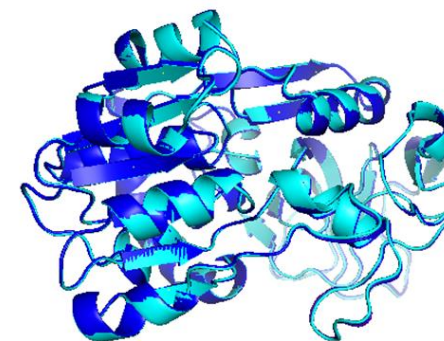
B



MA x MP
RMSD: 0.136 Å (303 to 303 atoms)



MA x MSC
RMSD: 0.049 Å (270 to 270 atoms)

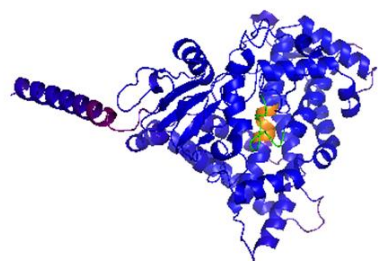


MP x MSC
RMSD: 0.154 Å (306 to 306 atoms)

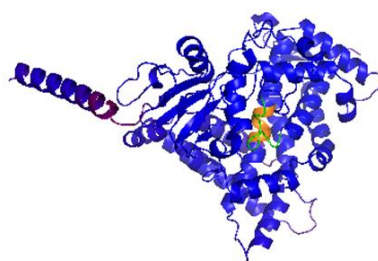
Figure 15: 3D protein structures of PR of the three different *Mentha* species. In **A**, the 3D protein structures of the three *Mentha* species predicted by AlphaFold 1.3 are shown. The per-residue confidence score (pLDDT) was 100 %. The catalytic N-terminal domain is indicated in yellow, whereas the C-terminal domain is indicated in blue, according to Liu *et al.* (2021). In **B**, an alignment of two single protein structures is demonstrated. The value of the root-mean-square deviation (RMSD) of each alignment was calculated. All protein structures were visualized with PyMOL 2.5.4. MA = *M. aquatica*; MP = *M. x piperita*; MSC = *M. spicata var. crispa*.

4. Results

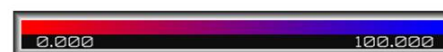
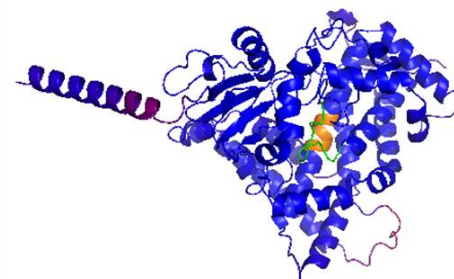
A



M. aquatica

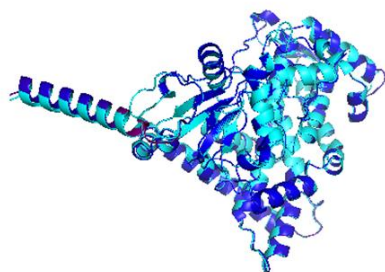


M. x piperita
Q947B7

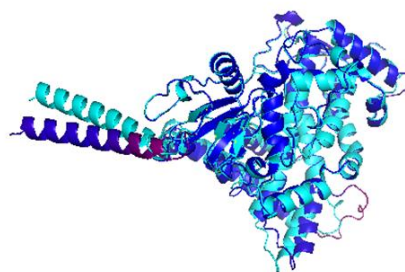


M. spicata var. *crispa*

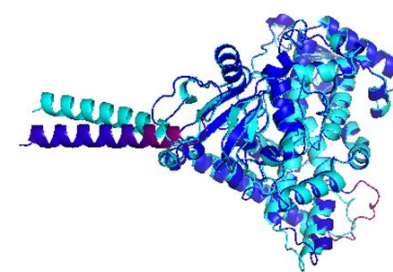
B



MA x MP
RMSD: 0.105 Å (376 to 376 atoms)



MA x MSC
RMSD: 0.437 Å (373 to 373 atoms)



MP x MSC
RMSD: 0.429 Å (384 to 384 atoms)

Figure 16: 3D protein structures of MFS of the three different *Mentha* species. In **A**, the 3D protein structures of the three *Mentha* species predicted by AlphaFold 1.3 are shown. The color code from red (low) to blue (high) indicates the per-residue confidence score (pLDDT) between 0 and 100 %. The oxygen-binding region is represented in orange, and the heme-binding region is represented in green, according to Berteau *et al.* (2001). In **B**, an alignment of two single protein structures is demonstrated. The value of the root-mean-square deviation (RMSD) of each alignment was calculated. All protein structures were visualized in PyMOL 2.5.4. MA = *M. aquatica*; MP = *M. x piperita*; MSC = *M. spicata* var. *crispa*.

4. Results

Figure 15A and **Figure 16A** demonstrate the 3D protein structures of PR and MFS of *M. aquatica*, *M. x piperita*, and *M. spicata* var. *crispa*. The per-residue confidence score (pLDDT) between 0 and 100 % was calculated. The protein structures of PR and MFS showed a pLDDT of 100 %, except for a protruding α -helix of MFS, where a small part was purple, suggesting a pLDDT of about 50 %. PR has two domains. A catalytic N-terminal domain that is represented in yellow and a C-terminal domain that is indicated in blue. In MFS, the oxygen-binding region is shown in orange and the heme-binding region in green. PR and MFS could be easily distinguished, but the protein structures of one enzyme within the three *Mentha* species were hardly distinguishable because of the high similarity. They showed almost the same arrangement of α -helices and β -sheets except for the MFS of *M. spicata* var. *crispa*, where minor differences in a loop on the right bottom side and a slightly different orientation of the α -helix protruding from the protein could be observed compared to *M. aquatica* and *M. x piperita*. To get a deeper insight into the similarity of the protein structures, alignments of two individual protein structures were created. These are presented in **Figure 15B** and **Figure 16B**. The root-mean-square deviation (RMSD) value of each alignment is given. A low RMSD value refers to a high similarity. *M. aquatica* and *M. spicata* var. *crispa* seemed to have the most similar protein structures in PR with a RMSD value of 0.049 Å, followed by *M. aquatica* and *M. x piperita* with a RMSD value of 0.136 Å and *M. x piperita* and *M. spicata* var. *crispa* with a RMSD value of 0.154 Å, while for MFS, *M. aquatica* and *M. x piperita* showed most similar protein structures. Here, a RMSD value of 0.105 Å was determined, followed by *M. x piperita* and *M. spicata* var. *crispa* with a RMSD value of 0.429 Å and *M. aquatica* and *M. spicata* var. *crispa* with a RMSD value of 0.437 Å.

In summary, the protein structures of PR and MFS could be distinguished easily. In general, PR was more similar between the three *Mentha* species than MFS, for which higher RMSD values were obtained. Similar protein structures could often be assigned to a close phylogenetic relationship, e.g., for MFS, but not for PR. Previously, the PR of *M. aquatica* and that of *M. x piperita* were shown to have the closest phylogenetic relationship, but the PR protein structure of *M. aquatica* was more similar to that of *M. spicata* var. *crispa*. This fits when the relative substitution rates based on exon level are considered, which were lowest for these two.

4. Results

4.2 Species-specific chemical profiles in a non-additive manner

To obtain the essential oil of six individual plants of *M. aquatica*, *M. x piperita*, and *M. spicata* var. *crispa* 50 g of fresh leaf material was hydro distilled. A rough overview of the qualitative differences in the composition of the essential oils was obtained using gas chromatography. Chromatograms can be found in the appendix, **Figure 43**. To completely elucidate the chemical profile and quantify the compounds of the three *Mentha* species, a GC-MS was conducted.

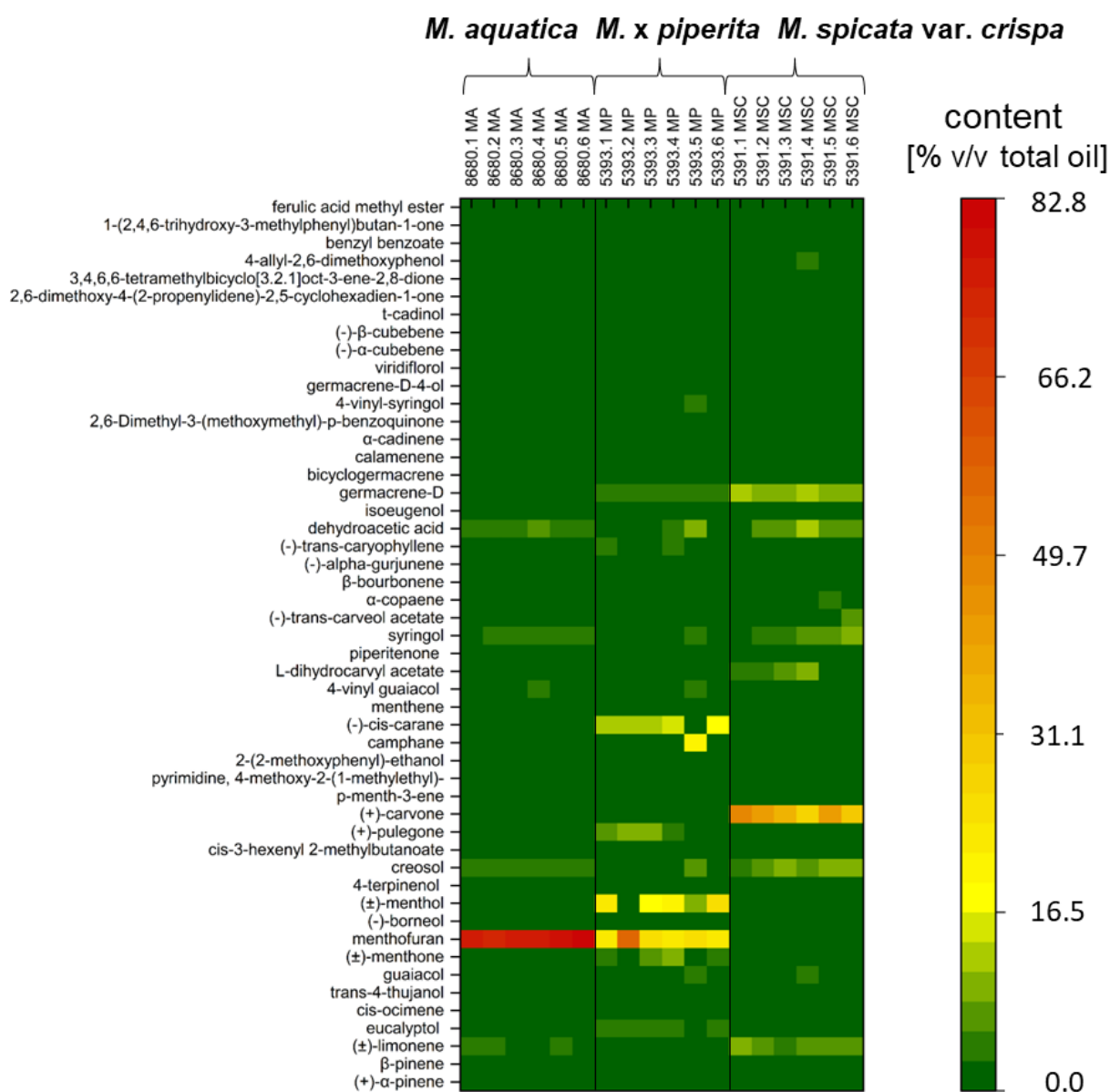


Figure 17: Heatmap of the relative content of different compounds detected in the essential oils of the three *Mentha* species using GC-MS. Relative contents are given as % v/v of the extracted oil. The compounds detected by GC-MS are ordered according to their retention time from bottom to top. Six biological replicates of each species were analyzed.

4. Results

The heatmap in **Figure 17** demonstrates the relative content of different compounds to the total percentage of the analyzed essential oil compounds using GC-MS. The available trivial names of the compounds are listed. The color code, from green (= low) over yellow (= moderate) to red (= high), ranges the relative content of the compounds. The study revealed that closely related species were chemically hugely different, while no different chemotypes were observed among individual plants of a species. All individuals of *M. aquatica* showed a relative content of 73 – 83 % of menthofuran as their main compound in the essential oil. Menthofuran was also the main compound of *M. x piperita*, with a relative content of 22 – 27 %, except for one individual plant, where a relative content of 55 % was detected. Additionally, a relative content of 10 – 26 % of the second main compound, menthol, was demonstrated except in the one individual plant with the high relative content of menthofuran in its oil. Here, no menthol was detected at all. Carvone was the main compound of the essential oil of *M. spicata* var. *crispa*, with a relative content of 28 – 50 %. It can be recognized that the relative content of compounds varied slightly even within the individual species.

In addition, some species-specific compounds with lower relative contents could be detected. A compound that could only be found in the essential oil of *M. aquatica* is 3,4,6,6-tetramethylbicyclo[3.2.1]oct-3-ene-2,8-dione (< 2 %). Unique compounds in the essential oil of *M. x piperita* were camphane (< 22 %), cis-carane (< 18 %), pulegone (< 11 %), menthone (< 9 %), eucalyptol (< 4 %), trans-4-thujanol (< 2 %), p-menth-3-ene (< 2 %), menthene (< 2 %), and benzyl benzoate (< 1 %). In *M. spicata* var. *crispa*, several compounds were determined that were only occurring in its essential oil, namely L-dihydrocarvyl acetate (< 10 %), trans-carveol acetate (< 8 %), α -copaene (< 5 %), 2,6-Dimethyl-3-(methoxymethyl)-p-benzoquinone (< 3 %), 2,6-dimethoxy-4-(2-propenylidene)-2,5-cyclohexadien-1-one (< 3 %), cis-ocimene (< 2 %), pyrimidine, 4-methoxy-2-(1-methylethyl) (< 2 %), 2-(2-methoxyphenyl)-ethanol (< 2 %), isoeugenol (< 2 %), t-cadinol (< 2 %), 1-(2,4,6-trihydroxy-3-methylphenyl)butan-1-one (< 2 %), borneol (< 1 %), 4-terpinenol (< 1 %), cis-3-hexenyl 2-methylbutanoate (< 1 %), piperitenone (< 1 %), α -gurjunene (< 1 %), calamenene (< 1 %), α -cadinene (< 1 %), germacrene-D-4-ol (< 1 %), cubebene (< 1 %), and ferulic acid methyl ester (< 1 %).

4. Results

Additionally, further minor compounds were detected that could be found in several species, e.g., *M. aquatica* and *M. x piperita* showed both the abundance of 4-vinyl-syringol (< 2 %; < 3 %) and viridiflorol (< 2 %; < 2 %), *M. aquatica* and *M. spicata* var. *crispa* of limonene (< 4 %; < 11 %), and *M. x piperita* and *M. spicata* var. *crispa* of germacrene-D (< 5 %; < 13 %), bicyclogermacrene (< 1 %; < 3 %), β -bourbonene (< 1 %; < 3 %), and α -pinene (< 1 %; < 1 %). All three species had dehydroacetic acid (< 6 %; < 9 %; < 13 %), creosol (< 6 %; < 8 %; < 11 %), syringol (< 4 %; < 5 %; < 9 %), guaiacol (< 3 %; < 4 %; < 4 %), 4-vinyl guaiacol (< 3 %; < 5 %; < 1 %), 4-allyl-2,6-dimethoxyphenol (< 2 %; < 3 %; < 3 %), (–)-trans-caryophyllene (< 2 %; < 3 %; < 1 %), and β -pinene (< 1 %; < 1 %; < 1 %) abundant in their essential oils.

In general, all *Mentha* species had unique chemical profiles in a non-additive manner, as the offspring *M. x piperita* has not inherited all compounds from the parental species. Nevertheless, *M. aquatica* and *M. x piperita* have the main compound menthofuran in common, albeit in different abundances. This suggests a closer chemical relationship, as expected based on the closer phylogenetic relationship and the similar protein structures of the key enzyme MFS that controls the metabolic flux to this compound.

4.3 Bioactivity studies

4.3.1 Dose-dependent germination inhibition of cress and poppy by carvone

Germination assays with *Lepidium sativum* and *Papaver rhoeas* were conducted to determine whether some compounds of the essential oils exert a specific bioactive potential. Therefore, 50 seeds of *L. sativum* or *P. rhoeas* were sown equidistantly on a Whatman filter paper wetted with 2 mL of distilled water and a cover slip containing different volumes of the pure compounds or the respective solvent control *n*-hexane were placed in a Petri dish. After incubation, the inhibition rate was quantified.

4. Results

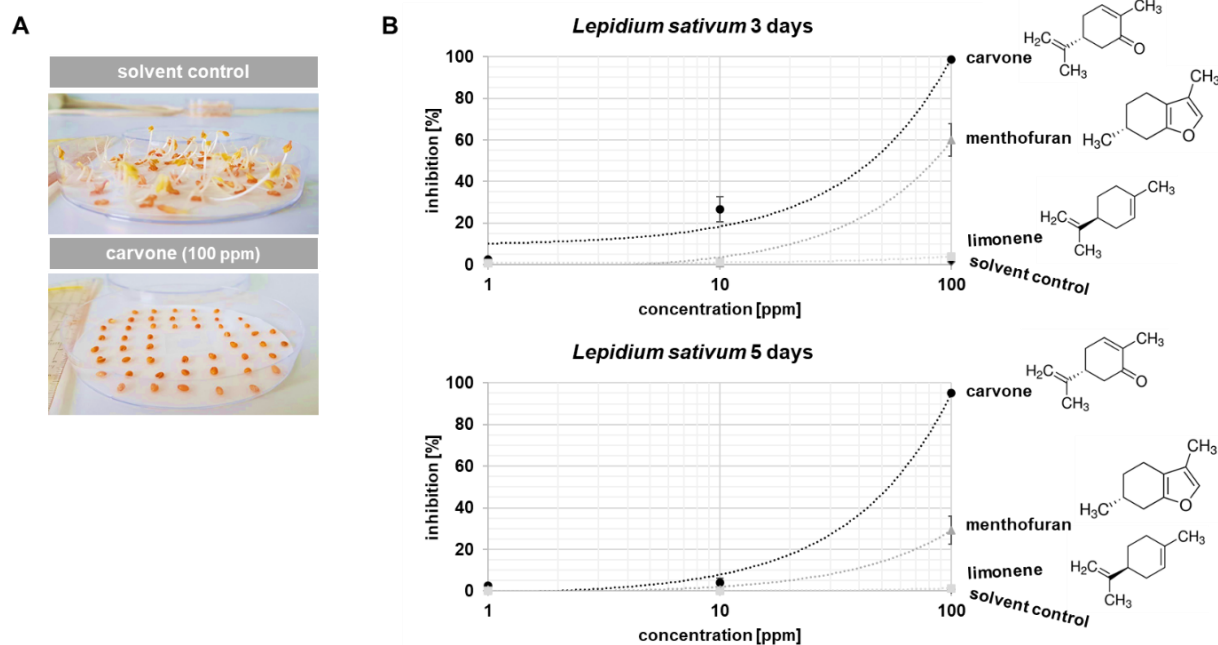


Figure 18: Carvone strongly inhibited the germination of *L. sativum*. **A** Representative images of the experimental setup **B** Dose-response of germination inhibition over the concentration of the monoterpenes carvone, menthofuran, and limonene as compared to the solvent control after incubation in darkness at 25 °C for 3 or 5 days. Data represent means and SE from biological triplicates.

Figure 18A shows representative images of the experimental setup of the standard cress germination test. The upper image illustrates the germination after applying *n*-hexane as solvent control through the gas phase, and the lower image after application of 100 ppm carvone, where almost no germination was observed after 3 days of incubation. In **Figure 18B**, the dose-response curves of germination inhibition over the concentration of the monoterpenes carvone, menthofuran, and limonene as compared to the solvent control *n*-hexane after incubation in darkness at 25 °C for 3 or 5 days are demonstrated. The solvent control *n*-hexane did not appear to have any effect on germination, as an inhibition rate of 1.33 % (SE ± 1.33) was determined after 3 days and 0.67 % (SE ± 0.67) after 5 days. Therefore, the effects could be attributed solely to the monoterpenes used in this assay. The application of 100 ppm carvone resulted in an inhibition rate of 98.67 % (SE ± 0.67) after 3 days, which remained almost stable with 95.33 % (SE ± 1.33) after 5 days, while the application of 100 ppm menthofuran only achieved an inhibition rate of 60.00 % (SE ± 7.69) after 3 days, which even halved to 29.33 % (SE ± 6.77) after 5 days of incubation. With decreasing concentration, the germination inhibition rates declined for all monoterpenes analyzed, implying a dose dependence.

4. Results

The monoterpene limonene showed an extremely low germination inhibition rate at a concentration of 100 ppm of 4 % (SE \pm 1.15) after 3 days and 1.33 % (SE \pm 1.33) after 5 days and was therefore not considered in further bioactivity assays.

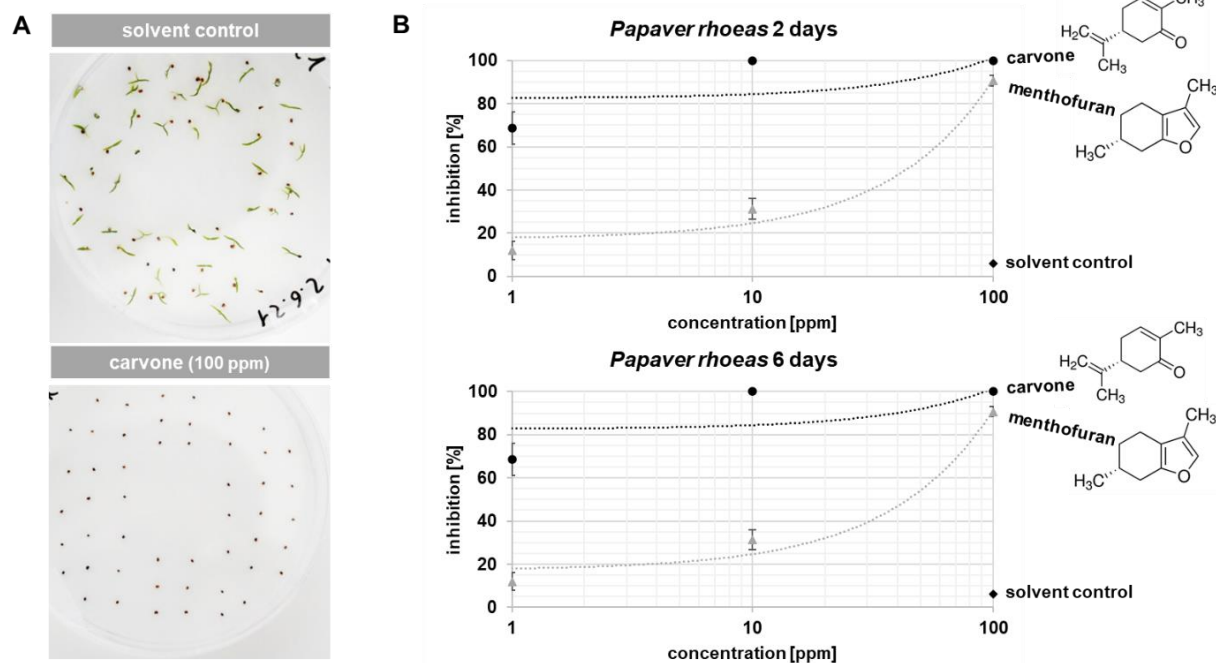


Figure 19: Carvone strongly inhibited the germination of *P. rhoeas*. **A** Representative images of the experimental setup **B** Dose-response of germination inhibition over the concentration of the monoterpenes carvone and menthofuran as compared to the solvent control after incubation on a 12 h light / 12 h dark cycle at 20 °C for 2 or 6 days. Data represent means and SE from biological triplicates. Another germination assay was performed with poppy to determine the specificity of the effects caused by the different monoterpenes. **Figure 19A** shows representative images of the germination after applying *n*-hexane as solvent control through the gas phase in the upper image and after application of 100 ppm carvone in the lower image, where no germination was observed after 6 days of incubation. In **Figure 19B**, the dose-response curves of carvone, menthofuran, and the solvent control are demonstrated. Again, the solvent control, *n*-hexane, exerted no significant effect on germination inhibition, so all effects were due to the monoterpenes tested. In general, the effects of both monoterpenes were much stronger than those in cress, even at lower concentrations, indicating specific responses. Moreover, all observed effects persisted over the complete experimental period. Application of carvone at the lowest concentration of 1 ppm achieved a considerable germination inhibition of 68.67 % (SE \pm 7.42).

4. Results

With and increasing 10-fold concentration, germination was completely inhibited. In contrast, exposure of poppy seeds to 1 ppm menthofuran reached only 12.00 % (SE \pm 4.16), but at a concentration of 10 ppm germination was inhibited by 31.33 % (SE \pm 4.67) and at 100 ppm by 90.67 % (SE \pm 2.40). Thus, a 10-fold higher concentration of 100 ppm menthofuran was required to provide approximately the same effect as 10 ppm carvone.

In summary, carvone is a highly bioactive monoterpene with a dose-dependent effect on the weeds tested, whereas a higher concentration of menthofuran was always required to achieve a similar germination-inhibiting effect. Both compounds were more efficient and more persistent in *P. rhoeas* as compared to *L. sativum*. Consequently, germination inhibition is not only dose-dependent but also target-specific.

4.3.2 Strong cytotoxicity in transgenic BY-2 lines caused by carvone

To test the cytotoxicity of the essential oils of *M. aquatica* and *M. spicata* var. *crispa* and their main compounds, carvone and menthofuran, an Evans Blue Dye Exclusion Assay according to Gaff and Okong'o-Ogola (1971) was conducted using non-transformed tobacco BY-2 cells (WT) and transformed BY-2 cell lines expressing the actin-binding domain 2 of fimbrin fused to GFP (GF11) and GFP-tubulin α 3 (TuA3). For an approach, 3-day-old cells were incubated with 0.5 % (v/v) of the essential oil, the respective compound, or the solvent control *n*-hexane for 30 min, stained with Evans Blue for 5 min, washed three times, and observed under the Axio Imager.Z1 ApoTome.

4. Results

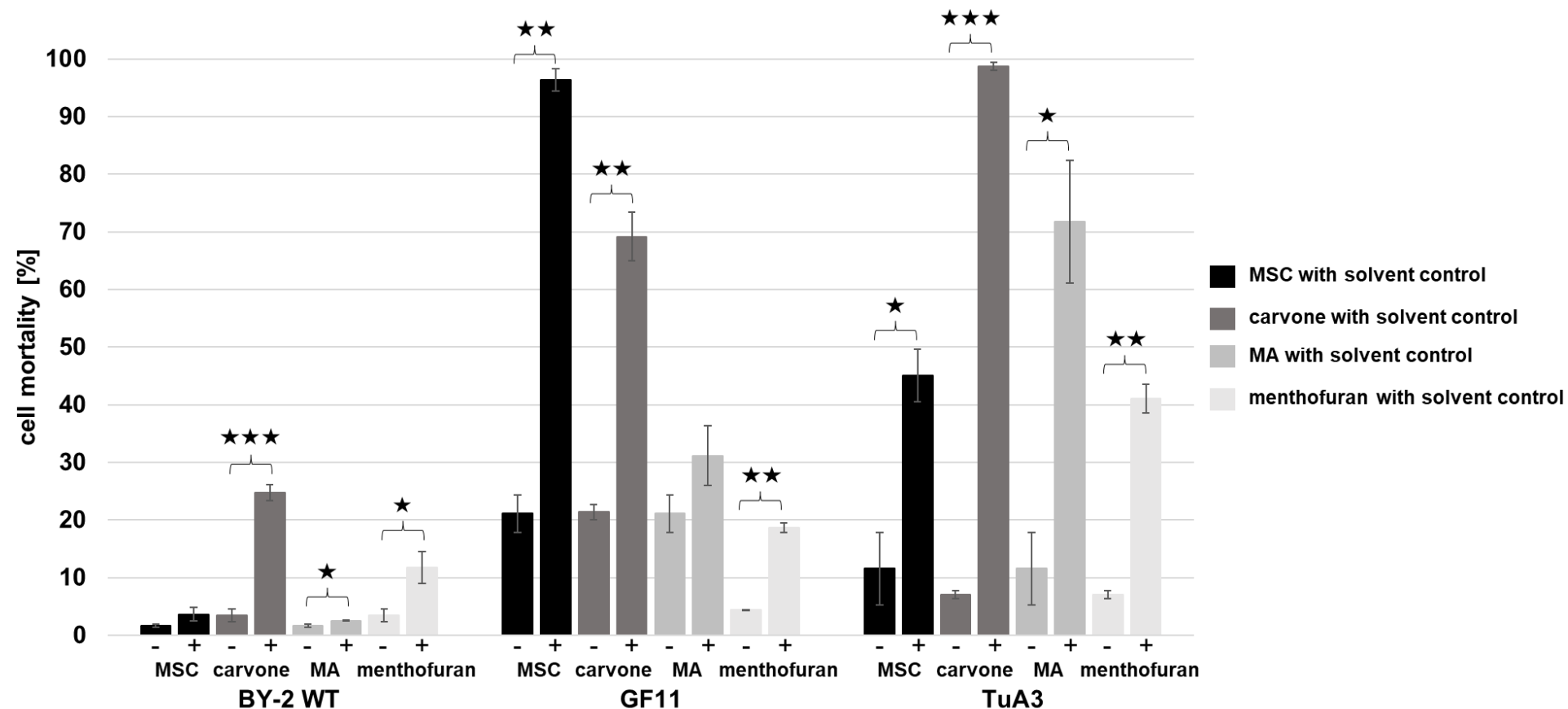


Figure 20: Cytotoxicity of the essential oils of *M. spicata* var. *crispa* and *M. aquatica* and their main compounds, carvone and menthofuran, on non-transformed BY-2 cells (WT) and transformed BY-2 cell lines expressing the actin-binding domain 2 of fimbrin fused to GFP (GF11) and GFP-tubulin α 3 (TuA3). Cell mortality is given in percent. For each oil or compound analyzed, two bars are shown. The left bar indicates the solvent control, *n*-hexane, and the right bar, a treatment with 0.5 % (v/v) oil or compound. The significance was tested by a one-tailed paired Student's t-test and is indicated by asterisks (*: p-value<0.05, **: p-value<0.01, *: p-value<0.001). MA = *M. aquatica*; MSC = *M. spicata* var. *crispa*.**

4. Results

The relative number of dead cells was represented by the cell mortality percentage shown in **Figure 20**. Three independent replicates were conducted with a population of 2500 individual cells per replicate. A one-tailed paired Student's t-test was performed to test significance. An influence of the solvent control *n*-hexane could be excluded, as the cell mortality rate was significantly lower in all cell lines than when treated with either the essential oil or the compound. It was remarkable that a treatment with carvone always resulted in a higher cell mortality rate than a treatment with menthofuran. Cells of the tubulin-marker cell line treated with carvone showed a cell mortality rate of 98.77 % (SE \pm 0.69) compared with 69.20 % (SE \pm 4.25) in the actin-marker cell line, and only 24.81 % (SE \pm 1.40) in the wild-type cell line. Menthofuran was also moderately effective against the TuA3 cell line with a cell mortality rate of 41.02 % (SE \pm 2.48), followed by the GF11 cell line with 18.64 % (SE \pm 0.82) and the WT cell line with 11.78 % (SE \pm 2.72). This again confirmed the higher bioactivity of carvone compared to menthofuran in all cell lines, as shown in the previous germination assays. Application of *M. spicata* var. *crispa* essential oil to the GF11 cell line resulted in a cell mortality rate of 96.38 % (SE \pm 1.90), which was higher than for a treatment with carvone. Moreover, TuA3 cells treated with the essential oil of *M. spicata* var. *crispa* showed a cell mortality rate of 45.16 % (SE \pm 4.58) and WT cells of only 3.66 % (SE \pm 1.18). The essential oil of *M. aquatica* exhibited a higher cell mortality rate of 71.77 % (SE \pm 10.66) in the tubulin-marker cell line compared to menthofuran and *M. spicata* var. *crispa* essential oil, but lower than carvone. Moreover, a treatment of GF11 or WT cells with the essential oil of *M. aquatica* resulted in cell mortality rates of 31.14 % (SE \pm 5.20) and 2.56 % (SE \pm 0.10), respectively.

In conclusion, carvone exerted a strong cytotoxicity in contrast to menthofuran, especially in the TuA3 cell line, reconfirming that it is a potent bioactive compound. However, MSC essential oil containing carvone exhibited stronger cytotoxicity against GF11 than TuA3 cells, suggesting that there are other bioactive compounds in this essential oil that have synergistic or antagonistic effects with carvone.

4.3.3 Microtubules and actin filaments as cellular target of carvone

Time-course live cell imaging was performed *in vivo* using the different transgenic BY-2 tobacco cell lines TuA3 and GF11 to elucidate the cellular mode of action of *M. spicata* var. *crispa* and *M. aquatica* essential oils and their main compounds, carvone and menthofuran.

4. Results

For this purpose, 0.5 μL of the essential oil, the respective compound, or the solvent control *n*-hexane was placed in the vicinity of 20 μL of a 3-day-old suspension culture on both sides, which allowed the cells to be only interfered with via the gas phase, as described in Sarheed *et al.* (2020).

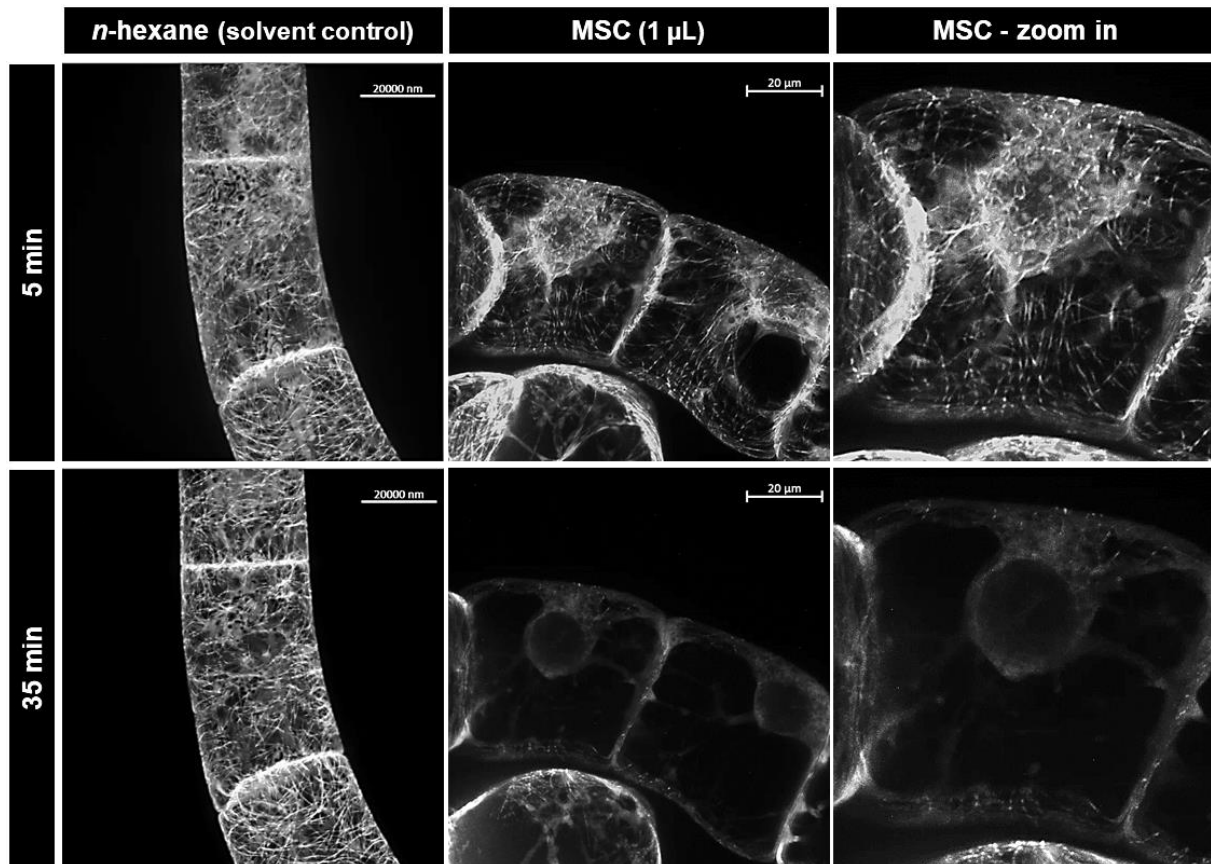


Figure 21: Cellular effect of the essential oil of *M. spicata var. crispa* on microtubules. Representative BY-2 cells expressing GFP-tubulin $\alpha 3$ followed by spinning disc confocal microscopy after treatment with either 1 μL of *n*-hexane as solvent control or the essential oil of MSC at proliferation phase, day 3 after subcultivation. Images show geometric projections of confocal z-stacks. MSC = *M. spicata var. crispa*.

Figure 21 shows the cellular effect of *M. spicata var. crispa* essential oil on microtubules *in vivo*. The observed effects could be attributed to the essential oil, as the fine network of microtubule strands was still present after 35 minutes of treatment with 1 μL of *n*-hexane as solvent control. When cells were exposed to *M. spicata var. crispa* essential oil, microtubules began to degrade after 5 minutes, but some were still visible, especially around the nucleus. After 35 minutes, the network was completely degraded.

4. Results

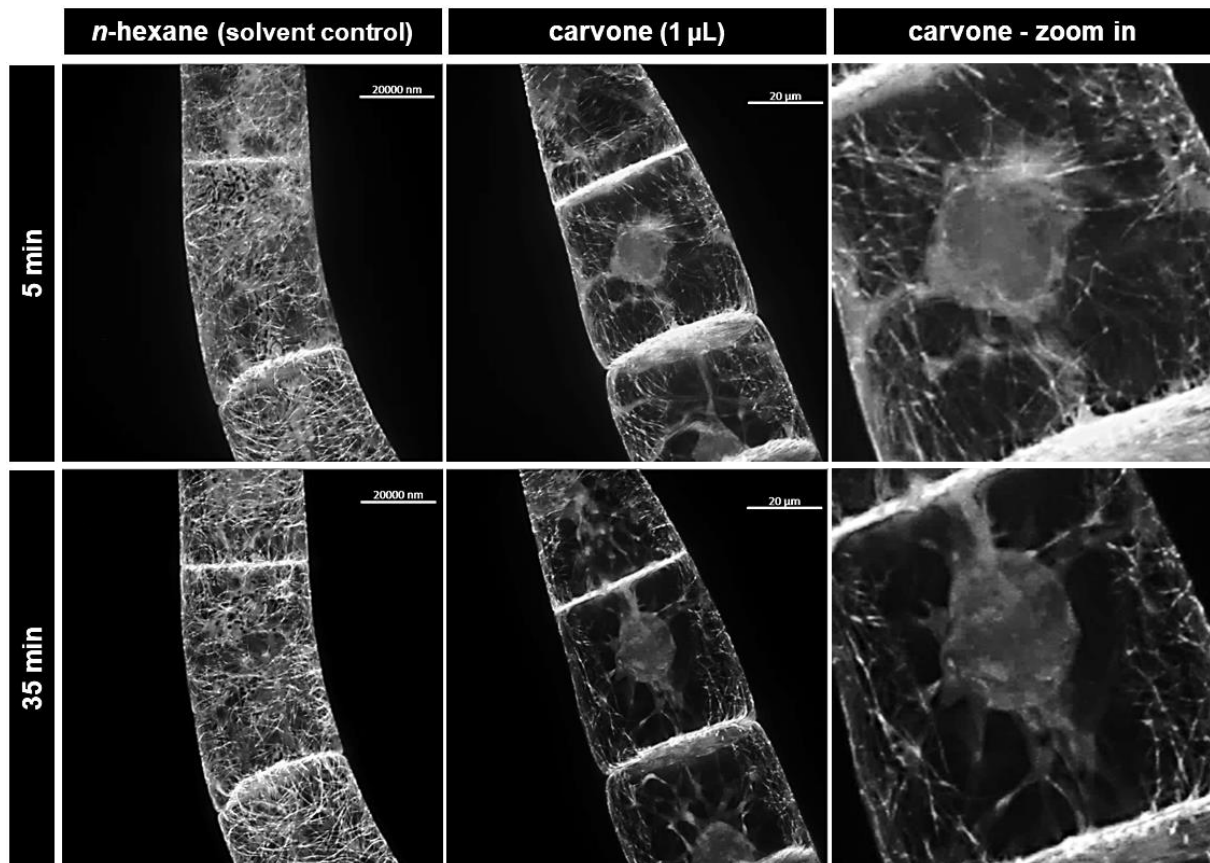


Figure 22: Cellular effect of carvone on microtubules. Representative BY-2 cells expressing GFP-tubulin α 3 followed by spinning disc confocal microscopy after treatment with either 1 μ L of *n*-hexane as solvent control or carvone at proliferation phase, day 3 after subcultivation. Images show geometric projections of confocal z-stacks.

Figure 22 demonstrates time-course live cell imaging with TuA3 cells exposed to carvone, the main compound of *M. spicata* var. *crispa*, *in vivo*. The control was the same as in the previous figure, with no cellular effect on microtubules. Carvone caused a rapid degradation of the microtubule network and therefore had a similar cellular effect to *M. spicata* var. *crispa* essential oil. After 5 minutes, some fine microtubule strands remained, which were almost degraded within 35 minutes.

4. Results

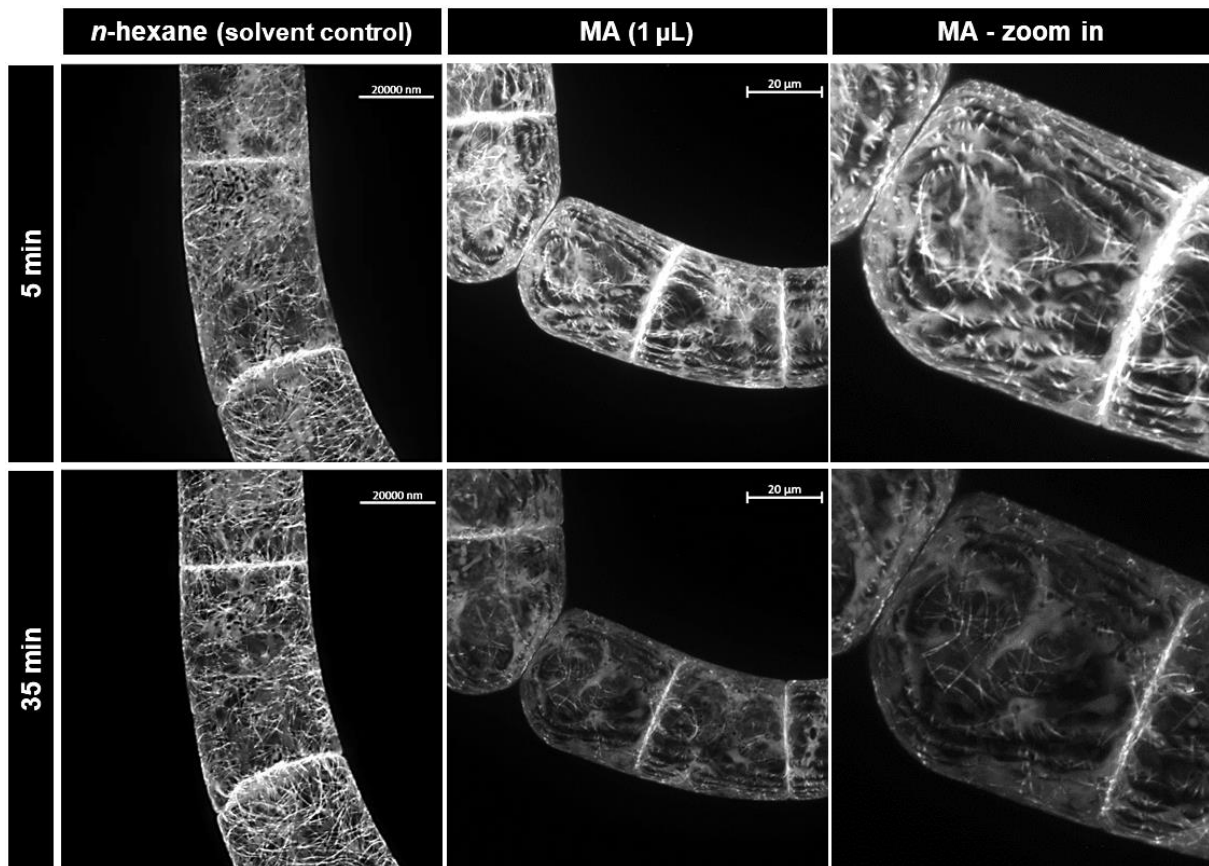


Figure 23: Cellular effect of the essential oil of *M. aquatica* on microtubules. Representative BY-2 cells expressing GFP-tubulin $\alpha 3$ followed by spinning disc confocal microscopy after treatment with either 1 μL of *n*-hexane as solvent control or essential oil of MA at proliferation phase, day 3 after subcultivation. Images show geometric projections of confocal z-stacks. MA = *M. aquatica*.

The cellular effect of *M. aquatica* essential oil on microtubules *in vivo* can be seen in **Figure 23**. The control was the same as in the previous figures, with no cellular effect on microtubules. Here, the mode of action seemed to be different and delayed. The microtubules were still present and intact after 5 minutes. Half an hour later, there was evidence of disintegration. The fluorescent α -tubulin monomers gave a diffuse signal in the cytoplasm of the cell. However, some fine microtubule strands were still visible.

4. Results

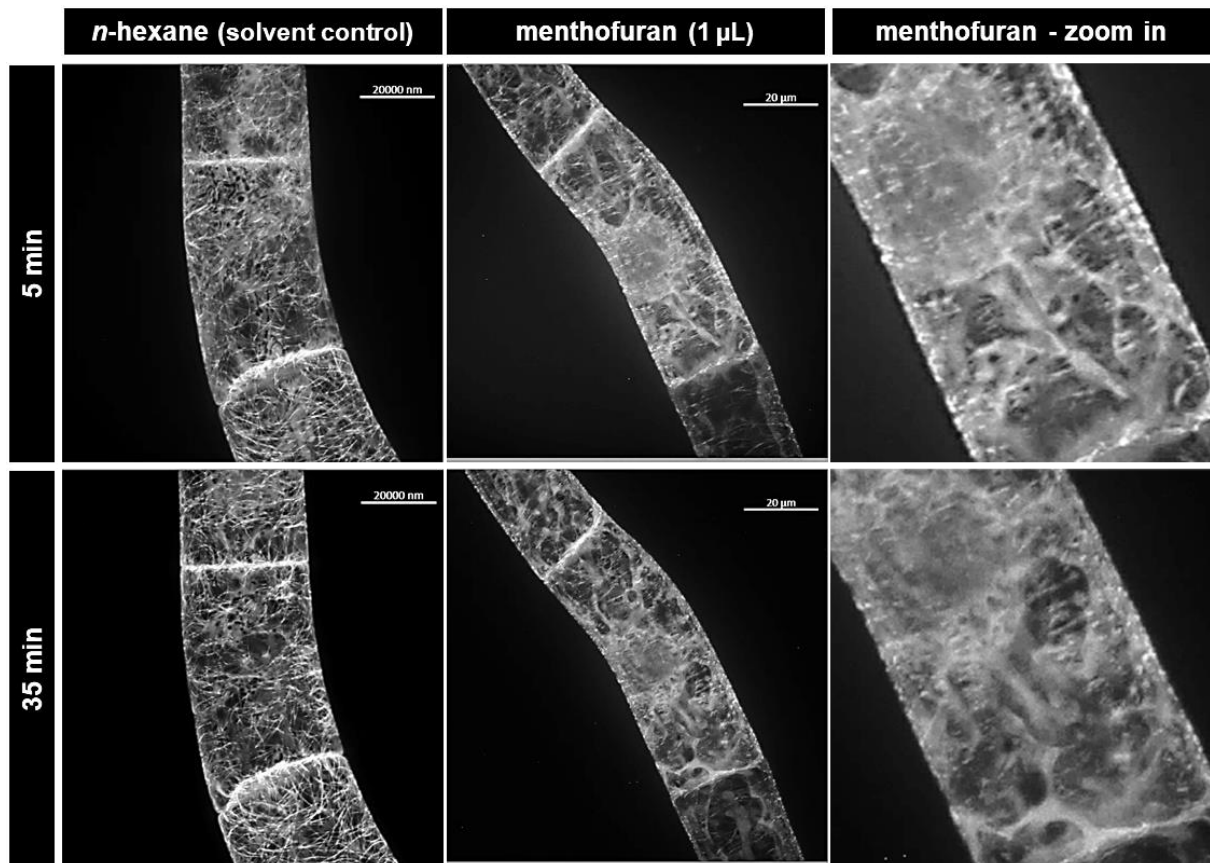


Figure 24: Cellular effect of menthofuran on microtubules. Representative BY-2 cells expressing GFP-tubulin $\alpha 3$ followed by spinning disc confocal microscopy after treatment with either 1 μL of *n*-hexane as solvent control or menthofuran at proliferation phase, day 3 after subcultivation. Images show geometric projections of confocal z-stacks.

Figure 24 shows time-course live cell imaging with TuA3 cells exposed to menthofuran, the main compound of *M. aquatica*, *in vivo*. The control was the same as in the previous figures, with no cellular effect on microtubules. Menthofuran had a similar but weaker effect on the cells compared to the essential oil of *M. aquatica*. The microtubule network was almost intact after 5 minutes, although some diffuse signals were already present. These diffuse signals became a bit stronger half an hour later. However, almost all the microtubule strands were still present.

4. Results

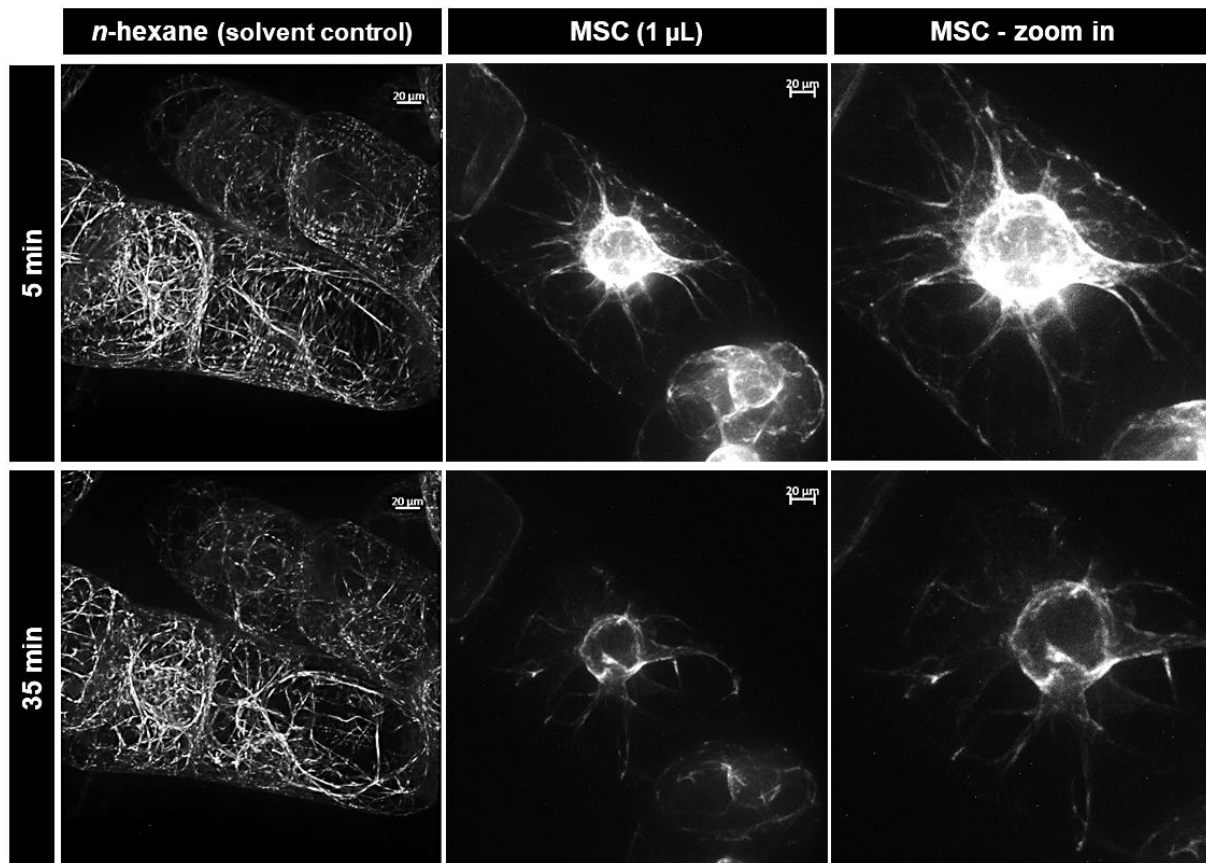


Figure 25: Cellular effect of the essential oil of *M. spicata* var. *crispa* on actin filaments. Representative BY-2 cells expressing the actin-binding domain 2 of fimbrin fused to GFP followed by spinning disc confocal microscopy after treatment with either 1 μL of *n*-hexane as solvent control or essential oil of MSC at proliferation phase, day 3 after subcultivation. Images show geometric projections of confocal z-stacks. MSC = *M. spicata* var. *crispa*.

Figure 25 displays time-course live cell imaging with GF11 cells exposed to *M. spicata* var. *crispa* essential oil *in vivo*. Since treatment with the solvent control *n*-hexane showed no significant difference between the start and end time points, it could be assumed that the solvent control had no effect on the actin network and that all observed effects were due to the essential oil of MSC. After 5 minutes, GF11 cells exposed to the essential oil of *M. spicata* var. *crispa* had already formed thick actin cables around the nucleus, the perinuclear cage, which were attached to the membrane at specific sites. Half an hour later, they were still present but with less fluorescence.

4. Results

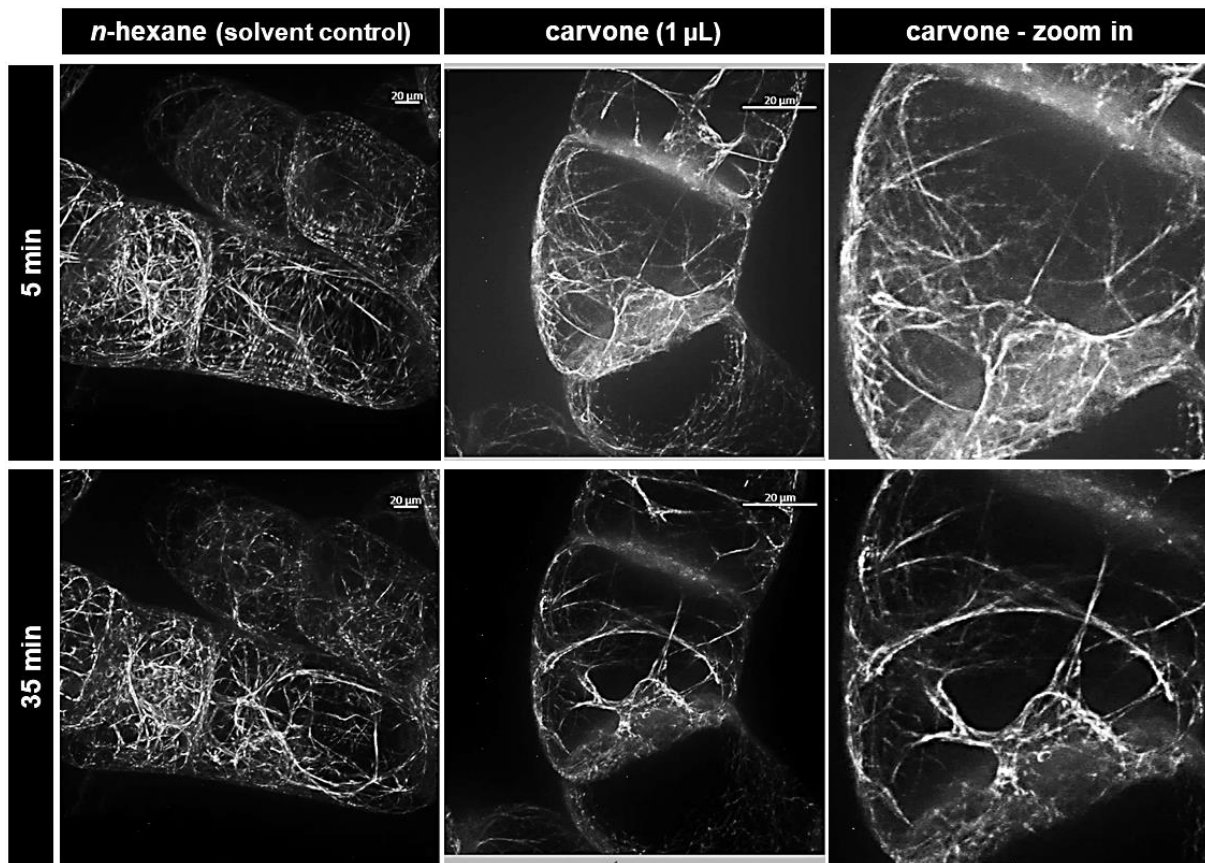


Figure 26: Cellular effect of carvone on actin filaments. Representative BY-2 cells expressing the actin-binding domain 2 of fimbrin fused to GFP followed by spinning disc confocal microscopy after treatment with either 1 μL of *n*-hexane as solvent control or carvone at proliferation phase, day 3 after subcultivation. Images show geometric projections of confocal z-stacks.

Figure 26 demonstrates the cellular effect of carvone, the main compound of *M. spicata* var. *crispa*, on actin filaments *in vivo*. The control was the same as in the previous figure, with no cellular effect on actin filaments. When the cells were exposed to carvone, actin bundling occurred after 5 minutes. Half an hour later, the bundling was enhanced. The effect was similar to *M. spicata* var. *crispa* essential oil but slightly weaker.

4. Results

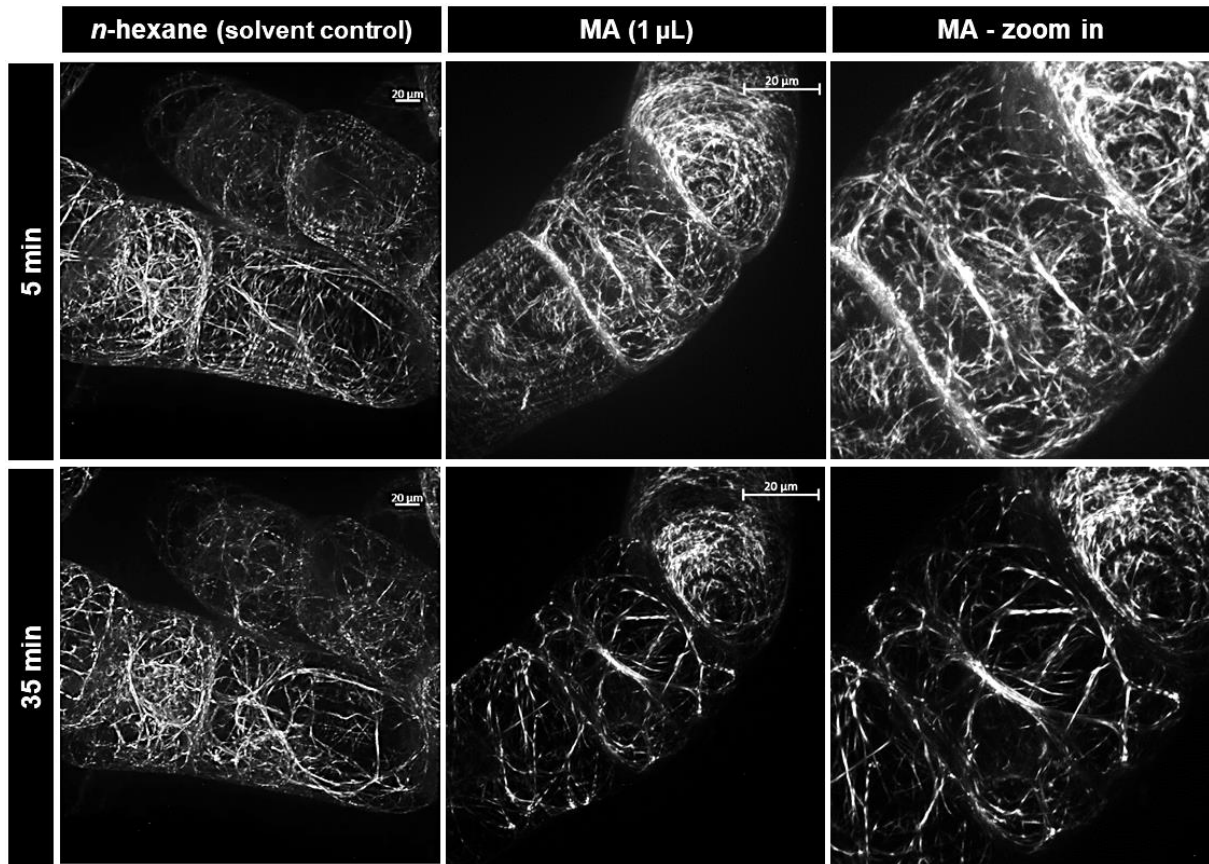


Figure 27: Cellular effect of the essential oil of *M. aquatica* on actin filaments. Representative BY-2 cells expressing the actin-binding domain 2 of fimbrin fused to GFP followed by spinning disc confocal microscopy after treatment with either 1 μL of *n*-hexane as solvent control or essential oil of MA at proliferation phase, day 3 after subcultivation. Images show geometric projections of confocal z-stacks. MA = *M. aquatica*.

Figure 27 shows the time-course live cell imaging with GF11 cells exposed to *M. aquatica* essential oil *in vivo*. The control was the same as in the previous figures, with no cellular effect on actin filaments. After 5 minutes, the actin network was still intact. However, half an hour later, a moderate actin bundling effect could be observed.

4. Results

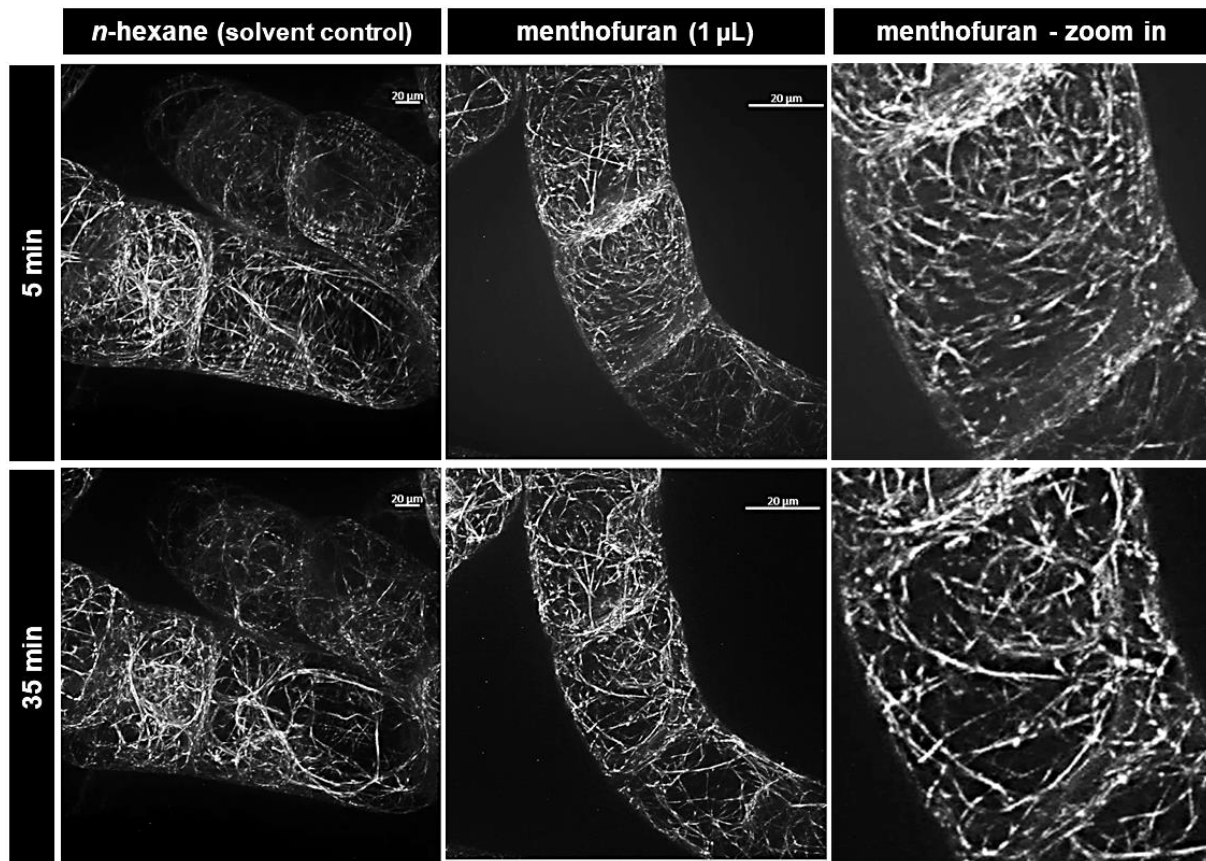


Figure 28: Cellular effect of menthofuran on actin filaments. Representative BY-2 cells expressing the actin-binding domain 2 of fimbrin fused to GFP followed by spinning disc confocal microscopy after treatment with either 1 μL of *n*-hexane as solvent control or menthofuran at proliferation phase, day 3 after subcultivation. Images show geometric projections of confocal z-stacks.

The cellular effect of menthofuran, the main compound of *M. aquatica*, on microtubules *in vivo* is visualized in **Figure 28**. The control was the same as in the previous figures, with no cellular effect on actin filaments. Exposure to menthofuran resulted in almost no cellular response. After 35 minutes, a very slight actin bundling effect could be observed.

To sum up the cellular effects, it could be shown that *M. spicata* var. *crispa* essential oil and its main compound, carvone, have an extremely strong effect on the cytoskeleton, as shown in the live cell imaging time series. It caused complete degradation of the microtubule network and strong actin bundling. For *M. aquatica* essential oil and its main compound, menthofuran, actin bundling was weaker and delayed. Furthermore, in terms of microtubules as targets, the mode of action seems to differ from that of *M. spicata* var. *crispa* essential oil and carvone.

4. Results

M. aquatica essential oil and menthofuran probably led to the disintegration of microtubules, whereas *M. spicata* var. *crispa* essential oil and its main compound, carvone, caused complete degradation. Consequently, microtubules could be the main target of these two essential oils and their main compounds, which appears to be the cause of strong cytotoxicity as well as germination failure.

4.4 Regulation of the monoterpene biosynthesis pathway

4.4.1 Predominant expression of key monoterpene synthases in young leaves and cases of heterochrony

The transcript levels of the key monoterpene synthases limonene-3-hydroxylase (L3H), limonene-6-hydroxylase (L6H), pulegone reductase (PR), and menthofuran synthase (MFS) of *M. aquatica*, *M. x piperita*, and *M. spicata* var. *crispa* were analyzed in leaves of different ages. RNA was extracted, cDNA was synthesized, a semi-qPCR was performed, and finally a qPCR was conducted to quantify the relative expression of the monoterpene synthases to the housekeeping genes 18 S and actin.

4. Results

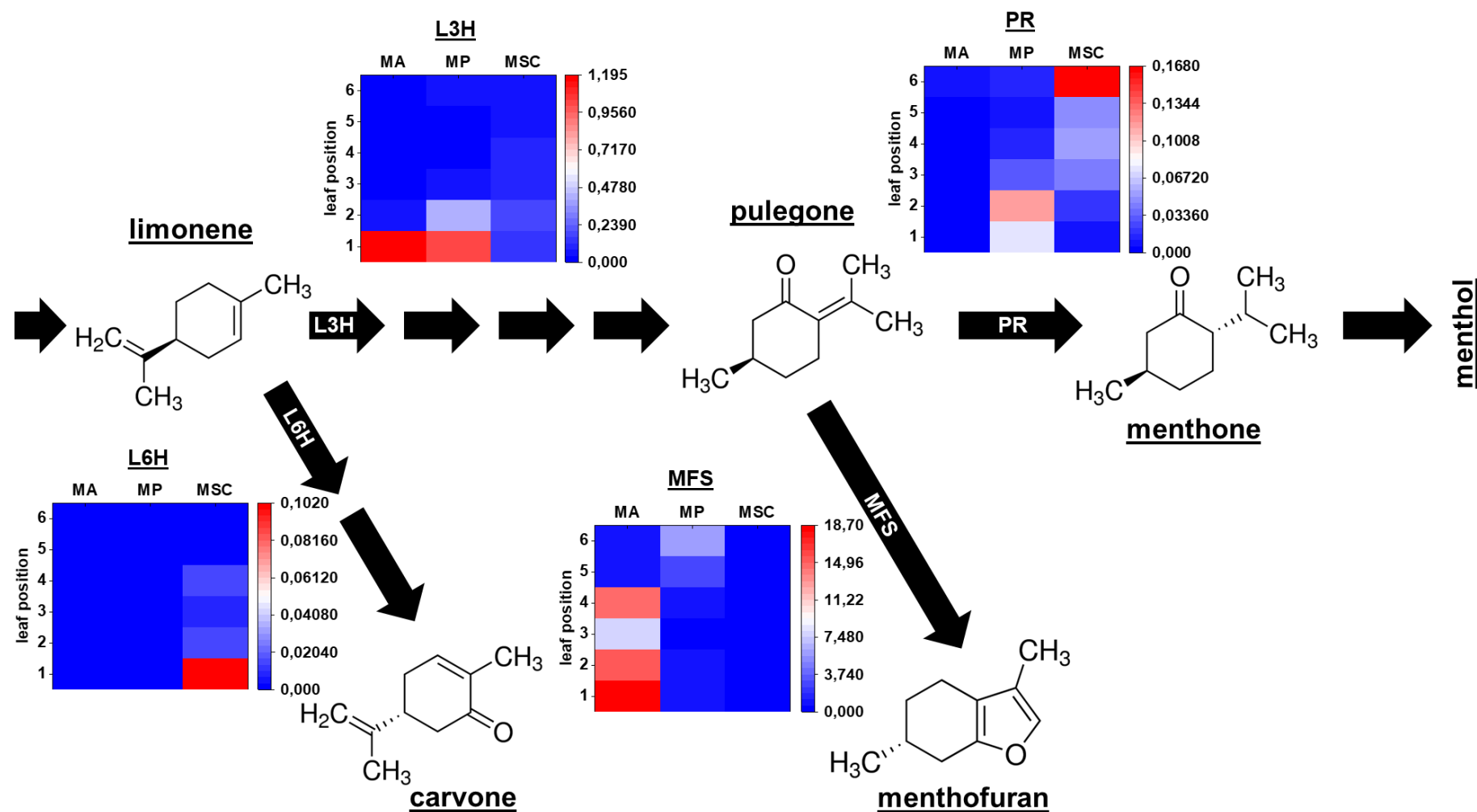


Figure 29: Monoterpene biosynthesis scheme and relative expression of key monoterpene synthases in *Mentha* leaves of different ages. The ct value of each sample was determined using a qPCR approach. The relative expression to the housekeeping genes 18 S and actin was calculated using the $2^{-\Delta ct}$ method according to Livak and Schmittgen (2001). The chemical formula was obtained from sigmaaldrich.com. Each arrow indicates an enzymatic step. L3H = limonene-3-hydroxylase; L6H = limonene-6-hydroxylase; PR = pulegone reductase; MFS = menthofuran synthase.

4. Results

In **Figure 29** the monoterpene biosynthesis pathway is demonstrated. The chemical structures of substrates and products of the relevant branching key monoterpene synthases are illustrated. Each arrow indicates an enzymatic step. Only the key monoterpene synthases (L3H, L6H, PR, and MFS) of interest are shown. The relative expression of L3H, L6H, PR, and MFS in *Mentha* leaves of different ages is represented as heat maps, ranging from low (blue) to moderate (white) to high (red). Leaf one was the youngest, apical leaf, while leaf six was the oldest, basal leaf. The two branching key monoterpene synthases L3H and L6H compete for the same substrate, limonene, and direct the monoterpene pathway towards either carvone or menthol and menthofuran. In general, the relative expression of the two key monoterpene synthases, L3H and L6H, was higher in younger than older leaves, regardless of which *Mentha* species was considered. Relative expression of L3H was abundant in all three *Mentha* species, whereas transcripts of L6H were only found in *M. spicata* var. *crispa*. Here, L6H was relatively expressed with a value of 0.102 (SE \pm 0.088) in the youngest leaf, with decreasing relative expression until no relative expression was detected in the oldest leaf. In addition, for *M. spicata* var. *crispa*, a quite similar relative expression of L3H was determined of 0.127 (SE \pm 0.015) in the youngest leaf and of 0.041 (SE \pm 0.041) in the oldest leaf. In contrast, *M. aquatica* and *M. x piperita* showed much higher relative expressions of 1.194 (SE \pm 0.704) and 1.010 (SE \pm 0.701) in the youngest leaf, which decreased to 0.008 (SE \pm 0.008) and 0.052 (SE \pm 0.006) in the oldest leaf. Moreover, the relative expression of two other branching key monoterpene synthases, namely PR and MFS, was analyzed. These two compete for pulegone as a substrate to enzymatically catalyze menthone or menthofuran. *M. aquatica* showed a very high relative expression of MFS of 18.675 (SE \pm 8.917) in the youngest leaf compared with 0.972 (SE \pm 0.972) in the oldest leaf, which was almost the same relative expression determined for L3H in the youngest leaf of 1.194 (SE \pm 0.704). On the contrary, the relative expression of PR in *M. aquatica* was very low in a young developmental stage but increased slightly with age, reaching a relative expression of 0.010 (SE \pm 0.010) in the sixth leaf. MFS of *M. x piperita* was relatively more expressed in older leaves, e.g., in the sixth leaf with 5.964 (SE \pm 5.964), than in younger leaves, e.g., in the first leaf with 1.130 (SE \pm 0.607). In contrast, the relative expression of PR of *M. x piperita* was higher in younger than in older leaves, but still low values were obtained, e.g., the relative expression in the first leaf was 0.073 (SE \pm 0.006) and in the sixth leaf 0.014 (SE \pm 0.014).

4. Results

In *M. spicata* var. *crispa*, the relative expression of MFS was very low and present only in the youngest leaf with a value of 0.003 (SE \pm 0.003), while a relative expression of PR of 0.006 (SE \pm 0.002) was detected in the youngest leaf, increasing to 0.168 (SE \pm 0.085) in the oldest leaf.

To summarize, the key monoterpene synthases were predominantly expressed at an early developmental stage of a leaf. A pattern could be discerned that within a *Mentha* species, monoterpene synthases competing for the same substrate were differentially expressed at different developmental stages. Moreover, a single monoterpene synthase, e.g., PR, may be expressed at different stages of leaf development in the various *Mentha* species, indicating heterochrony.

4.4.2 Temporal expression pattern correlates with the metabolite level

For qualitative analysis of monoterpenes in *Mentha* leaves of different ages, a solid phase microextraction (SPME) with GC-MS was performed.

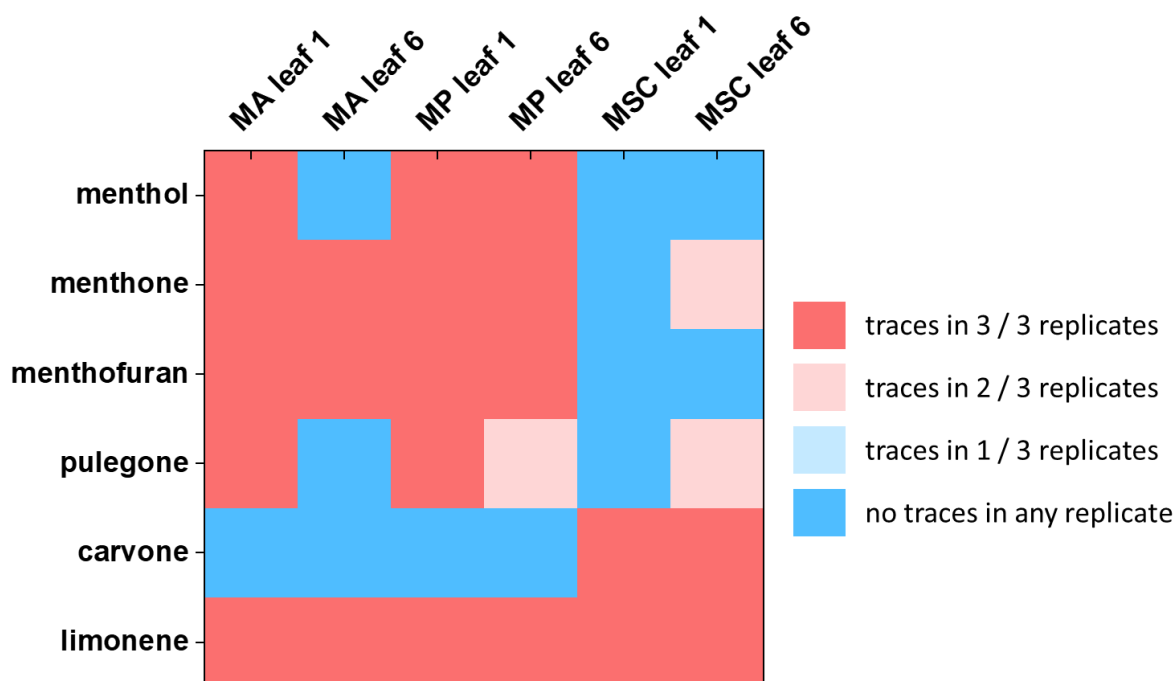


Figure 30: Heatmap of the abundance of traces of compounds in the youngest and oldest leaves of the three *Mentha* species detected by SPME GC-MS. The number of times that traces of a compound were detected in the three biological replicates of the freeze-dried leaf samples is indicated by a color code, ranging from blue (= no traces) to red (traces in 3 / 3 replicates). MA = *M. aquatica*; MP = *M. x piperita*; MSC = *M. spicata* var. *crispa*.

4. Results

Figure 30 shows a heatmap visualizing the abundance of traces of several compounds in the first and sixth leaf of the three *Mentha* species detected by SPME GC-MS. The abundance of traces in three biological replicates is illustrated by a color code. Limonene, the precursor for all monoterpenes, was abundant in all leaf samples examined, regardless of which *Mentha* species was considered. Carvon was found exclusively in the leaves of *M. spicata* var. *crispa*, independent of age. In addition, the sixth leaf of *M. spicata* var. *crispa* contained traces of pulegone and menthone in two out of three replicates. Both compounds were also detected in the leaves of *M. aquatica* and *M. x piperita*. In contrast to *M. spicata* var. *crispa*, these monoterpenes even occurred in all three replicates of the first leaf. Furthermore, in both species, traces of menthone were found in all three replicates of the sixth leaf as well. Traces of pulegone could be determined in two out of three replicates for *M. x piperita* compared to *M. aquatica*, where no traces were found in the sixth leaf. Traces of menthol were found in all three replicates of *M. x piperita*, independent of leaf age. In contrast, in the leaves of *M. aquatica*, the abundance of traces of menthol decreased from abundance in all replicates of the first leaf to none in the sixth leaf. Moreover, traces of menthofuran were detected in all three replicates of leaves of *M. aquatica* and *M. x piperita*, independent of leaf age.

In conclusion, the chemical profile of *M. spicata* var. *crispa* differed greatly from that of the chemically closely related *Mentha* species *M. aquatica* and *M. x piperita*. Moreover, the developmental stage of the leaf played a role in some cases.

4.4.3 Predicted promoter motifs suggest interaction with abiotic factors and various phytohormones

To get a more comprehensive view of the regulation of the key monoterpene synthases PR and MFS of *M. aquatica*, *M. x piperita*, and *M. spicata* var. *crispa*, the promoter regions were investigated. Upstream regions were cloned from DNA samples. The sequences obtained were analyzed *in silico* with PLANTCare (Lescot *et al.*, 2002), a database of cis-acting regulatory elements in plants. All predicted promoter motifs, which were present in the two promoters considered, are demonstrated. For clarity, the many predicted binding sites for MYC- and MYB-transcription factors with unknown downstream functions and other light responsive elements were omitted.

4. Results

Promoter motifs of PR

PR upstream – *M. aquatica*

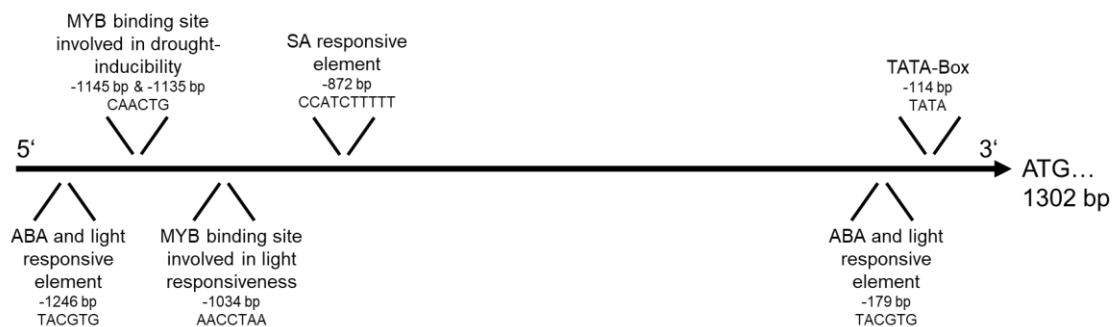


Figure 31: Predicted promoter motifs of PR of *M. aquatica*. Upstream sequence of the interested key monoterpene synthase gene was cloned, and motifs were analyzed *in silico* with PLANTCare (Lescot *et al.*, 2002), a database of plant cis-acting regulatory elements. The promoters and their motifs are drawn to scale.

In **Figure 31** predicted promoter motifs of PR of *M. aquatica* are shown with their sequence and position in 5' - 3' sequence orientation to scale. From 5'-end following motifs were found: an abscisic acid (ABA) and light responsive element at -1246 bp with the sequence TACGTG, a MYB-binding site involved in drought-inducibility at -1145 bp and at -1135 bp with the sequence CAACTG, a MYB-binding site involved in light responsiveness at -1034 bp with the sequence AACCTAA, a salicylic acid (SA) responsive element at -872 bp with the sequence CCATCTTTTT, again an ABA and light responsive element at -179 bp with the same sequence TACGTG as the previous one, and the TATA-Box at -114 bp immediately before the transcription start.

PR upstream – *M. x piperita* and *M. spicata* var. *crispa*

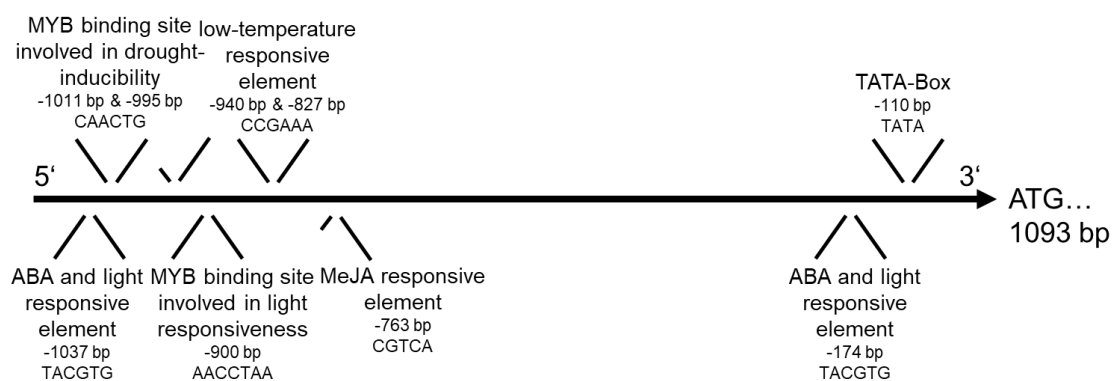


Figure 32: Predicted promoter motifs of PR of *M. x piperita* and *M. spicata* var. *crispa*. Upstream sequences of the interested key monoterpene synthase gene were cloned, and motifs were analyzed *in silico* with PLANTCare (Lescot *et al.*, 2002), a database of plant cis-acting regulatory elements. The promoters and their motifs are drawn to scale.

4. Results

Figure 32 presents the predicted promoter motifs of PR of *M. x piperita* and *M. spicata* var. *crispa* with their sequence and position in 5' - 3' sequence orientation to scale. The two analyzed sequences of the two *Mentha* species yielded completely identical motifs at the same position. From 5'-end following motifs were found: an abscisic acid (ABA) and light responsive element at -1037 bp with the sequence TACGTG, a MYB-binding site involved in drought-inducibility at -1011 bp and at -995 bp with the sequence CAACTG, a MYB-binding site involved in light responsiveness at -900 bp with the sequence AACCTAA, a low-temperature responsive element at -940 bp and at -827 bp with the sequence CCGAAA, a methyl jasmonate (MeJA) responsive element at -763 bp with the sequence CGTCA, again an ABA and light responsive element at -174 bp with the same sequence TACGTG as the previous one, and the TATA-Box at -110 bp immediately before the transcription start.

To summarize, motifs indicating a response to abiotic factors such as drought and light were found in all PR promoters regardless of which *Mentha* species was investigated, while low-temperature responsive elements could only be determined in the promoters of *M. x piperita* and *M. spicata* var. *crispa*. All *Mentha* species show interaction with the phytohormone ABA. Moreover, *M. aquatica* seems to respond to SA, while *M. x piperita* and *M. spicata* var. *crispa* are more likely to respond to MeJA, as the respective motifs were found in their promoters. In addition, the promoter of *M. x piperita* was identical to that of *M. spicata* var. *crispa*.

Promoter motifs of MFS

MFS upstream – *M. aquatica*

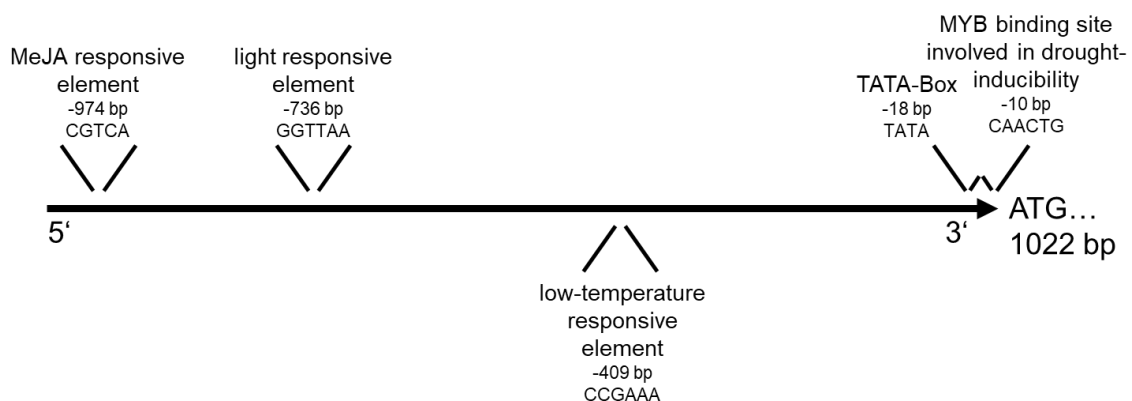


Figure 33: Predicted promoter motifs of MFS of *M. aquatica*. Upstream sequence of the interested key monoterpene synthase gene was cloned, and motifs were analyzed *in silico* with PLANTCare (Lescot *et al.*, 2002), a database of plant cis-acting regulatory elements. The promoters and their motifs are drawn to scale.

4. Results

Figure 33 shows the predicted promoter motifs of MFS of *M. aquatica* with their sequence and position in 5' - 3' sequence orientation to scale. From 5'-end following motifs were found: a MeJA responsive element at -974 bp with the sequence CGTCA, a light responsive element at -736 bp with the sequence GGTTAA, a low-temperature responsive element at -409 bp with the sequence CCGAAA, the TATA-Box at -18 bp, and a possible MYB-binding site involved in drought-inducibility at -10 bp with the sequence CAACTG immediately before the transcription start.

MFS upstream – *M. x piperita*

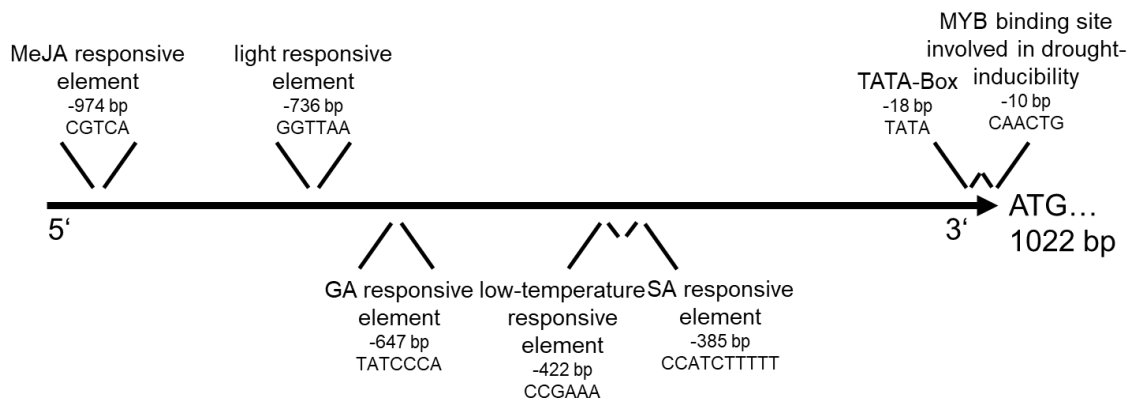


Figure 34: Predicted promoter motifs of MFS of *M. x piperita*. Upstream sequence of the interested key monoterpene synthase gene was cloned, and motifs were analyzed *in silico* with PLANTCare (Lescot *et al.*, 2002), a database of plant cis-acting regulatory elements. The promoters and their motifs are drawn to scale.

In **Figure 34** the predicted promoter motifs of MFS of *M. aquatica* are demonstrated with their sequence and position in 5' - 3' sequence orientation to scale. From 5'-end following motifs were found: a MeJA responsive element at -974 bp with the sequence CGTCA, a light responsive element at -736 bp with the sequence GGTTAA, a gibberellic acid (GA) responsive element at -647 bp with the sequence TATCCCA, a low-temperature responsive element at -422 bp with the sequence CCGAAA, a SA responsive element at -385 bp with the sequence CCATCTTTTT, the TATA-Box at -18 bp, and a possible MYB-binding site involved in drought-inducibility at -10 bp with the sequence CAACTG immediately before the transcription start.

4. Results

MFS upstream – *M. spicata* var. *crispa*

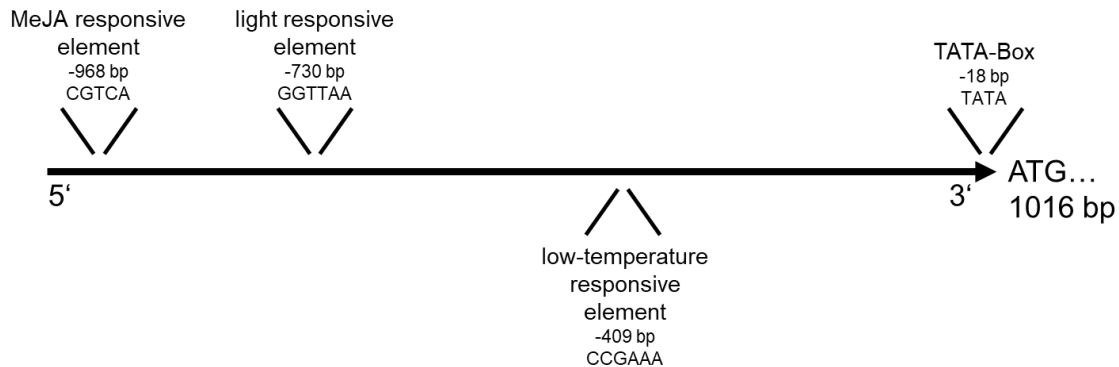


Figure 35: Predicted promoter motifs of MFS of *M. spicata* var. *crispa*. Upstream sequence of the interested key monoterpene synthase gene was cloned, and motifs were analyzed *in silico* with PLANTCare (Lescot *et al.*, 2002), a database of plant cis-acting regulatory elements. The promoters and their motifs are drawn to scale.

Figure 35 illustrates the predicted promoter motifs of MFS of *M. spicata* var. *crispa* with their sequence and position in 5' - 3' sequence orientation to scale. From 5'-end following motifs were found: a MeJA responsive element at -968 bp with the sequence CGTCA, a light responsive element at -730 bp with the sequence GGTTAA, a low-temperature responsive element at -409 bp with the sequence CCGAAA, and the TATA-Box at -18 bp immediately before the transcription start.

In conclusion, all *Mentha* species contained motifs in the MFS promoter indicating that they respond to abiotic factors such as light and low temperatures. Additionally, *M. aquatica* and *M. x piperita* had a MYB-binding site involved in drought-inducibility. Furthermore, all *Mentha* species seem to respond to MeJA, while *M. x piperita* appears to have additional specific responses to SA and GA. Compared to the PR promoter, there is probably no interaction with ABA within all the analyzed *Mentha* species.

All in all, the PR and MFS promoters were quite similar. Both promoters indicated a possible interaction with different abiotic factors and various phytohormones, including some specific motifs that could be either assigned to the PR or MFS promoter or to a certain *Mentha* species.

4. Results

4.5 Localization of MFS of all three *Mentha* species in the ER

The transcript of the MFS of *M. spicata* var. *crispa* was found, but the metabolite was absent. Moreover, the evolutionary distance of its sequence and the rather different protein structure compared to the other two *Mentha* species, *M. aquatica* and *M. x piperita*, indicate that this gene has already diversified in a different evolutionary direction and probably adopted a new function. In addition, two amino acid changes were detected in the transmembrane domain, suggesting that the localization may have been altered. Therefore, a localization study was conducted *in vivo* using fusion proteins with a fluorescent marker. For this approach, the coding sequence of MFS of *M. aquatica*, *M. x piperita*, and *M. spicata* var. *crispa* was fused to GFP. For this approach, each coding sequence of MFS was cloned into an expression vector carrying the coding sequence for GFP via Gateway® Technology using the Clonase™ II system. The vector was first transformed into *A. tumefaciens* using a freeze-thaw transformation protocol and later into *N. tabacum* L. cv Bright Yellow-2 cells using a protocol for stable transformation. To verify the overexpression of the transgenic cell lines, RNA was extracted, cDNA was synthesized, and quality control was done by semi-qPCR, followed by qPCR to quantify the expression of MFS in the different cell lines (appendix, **Figure 44**). To finally localize the MFS of the three *Mentha* species in each transgenic cell line, spinning disc confocal microscopy was performed using a 3-day-old, mitotically highly active cell culture. A colocalization study was conducted using 1 µM ER-Tracker™ Red.

4. Results

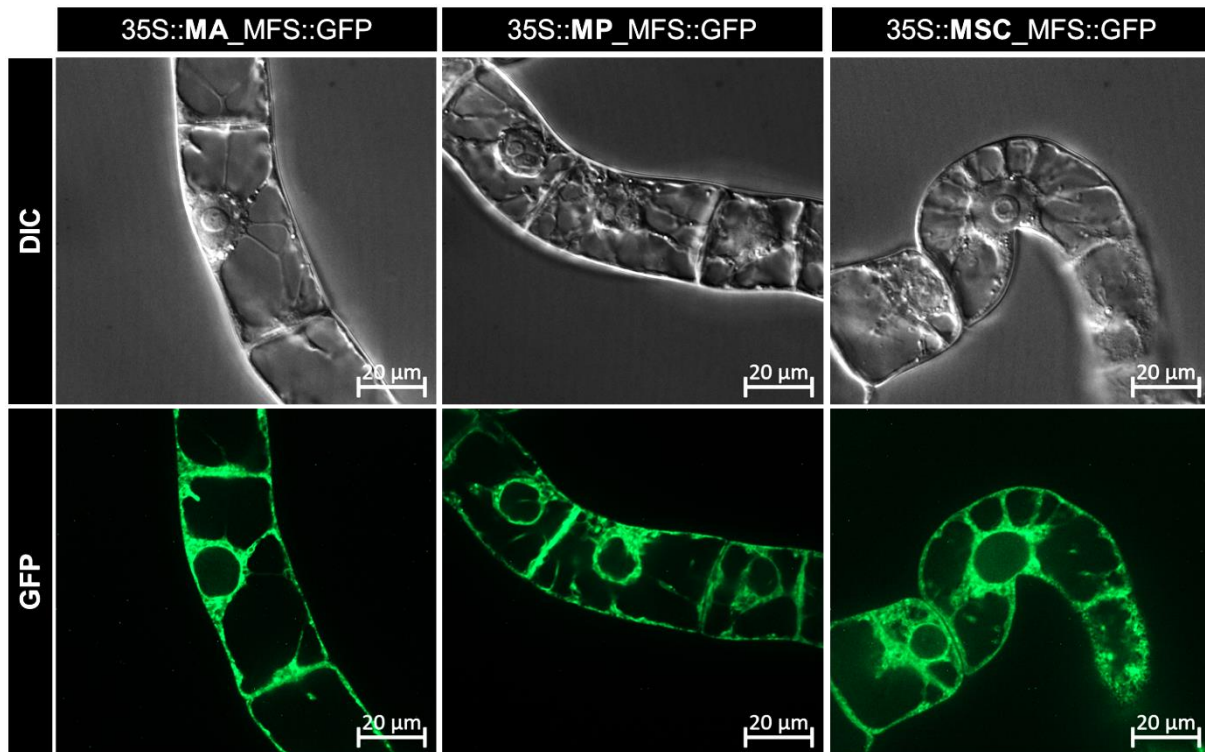


Figure 36: Localization of MFS in the three established transgenic BY-2 tobacco cell lines. Representative BY-2 cells expressing the gene of MFS of different *Mentha* species fused to GFP under the control of the cauliflower mosaic virus (CaMV) 35S promoter were visualized by spinning disc confocal microscopy on day 3 after subcultivation. Differential interference contrast (DIC) as well as the GFP channel are shown.

Live cell imaging was performed *in vivo* to localize the MFS of the three different *Mentha* species. The transgenic cell lines were named according to which *Mentha* species the MFS originated from, e.g., 35S::MA_MFS::GFP is a transgenic BY-2 tobacco cell line expressing MFS of *M. aquatica* fused to GFP under the control of the cauliflower mosaic virus (CaMV) 35S promoter. In the DIC channel, it is visible that the cells were healthy and intact. It could be excluded that MFS is located in the nucleus or the vacuole because, in all three transgenic cell lines, a reticular structure was found in the cytosol. This indicates that MFS occurs in the endoplasmic reticulum (ER).

4. Results

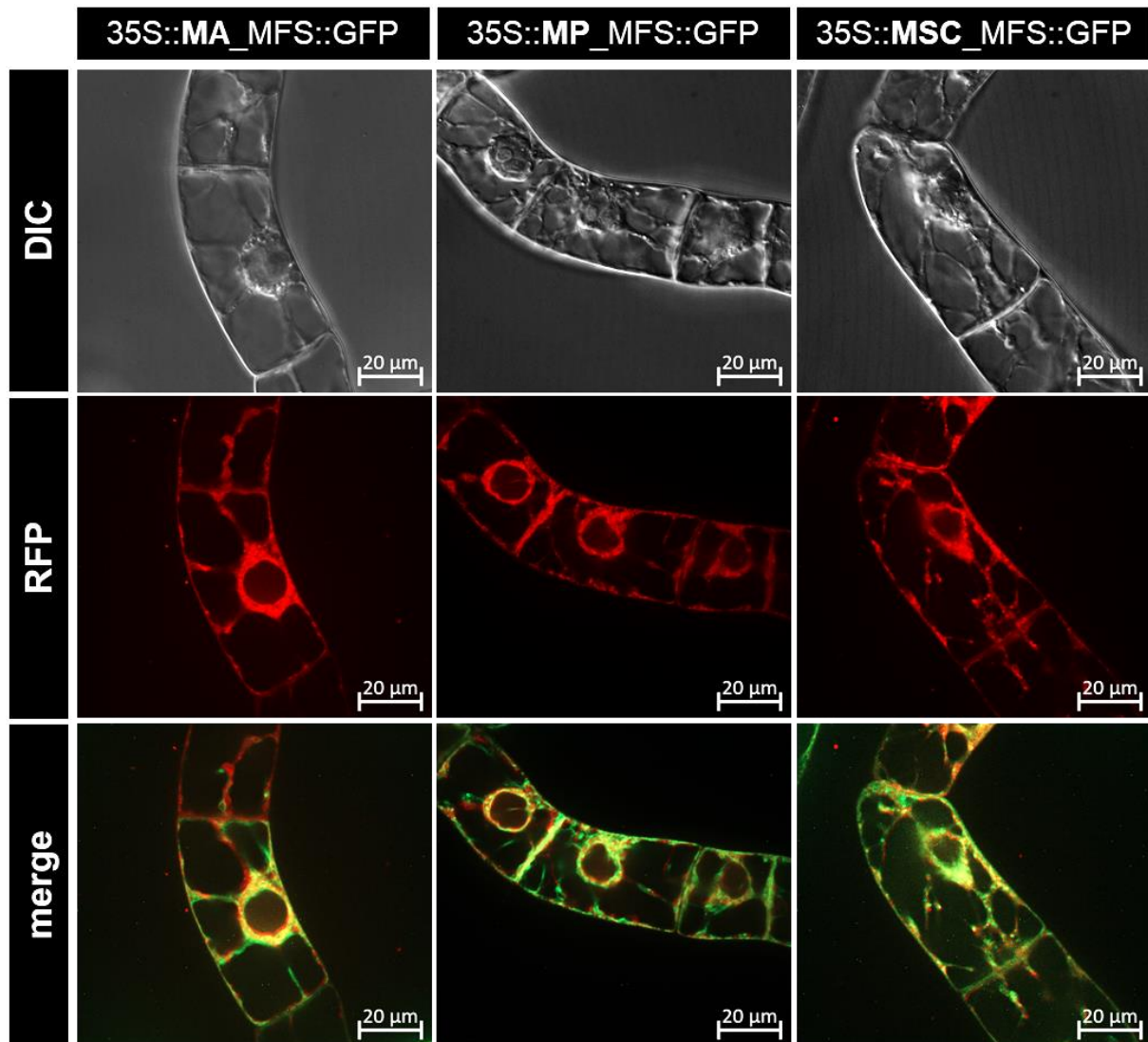


Figure 37: Colocalization study of MFS of the three transgenic BY-2 tobacco cell lines with the ER-Tracker™ Red. BY-2 cells expressing the MFS of different *Mentha* species fused to GFP under the control of the cauliflower mosaic virus (CaMV) 35S promoter were stained with 1 µM ER-Tracker™ Red to investigate the colocalization with the ER. Representative BY-2 cells were visualized by spinning disc confocal microscopy on day 3 after subcultivation. Differential interference contrast (DIC), RFP, and the merge channel of RFP with GFP are shown.

To verify the localization of the MFS of three different *Mentha* species in the ER, a colocalization study with the ER-Tracker™ Red was conducted. In the DIC channel, it can be seen that the cells were healthy and intact. In the RFP channel, the ER is visualized. An overlay of the GFP channel, where the fluorescence of the GFP-tagged MFS of each transgenic cell line was observed, with the RFP channel resulted in yellowish structures, indicating a colocalization of the MFS with the ER.

In conclusion, no differences in localization could be detected. The MFS of all three *Mentha* species was present in the ER.

4. Results

4.6 Summary of results

Phylogenetic studies of *Mentha* species

- Species authentication based on floral traits with determination keys as well as genetic barcoding is essential to having a reliable foundation for statements.
- *M. x piperita* is a hybrid derived from *M. aquatica* and *M. spicata* var. *crispa*.
- *M. spicata* var. *crispa* was identified as the mother of *M. x piperita* because of the higher sequence similarity of the plastid barcoding marker *ycf1b*.
- A phylogenetic tree based on PR sequences revealed that *M. aquatica* and *M. x piperita* are very closely related in this trait, but a further analysis elucidated that *M. aquatica* and *M. spicata* var. *crispa* showed the lowest relative substitution rate based on exon and amino acid level.
- The 3D protein structures of PR did not differ greatly among the three *Mentha* species, with those of *M. aquatica* and *M. spicata* var. *crispa* being almost identical.
- MFS of *M. aquatica* and of *M. x piperita* are phylogenetically very closely related, which was confirmed by a low relative substitution rate on every sequence level investigated compared to *M. spicata* var. *crispa*.
- The most similar 3D protein structures of MFS were determined for *M. aquatica* and *M. x piperita*, whereas that of *M. spicata* var. *crispa* differed greatly.

Elucidation of chemical profiles of closely related *Mentha* species

- All *Mentha* species had unique chemical profiles in a non-additive manner.
- Menthofuran was the main compound of *M. aquatica* and *M. x piperita*. In addition, *M. x piperita* had a high amount of menthol. *M. spicata* var. *crispa* was chemically more distant, with carvone as the main compound.

Bioactivity studies

- Carvone seems to mainly attack microtubules until complete degradation and leads to strong actin bundling. This could be the cause of strong cytotoxicity in BY-2 tobacco cells and dose-dependent germination inhibition in certain weeds.

4. Results

- Compared with carvone, menthofuran exerted a weaker, different, and delayed mode of action by probably leading to the disintegration of microtubules and only slight actin bundling. Moreover, a lower cytotoxicity was determined, and higher concentrations were always required to achieve a similar germination-inhibiting effect on weeds as carvone.
- Both compounds, carvone and menthofuran, were more efficient and persistent in poppy compared to cress, indicating specificity.
- The mode of action was represented by the essential oils, from which the compounds were derived.

Regulation of the monoterpene biosynthesis pathway

- Monoterpene synthases appeared to be predominantly expressed in the early developmental stage of a leaf.
- The gene expression of monoterpene synthases can vary within a species, i.e., branching enzymes that compete for a common substrate were expressed at different developmental stages.
- The gene expression of a single monoterpene synthase can vary between species, i.e., the same monoterpene synthase of different *Mentha* species might be expressed at different stages of leaf development, indicating heterochrony.
- The gene expression pattern of monoterpene synthases correlated with the metabolite level, with an exception for MFS of *M. spicata* var. *crispa*.
- The promoters of PR and MFS of the different *Mentha* species were, in general, quite similar. There was evidence for interactions with abiotic factors and phytohormones.
- Some minor, interspecific differences in the promoter motifs as well as between the PR and MFS promoters were determined, allowing specific regulation of gene expression.

Localization of the MFS

- The MFS of all three *Mentha* species occurred in the ER.

5. Discussion

5.1 Is the species being examined the one it claims to be?

Hybridization events followed by fusion of unreduced gametes or duplication of genomes have happened many times in the plant kingdom, resulting in polyploid and viable offspring. It is a common mechanism for plants to adapt to their environment. In addition, a plant hybrid may have a similar phenotype to its parental species but be genetically related to a different species (Tate *et al.*, 2005). All this leads to difficulties in species delimitation and thus complicates the problems of systematics and phylogenetics. Therefore, verifying the identity of model organisms is crucial, especially when hybridization events are common in a species such as in the mints. Therefore, an authentication study was conducted for the different *Mentha* species analyzed, using morphology-based determination keys and different nuclear and plastid barcoding markers. Using different determination keys, all *Mentha* species could be confirmed, except 7580 *M. suaveolens*, which could not be assigned to this species because its morphological characteristics belong to another species, *M. arvensis*. Moreover, the limitations of determination keys quickly became apparent, as cultivars or varieties were often not described.

Hence, an additional phylogenetic authentication approach was performed using the nuclear barcoding marker ITS AB, which flanks the region of ITS1, 5.8 S, ITS2 between the ribosomal subunits 18 S and 26 S in plants (Blattner 1999), and the plastid barcoding marker *ycf1b*, which encodes a protein that is essential for the TIC complex in plastids containing highly variable small single copy and the conserved inverted repeat regions (Dong *et al.*, 2015). Two additional plastid barcoding markers, *rbcLa* and *psbA - trnH*, were analyzed, but the sequence differences were not big enough to allow precise differentiation of the mints (see appendix, **Figure 41** and **Figure 42**). Therefore, conclusions were only drawn by comparing the phylogenetic trees of ITS AB and *ycf1b*, where high relative base substitution rates were abundant, indicating that evolution has led to species-specific variation in these two markers within *Mentha*.

The comparative approach of nuclear and plastid barcoding markers allows assumptions to be made about possible hybrids and their parental species, including whether they belong to the maternal or paternal part.

5. Discussion

Nuclear barcoding markers can elucidate the parental origin of hybrids, while plastid markers only identify the maternal ancestor. This is due to the fact that plastids are primarily maternally inherited (Hagemann and Schröder, 1989). However, recent studies showed that paternal inheritance of plastids is also possible in some species under specific environmental conditions, allowing rapid adaptation (Chung *et al.*, 2023). Since the sampling for this study was done under normal conditions and there is no available information within the *Mentha* species, paternal inheritance was excluded. Therefore, the small evolutionary divergence of the *ycf1b* gene between two species is assumed to be due to maternal linkage, which is more evident for *M. x piperita* and *M. spicata* var. *crispa* than for *M. x piperita* and *M. aquatica*. This suggests that *M. spicata* var. *crispa* represents the maternal part of this hybrid.

Based on morphological characteristics and basic chromosome number, five sections for the genus *Mentha* have been classified: *Audibertia*, *Eriodontes*, *Preslia*, *Pulegium*, and *Mentha*, whereas the section *Mentha* is taxonomically the most complex one (Harley and Brighton, 1977). All species used in this study belong to this section. It was verified that the mints are a monophyletic group within the Lamiaceae family, which has already been confirmed in a previous phylogenetic study using genetic barcoding and fingerprinting (Gobert *et al.*, 2006).

Within this monophylum, the *Mentha* species were divided into two clusters based on the nuclear and plastid barcoding markers. Cluster one contains *M. canadensis*, *M. longifolia*, *M. spicata* and its variety, *M. x piperita*, *M. rotundifolia* cv. *variegata*, *M. suaveolens*, and *M. spec.*, and cluster two includes *M. arvensis* and *M. aquatica*. However, there were two discrepancies. The first is that in the phylogenetic tree based on the nuclear barcoding marker ITS AB, 9617 *M. arvensis* was present in the first cluster. This could be due to pseudogenes that can appear in allopolyploid species, because if only the plastid region *ycf1b* was considered, 9617 *M. arvensis* belonged to cluster two, as expected. The second is that 7580 *M. suaveolens* occurs in cluster two for both markers, which was unexpected for this species. Considering the morphological characters more consistent with *M. arvensis* and the results of genetic barcoding, where 7580 clustered with *M. arvensis*, it is assumed that this species is not *M. suaveolens* but *M. arvensis* or a cultivar thereof.

5. Discussion

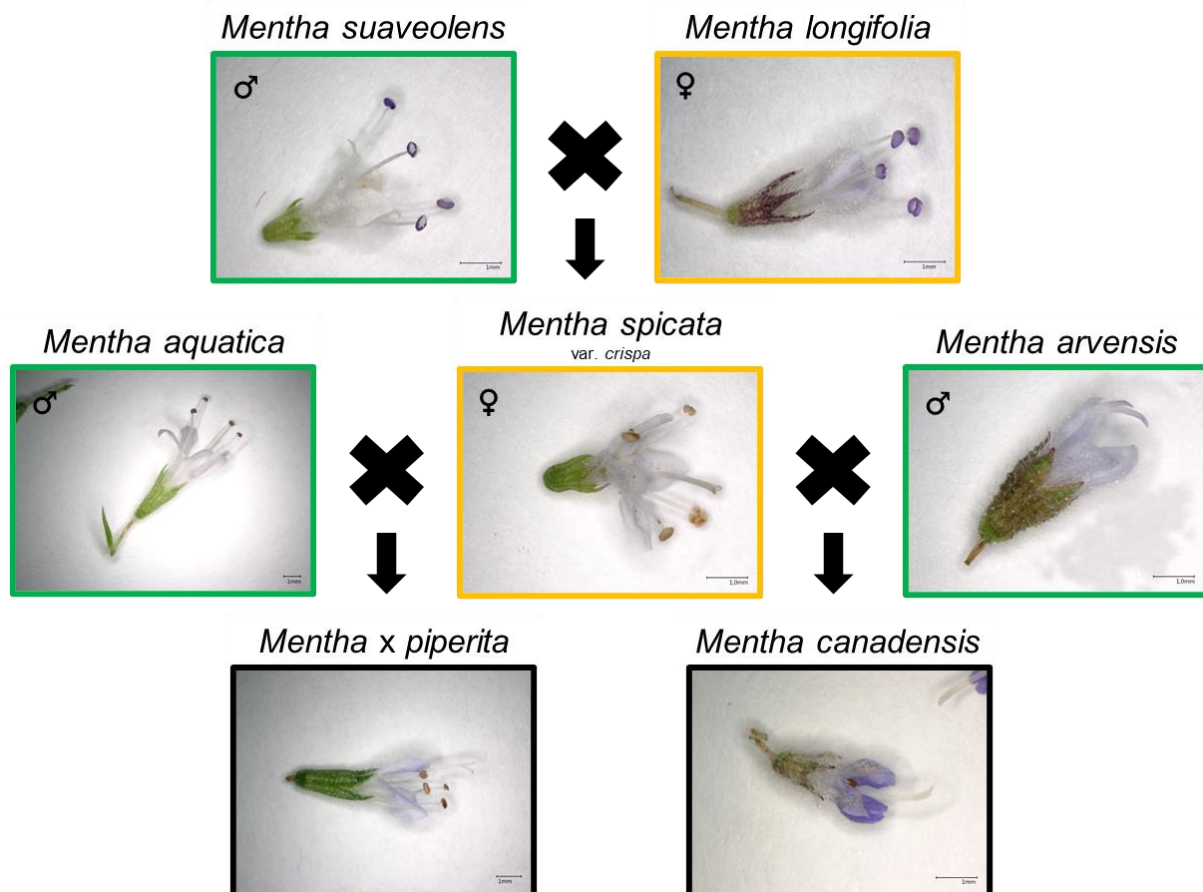


Figure 38: Phylogeny and flower morphology within the *Mentha* genus. The color code and gender symbol indicate the assumed parental role of a hybrid. Yellow demonstrates maternal part, green paternal part, black hybrid. The flower images were taken using the Keyence microscope. Scale 1 mm. The assumed phylogeny of some *Mentha* hybrids is illustrated in **Figure 38**. The phylogenetic analysis of several barcoding markers confirms that *M. x piperita* is a hybrid of *M. aquatica* as the paternal and *M. spicata* var. *crispa* as the maternal part. In addition, the species from which this cultivar is derived is a hybrid of *M. longifolia* as maternal and *M. suaveolens* as paternal part. This is consistent with a study based on plastid barcoding markers in which *M. longifolia* was also found as the maternal part of *M. spicata* (Bunsawat *et al.*, 2004). *M. spicata* further hybridized with *M. arvensis* and gave rise to the new species *M. canadensis*. Here, the results are incongruent with Bunsawat *et al.* (2004), who suggested *M. arvensis* as the maternal part of the hybrid. This species is located in a different cluster than the hybrid in the phylogenetic tree based on *ycf1b*, which strengthens the hypothesis that it is here rather the paternal part of *M. canadensis*. Furthermore, the floral morphology of a hybrid appears to be derived from the paternal part and can therefore be assigned to a certain gender. This suggests that the floral traits of a hybrid are anchored in nuclear DNA rather than plastid DNA and that the floral phenotype is mainly controlled by male genetics.

5. Discussion

5.2 How could such a chemical diversity arise within a single genus?

To understand how such a chemical diversity could arise within a single genus, three closely related but chemically diverse *Mentha* species were selected as model organisms for the investigation of their chemical evolution, namely the hybrid species *M. x piperita* and its parents *M. aquatica* and *M. spicata* var. *crispa*.

First, the chemical profiles of these species were analyzed by GC-MS to confirm differences in chemistry. A closer chemical relationship was found between *M. aquatica* and *M. x piperita*, as both contained menthofuran as their main compound, although the abundance in *M. x piperita* (22 - 27 %) was lower than in *M. aquatica* (73 - 83 %). In addition, *M. x piperita* included menthol (10 - 26 %) as a second main compound. Carvone was only present in the essential oil of *M. spicata* var. *crispa* (28 - 50 %) and represents the main compound of this species. These compounds have also been found by Lange Laboratory (2014 – 2021) to be the main compounds of the three *Mentha* species, albeit in different quantities. Furthermore, several compounds were unique to a species, and some compounds were detected in two species or even in all species. Nevertheless, the hybrid *M. x piperita* has not inherited all compounds in an additive manner. It has evolved a new, unique chemical profile.

This raises the question, “How?” To answer this question, a phylogenetic study was performed using two exemplary important monoterpene synthases that control the metabolic flux to various compounds to determine whether sequence differences in an enzyme could be a possible driver of new functions and thus different chemistry. The first enzyme studied is pulegone reductase (PR), which uses pulegone as a substrate and reduces it to menthone, which can be further catabolized to menthol (Croteau *et al.*, 2005), one of the main compounds of *M. x piperita*. The second enzyme investigated is menthofuran synthase (MFS), which catabolizes the reaction of pulegone to menthofuran (Croteau *et al.*, 2005), the main compound present in *M. aquatica* and *M. x piperita*. These two enzymes use the same substrate but guide the metabolic flux in different directions and are therefore an essential branch point within monoterpene biosynthesis to create chemical diversity. The coding sequences of both enzymes of *M. x piperita* and *M. aquatica* were found to cluster together in a phylogenetic tree, whereas *M. spicata* var. *crispa* forms a monophyletic group. This supports the closer chemical relationship between *M. x piperita* and *M. aquatica*, both of which contain the metabolite menthofuran in their essential oils.

5. Discussion

However, menthone and menthol were only found in *M. x piperita*, suggesting that regulatory mechanisms are involved at this branch point. The very high content of menthofuran in *M. aquatica* could explain why no menthone or menthol were abundant. The MFS is very active in this species and uses the entire substrate for menthofuran production. Therefore, no pulegone remains that could be catabolized by the competing PR to produce the other compounds. In the hybrid *M. x piperita*, the abundance of menthofuran was lower, leading to the assumption that some pulegone can still be used by PR to produce the commonly known main compound menthol of *M. x piperita*. Due to the close phylogenetic relationship and very similar coding sequences of the two enzymes within the two mints, it cannot be excluded that one of the enzymes has evolved into a less productive variant. Consequently, the enzyme activity must be controlled in some way. One possibility could be regulation at the transcript level. This was confirmed by Mahmoud and Croteau (2003), who showed that menthofuran itself acts as a negative regulator of PR and downregulates its transcript level. Since the amount of the negative regulator menthofuran is lower in *M. x piperita*, this could be the reason for the abundance of menthol as a second main compound. Furthermore, the MFS of *M. aquatica* and *M. x piperita* appeared to be more closely related than the competing PR. This was supported by lower relative substitution rates at each sequence level. For example, the relative substitution rate on exon level of *M. aquatica* and *M. x piperita* for MFS was 0.27 % (4 SNPs in 1482 bp) compared to 0.49 % (5 SNPs in 1029 bp) for PR. In addition, the introns of MFS of *M. aquatica* and *M. x piperita* were completely identical, resulting in a single cluster of DNA and coding sequences of *M. aquatica* and *M. x piperita* in the phylogenetic tree based on MFS sequences. This suggests, first, that the evolutionary distance between the two *Mentha* species is very small with respect to this enzyme, and second, that the MFS is subject to high selection pressure that allows only minor variation since both species contain the metabolite menthofuran in their essential oil, which is produced by this enzyme. In contrast, the PR DNA sequences of *M. aquatica* formed a monophyletic group within the phylogenetic tree. This could be explained by highly divergent PR intron sequences compared to the other two species. It suggests continuous variation in this trait of *M. aquatica*, which could be easily established due to low selection pressure. A factor contributing to this low selection pressure could be that *M. aquatica* does not necessarily need the metabolites produced by PR for survival and therefore suppresses its expression, enabling variations to be established.

5. Discussion

As mentioned earlier, *M. spicata* var. *crispa* formed a monophyletic group in the phylogenetic trees of PR and MFS, respectively, indicating a large evolutionary distance of the enzymes to them of *M. aquatica* and *M. x piperita*. This is supported by intron analysis, which reveals many sequence differences. Surprisingly, for PR, the lowest relative substitution rate on exon level was determined for *M. spicata* var. *crispa* and *M. aquatica* (0.29 % \pm 3 SNPs) compared to the other pairs (*M. aquatica* and *M. x piperita* with 0.49 % \pm 5 SNPs and *M. x piperita* and *M. spicata* var. *crispa* with 0.58 % \pm 6 SNPs), but in general, the sequence differences of PR were very low between all species, leading to the conclusion that this enzyme is conserved within the *Mentha* genus. Low relative substitution rates at the exon level imply high similarity of protein structures. This could be confirmed when the 3D models of protein structures were considered. The most similar protein structures of PR were found for *M. spicata* var. *crispa* and *M. aquatica*, with the lowest RMSD value of 0.049 Å, while the other two pairs have RMSD values about three times higher. This suggests greater differences, but all in all, the RMSD values are quite low, reconfirming that PR is a conserved enzyme within the genus *Mentha*.

In contrast, the protein structures of MFS were in general more diverse than those of PR, as reflected by their overall higher RMSD values. The MFS protein structures of *M. spicata* var. *crispa* were significantly different from those of *M. aquatica* (0.437 Å) and *M. x piperita* (0.429 Å), whereas *M. aquatica* and *M. x piperita* were quite similar (0.105 Å). This was expected from the distant phylogenetic relationship and the high relative substitution rates on the exon level of MFS of *M. spicata* var. *crispa* compared to the other two *Mentha* species. For example, the relative substitution rate on exon level of MFS was 5.78 % (86 SNPs) for *M. spicata* var. *crispa* and *M. aquatica* and 5.65 % (84 SNPs) for *M. spicata* var. *crispa* and *M. x piperita*, compared with *M. aquatica* and *M. x piperita* at 0.27 % (4 SNPs). All this indicates that lineage-specific independent evolution of this enzyme occurred in *M. spicata* var. *crispa*, which shifted the evolution of MFS in a different direction, probably to generate a new monoterpene synthase with an advantageous function. Diversification of gene clusters, e.g., through sequence divergence, has already been proposed as the main driver of the chemical diversity of diterpenes within the Lamiaceae family (Bryson *et al.*, 2023).

5. Discussion

In addition, the localization of the MFS of the three *Mentha* species was checked to determine whether the MFS of *M. spicata* var. *crispa* has already shifted its enzyme localization from that of the other two species since two different amino acids were detected in the transmembrane domain, but this was not the case. All three enzymes were located in the ER, as it is common for cytochrome P450-dependent monooxygenases (Chapple 1998). This suggests that evolution has not yet altered the location of MFS in *M. spicata* var. *crispa*, but it is possible that the further sequence differences have led to changes in other protein regions that cause a shift in function. This would demonstrate that evolution could do big things through small changes, so called microevolution (Hendry and Kinnison, 2001). Although transcripts of MFS were present in *M. spicata* var. *crispa*, none of the resulting metabolites were found in the essential oil of this species. Further studies are therefore needed to test the hypothesis whether this enzyme is a functionless remnant, post-transcriptionally silenced, or whether this gene has evolved in a different direction and may represent a new monoterpene synthase with unknown function in this species. If the latter is the case, the question of how such chemical diversity evolved in a single genus could be partially answered. Rather, it arises by descent from a common ancestral gene through gene diversification followed by lineage-specific independent evolution than by promiscuity.

The hybrid *M. x piperita* has evolved a new, unique chemical profile and contains very similar genes for monoterpene synthases as *M. aquatica*. This raises the question of how these monoterpene synthases might be controlled within the different *Mentha* species, leading to different chemistry. Therefore, it would be interesting to gain a deeper understanding of the temporal regulation of gene expression of the monoterpene synthases and what factors might influence their the expression.

5.3 How is the monoterpene biosynthesis pathway regulated?

To investigate the temporal expression pattern of monoterpene synthases and its correlation to the metabolite level in leaves of different ages of the three *Mentha* species, four key enzymes were selected that channel the metabolic flux in different directions to the main compounds carvone, menthofuran, and menthol. The relative expression of the monoterpene synthases to the housekeeping genes 18 S and actin was quantified using qPCR.

5. Discussion

The first two competing enzymes are limonene 3-hydroxylase (L3H) and limonene 6-hydroxylase (L6H). Both use limonene as a substrate, whereas L3H generates precursors of menthofuran and menthol, while L6H directs the metabolic flux toward carvone (Turner and Croteau, 2004). The metabolite limonene was found in all *Mentha* species, regardless of leaf age, which was expected since it serves as a substrate for L3H and L6H, providing precursors for the production of the various main compounds. Carvone was identified as the main compound of *M. spicata* var. *crispa* in the previous GC-MS analysis. Here, carvone was found to be uniquely abundant in the leaves of *M. spicata* var. *crispa*. This is consistent with the finding that the L6H transcript was only present in *M. spicata* var. *crispa*, with a decrease in relative expression from the youngest to the oldest leaf. The relative expression of L3H was observed in all *Mentha* species. *M. spicata* var. *crispa* had a similar relative expression of L3H (0.127) compared with L6H (0.102) in the youngest leaf. However, the content of carvone dominated compared to that of pulegone, which was detected only in older leaves of *M. spicata* var. *crispa*. It indicates that L6H has a higher binding affinity for the substrate limonene than L3H. This could be a reason why no transcript of L6H was observed in the other two *Mentha* species, *M. aquatica* and *M. x piperita*. For these, pulegone is a very important precursor of their main compounds, menthofuran and menthol. Therefore, expression of L6H is suppressed in *M. aquatica* and *M. x piperita*, so that at an early stage of leaf development, L3H can be active to accumulate the valuable precursor pulegone. In addition, a ten-fold higher relative expression of L3H was found in those two mints compared to *M. spicata* var. *crispa*, supporting this hypothesis.

However, the relative expression of L3H and L6H was higher in younger than in older leaves, irrespective of the *Mentha* species analyzed. This suggests that the biosynthesis of monoterpenes occurs primarily at an early stage of leaf development, and the resulting compound is then retained throughout the whole leaf life, such as carvone in *M. spicata* var. *crispa*, or is further metabolized toward the main compound of a species, such as pulegone in *M. aquatica* and *M. x piperita*. This was also shown by Gershenzon *et al.* (2000), where the monoterpene content of young peppermint leaves increased rapidly during early leaf development and biosynthesis decreased after the leaf reached full leaf width. Thereafter, the essential oil content remained stable for the remainder of leaf life, as there was no evidence of monoterpene loss through catabolism or volatilization (Gershenzon *et al.*, 2000).

5. Discussion

The other two competing enzymes are pulegone reductase (PR) and menthofuran synthase (MFS). Both use pulegone as a substrate to produce either menthone by PR, which can be further converted to menthol, or menthofuran by MFS (Croteau *et al.*, 2005). Compared with L3H and L6H, where transcript repression and transcript levels appear to control metabolic flux, transcripts of both enzymes were observed in all three *Mentha* species. Here, temporal shifts in the relative expression of PR and MFS were detected between the *Mentha* species, suggesting heterochrony. Heterochrony is an evolutionary-induced temporal shift in the development of a species relative to its ancestor (Alberch *et al.*, 1979; Smith 2001). This may explain an evolutionary mechanism for how *M. x piperita* was able to develop its new, unique chemical profile. In *M. x piperita*, gene expression of PR is upregulated in younger leaves, which decreases with age, and vice versa for MFS, whereas the opposite is true for *M. aquatica*. In *M. x piperita*, one would expect almost no menthofuran to accumulate in younger leaves because of the very low expression of MFS. Here, the limitations of SPME GC-MS become apparent. This method detects trace amounts and does not allow quantification, which would be necessary to confirm a positive correlation with transcript and metabolite levels. Therefore, only statements about the overall abundance of a compound can be provided. Besides menthol, menthofuran was also abundant in the younger leaves of *M. x piperita*. In general, it is not an either-or decision; the small amount of transcript of MFS that is present in younger leaves of *M. x piperita* produces traces of menthofuran that are then detected by this sensitive method. However, as described above, menthofuran itself acts as a negative regulator of the PR transcript (Mahmoud and Croteau, 2003). This may explain why MFS transcript could only be found in small amounts in younger leaves of *M. x piperita*, so that menthol can predominantly be formed. Nevertheless, a quantification of metabolites is necessary to verify this hypothesis.

In *M. aquatica*, the situation is different. Here, the relative expression of MFS in a young leaf is very high (18,675) and probably produces a very high amount of menthofuran, which was detected by SPME GC-MS. This may explain the low amount of PR transcript found in *M. aquatica*, and it again confirms the results of the study by Mahmoud and Croteau (2003). It also explains that no pulegone was found in older leaves of *M. aquatica* because all pulegone is consumed for the production of menthofuran.

5. Discussion

M. spicata var. *crispa* differed strongly from the other two species in terms of MFS gene expression. MFS was expressed only in the youngest leaf of *M. spicata* var. *crispa*, albeit at very low levels, but no traces of menthofuran were detected. Together with the finding that MFS has a very large evolutionary distance compared with the MFS of *M. aquatica* and *M. x piperita*, it is suggested that this transcript originated from a newly evolved enzyme with a different function. However, as already mentioned in the previous discussion, further studies are needed for the verification of this hypothesis. Furthermore, the relative expression of PR increases with ongoing leaf age in *M. spicata* var. *crispa*, which is consistent with the finding that the metabolites pulegone and menthone were detected by SPME GC-MS in older leaves. As described above, it is hypothesized that at an early stage of leaf development, L6H directs metabolic flux to the commonly known main compound carvone. At a later stage, when L6H is downregulated, L3H could use the substrate and direct the metabolic flux to pulegone, which can be further catabolized by PR to menthone, which was found in older leaves. In the previous GC-MS analysis of essential oils, samples were collected at a different time than for gene expression analysis. No pulegone and no menthone were detected there, which implies that environmental conditions such as different seasons or times of day play a role in the composition of the chemical profile.

Figure 39 illustrates a summary of the gene expression study of L3H, L6H, MFS, and PR, the quantitative metabolite analysis of the essential oils using GC-MS (not the qualitative SPME GC-MS analysis), as well as the phylogenetic studies and the protein structure comparison of PR and MFS of the three different *Mentha* species.

5. Discussion

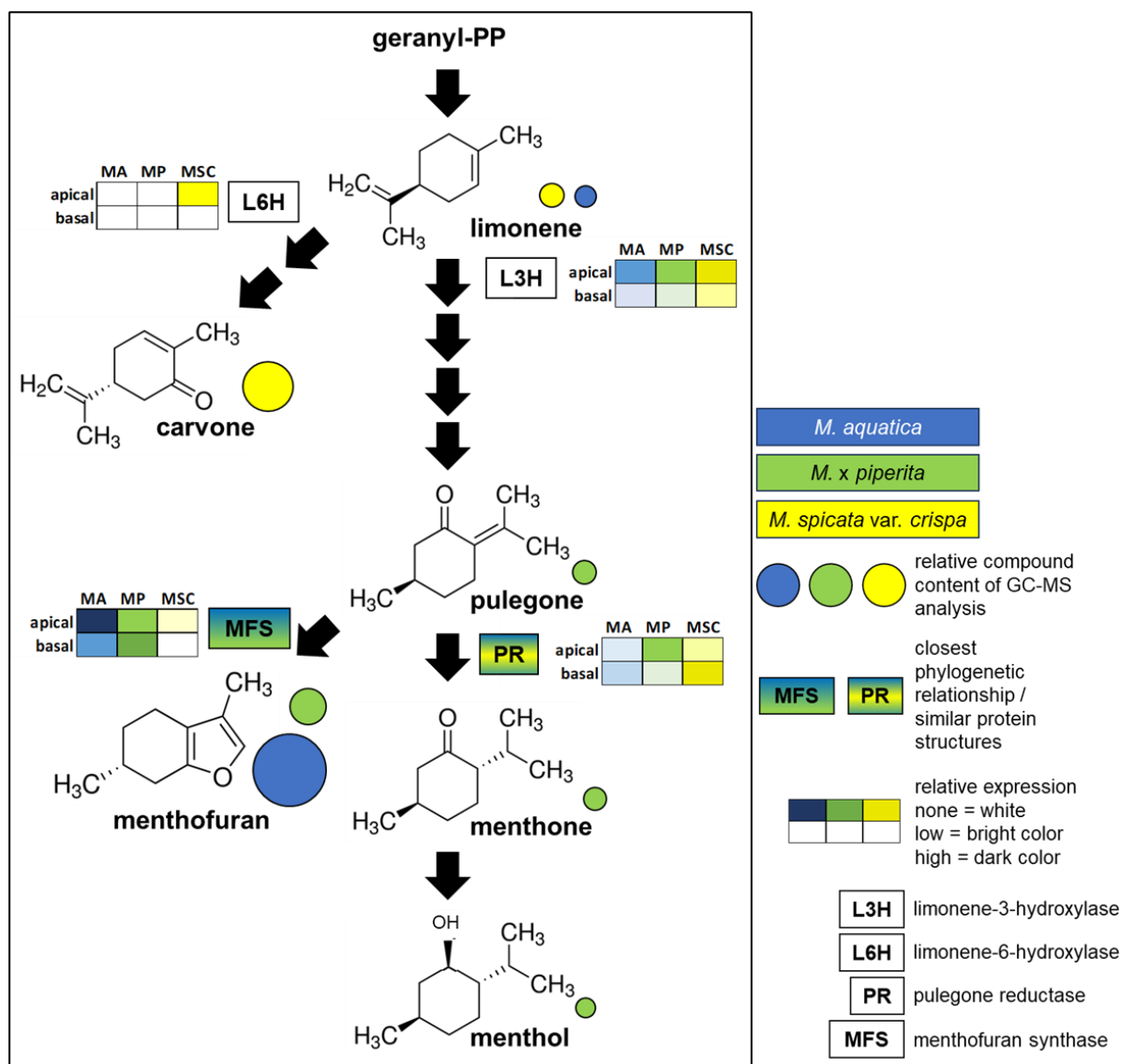


Figure 39: Summary of the gene expression study, the quantitative metabolite analysis, the phylogenetic studies, and the protein structure comparison of the three different *Mentha* species. The monoterpene biosynthesis pathway, with the most important intermediates at branching points and the end products, is demonstrated. Each arrow indicates an enzymatic step. The chemical formula was obtained from sigmaaldrich.com. One color always represents one *Mentha* species, while blue refers to *M. aquatica*, green to *M. x piperita*, and yellow to *M. spicata var. crispa*. The abundance of the main compounds in each species is shown as circles, with the size of the circles indicating the relative contents of the various compounds from low (=small) to high (=large) to the total percentage of essential oil compounds analyzed by GC-MS. Minor compounds were not displayed here. The branching enzymes studied, limonene-3-hydroxylase (L3H), limonene-6-hydroxylase (L6H), pulegone reductase (PR), and menthofuran synthase (MFS), are shown in the rectangles. Next to them is a small table showing the strength of relative expression in the apical and basal leaves from none (=white) to low (bright color) to high (=dark color). The phylogeny and the protein structures of PR and MFS of the *Mentha* species were investigated. Again, the colors appearing in the respective rectangles of the enzymes represent a close relationship or a similar protein structure between the *Mentha* species.

5. Discussion

In general, abiotic factors may be a different mechanism for regulating monoterpene synthases. Therefore, promoter studies of PR and MFS were performed to identify possible transcription factor binding sites or abiotic factors that might influence expression patterns. Upstream sequences were cloned, and the motifs were analyzed *in silico* using PLANTCare (Lescot *et al.*, 2002), a database of cis-acting regulatory elements in plants. In general, the promoters of PR and MFS were quite similar. Both promoters pointed to interactions with various abiotic factors and phytohormones but also possessed some specific motifs that could be assigned to either the PR or the MFS promoter or to a certain *Mentha* species.

Many light-responsive motifs were found in all promoters, regardless of which enzyme or *Mentha* species was considered. This suggests that monoterpene biosynthesis is highly dependent on light. The general precursor of monoterpenes comes from primary metabolism (Patra *et al.*, 2013), namely pyruvate, which is produced in glycolysis (Chandel 2021). Here, the substrate is glucose, which is produced in the Calvin cycle, which is part of plant photosynthesis, and for this, sunlight is required (Hall and Rao, 1999). Thus, it is a sequence of metabolic steps that leads back to primary metabolism that explains the need for light for monoterpene production and, moreover, shows how complex the metabolic network of plants is.

In addition, binding sites for MYC- and MYB-transcription factors (TFs) with unknown downstream functions were detected in all promoters of PR and MFS. MYC-TFs are involved in jasmonate signaling and regulate the expression of jasmonate-associated genes (Alves *et al.*, 2014), but they are also participating in other stress responses (Singh and Laxmi, 2015). MYB-TFs account for approximately 9 % of the total TF family in *Arabidopsis* and are one of the largest TF families in plants (Riechmann *et al.*, 2000), pointing to their importance. They play a role in regulating plant growth, developmental processes, stress responses, and the biosynthesis of secondary compounds, especially phenylpropanoids (Cao *et al.*, 2020). A MYB-TF from R2R3-MYB subgroup 7, namely MsMYB from spearmint, was found to regulate monoterpene biosynthesis at an early step (Reddy *et al.*, 2017), which could be one of the promoter motifs discovered. The exceedingly important role of MYC- and MYB-TFs is consistent with the finding that binding sites in the promoters of PR and MFS are abundant in all *Mentha* species. Nevertheless, some differences were also found that permit interspecific regulation of an enzyme or between the enzymes within a species.

5. Discussion

In addition to MYB-TFs with unknown downstream functions, a binding site for a MYB-TF involved in drought induction was detected in all promoters except in the MFS promoter of *M. spicata* var. *crispa*. In addition, all promoters contained low-temperature-responsive elements except the PR promoter of *M. aquatica*. Low temperature is a regulating factor for PR gene expression, as *M. x piperita* and *M. spicata* var. *crispa* appear to respond to this environmental change, whereas *M. aquatica* does not. This could be due to the different niches of the mints. *M. aquatica* occurs naturally in swamps and wetlands, while *M. x piperita* and *M. spicata* var. *crispa* are mostly grown in regions with warmer temperatures (Lange Laboratory, 2014 - 2021). Therefore, a decrease in temperature could be an important sign of a necessary change in chemistry to achieve better adaptation in these two species.

Moreover, the gene expression of PR and MFS seems to be dependent on different phytohormones. For example, gene expression of PR in *M. aquatica* appears to be dependent on SA, whereas *M. x piperita* and *M. spicata* var. *crispa*, which have an identical promoter, interact with MeJA. This enables specific regulation between the *Mentha* species, creating chemical diversity. As mentioned earlier, many variations occurred in the PR introns of *M. aquatica* due to low selection pressure, so it is hypothesized that this may have also happened in the PR promoter and created an SA promoter motif, but this is only a rough hypothesis and further studies are needed here. MeJA is indicative of pathogen attack (Alves *et al.*, 2014), and since menthol has been shown to have antimicrobial activity (Choi *et al.*, 2008), enrichment of this compound in response to MeJA recognition could be beneficial. *M. aquatica* contains high proportions of menthofuran in its oil, which could also be a bioactive compound against pathogens and therefore exert similar properties to menthol. Thus, the compound menthol produced by PR is not necessarily required for defense in this species, which is why no MeJA promoter motif was found here. Moreover, all *Mentha* species contained motifs for MeJA responsiveness in their MFS promoters, supporting the hypothesis of upregulation of MFS gene expression to accumulate the bioactive compound menthofuran in response to pathogen attack, as already hypothesized for *M. aquatica*. Furthermore, for *M. x piperita*, the MeJA-dependent gene expression of MFS and PR has already been confirmed in a study where MFS and PR transcripts were upregulated in response to MeJA (Soleymani *et al.*, 2017), verifying that the corresponding motifs were found in the promoters of *M. x piperita* in this study.

5. Discussion

In addition, PR gene expression appears to be dependent on abscisic acid (ABA), whereas MFS is not responsive to ABA in all three *Mentha* species. ABA is a phytohormone that plays a role in drought stress (Singh and Laxmi, 2015), but further studies are needed on how the compounds produced by PR might help the plant resist drought. A unique finding was that gene expression of MFS in *M. x piperita* can also be controlled by the phytohormones SA and GA, as the corresponding motifs were found in this promoter while they were absent in the other two mints. This could be an evolutionary adaptation of *M. x piperita* that led to the changes in its chemical profile compared to the chemically closely related parental species *M. aquatica*, which also contains menthofuran in its essential oil.

It follows that the monoterpene biosynthesis pathway is transcriptionally regulated and dependent on various abiotic factors as well as on phytohormones, allowing the establishment of chemically diverse species. Nevertheless, the question of why such chemical diversity arose remains elusive. To gain a deeper insight into this question, bioactive compounds were searched and investigated for their cellular mode of action.

5.4 Do mints have potent bioactive compounds with herbicidal character?

In order to find highly bioactive compounds with herbicidal character and elucidate their cellular mode of action, screening of the main compounds found for the three *Mentha* species was performed using germination assays. Since a previous work (Sarheed *et al.*, 2020) has already addressed menthol, the main compound of *M. x piperita*, the focus here was on carvone, the main compound of *M. spicata* var. *crispa*, and menthofuran, the main compound of *M. aquatica* and *M. x piperita*. First, a standard germination test was performed on cress with the main compounds, limonene (abundant in all three mints), and *n*-hexane as a solvent control. The dose-response curves of germination inhibition as a function of monoterpene concentration showed that carvone strongly inhibited germination of cress in a dose-dependent manner. In contrast, the effect of menthofuran was lower, and for limonene, the germination inhibition was not significantly different from that of the control, suggesting that monoterpenes are specific signals with different bioactivity. Another test was conducted with poppy, a widely known winter weed. Poppy is very competitive due to its high reproductive capacity (Codina-Pascual *et al.*, 2022) and its emerging resistance to various chemical herbicides (Torra *et al.*, 2021).

5. Discussion

Here, again, a dose dependence was observed as well as a very strong effect of carvone even at lower concentrations compared to that of cress, suggesting that monoterpenes can attack specific target plants. Furthermore, the effect on poppy was more persistent for both monoterpenes over the experimental period compared to cress. Some cress seeds were able to germinate after a period of time, e.g., those exposed to menthofuran, indicating that they were not toxified but rather inhibited by a weakening signal and therefore were able to germinate after a certain time. This can be transferred to Karl Bühler's organon model (Bühler, 1965). Depending on the recipient plant, the signal, in this case the monoterpene, can have a different information content, which leads to an altered effect since the context between sender and receiver is another. All this suggests that monoterpenes are specific signals that are interpreted differently by various weeds, enabling specificity.

In addition, the cytotoxicity of the essential oils of *M. aquatica* and *M. spicata* var. *crispa* and their main compounds, carvone and menthofuran, was assessed using the Evans Blue Dye Exclusion Assay according to Gaff and Okong'o-Ogola (1971) on non-transformed tobacco BY-2 cells (WT) and transformed BY-2 cell lines constitutively expressing the actin-binding domain 2 of fimbrin fused to GFP (GF11) (Sano *et al.*, 2005) and GFP-tubulin $\alpha 3$ (TuA3) (Kumagai *et al.*, 2001). In general, all effects were found to be stronger on transgenic BY-2 cell lines compared to WT, suggesting that cytoskeletal dynamics play an important role in the mode of action. The microtubules are more stable in the TuA3 cell line due to constitutive expression, whereas the microtubules in the WT cell line are more dynamic and allow for their innate turnover, polymerization and GTP hydrolysis, causing the typical dynamic instability (Hashimoto 2015). The same is true for the transgenic GF11 cell line, where overexpression leads to a denser actin network.

It was hypothesized that if a compound is alone responsible for the effect on the cytoskeleton, it will have a higher cell mortality rate than the essential oil from which it is derived, as shown for carvone on TuA3 cells, because of the higher concentration as a pure substance compared to the relative content in the essential oil. However, the compounds were often not solely responsible for the effect. For example, GF11 cells exposed to the essential oil of *M. spicata* var. *crispa* showed a higher cell mortality rate of 96.38 % compared to carvone, which was also significant at 69.20 %. This suggests that other compounds of this essential oil, despite carvone, promote the effect on actin filaments, leading to the measured high cell death.

5. Discussion

These unidentified compounds, together with carvone, may have a synergistic relationship. This was also observed when the essential oil of *M. aquatica* was applied, resulting in a higher mortality rate in both transgenic cell lines than with the single compound, indicating that menthofuran is not, or at least not alone, the bioactive compound of this essential oil causing the high cytotoxicity. Additionally, essential oil blends may also have antagonistic effects, as shown in TuA3 cells, where carvone alone causes the highest cell mortality rate of 98.77 %, whereas exposure to *M. spicata* var. *crispa* achieved only half of this. However, this could also be due to the high concentration of the pure compound, as mentioned above. Furthermore, the effect of carvone on WT cells was only a quarter as large compared to TuA3 cells, suggesting that stable microtubules may be the cellular target of carvone. Menthofuran, on the other hand, did not exert even a half-size effect on TuA3 cells. Moreover, the effect of carvone on GF11 cells was also substantial at 69.20 % and 3.5 times higher compared to menthofuran. This indicates that carvone has a stronger cytotoxicity than menthofuran, as assumed from the previous germination tests. Moreover, a combination of the modes of action on both cytoskeletal compounds could lead to the strong germination-inhibitory effect of carvone.

To further investigate the cellular mode of action of the compounds and essential oils, GF11 and TuA3 cells were followed *in vivo* for half an hour, as described in Sarheed *et al.* (2020). As expected from the strong cytotoxicity of carvone on TuA3 cells, a rapid disruption of the microtubule network was observed, whereas the extent of disruption was greater with *M. spicata* var. *crispa* essential oil, although the mortality rate was lower than with carvone. This could be due to technical limitations. A cell at the periphery comes into contact with the volatile substance more quickly than a cell located in the center of the slide and between many other cells. It appeared that the microtubules are completely degraded over time in cells exposed to carvone or *M. spicata* var. *crispa* essential oil, as no fluorescently tagged α -tubulin monomers were visible. Disruption of microtubules was also observed when TuA3 cells were exposed to *M. aquatica* essential oil and its main compound, menthofuran. However, the mode of action was delayed and differed from that of *M. spicata* var. *crispa* essential oil and carvone. Here, the microtubules appeared to disintegrate because a diffuse signal was visible, which could represent the fluorescently tagged α -tubulin monomers.

5. Discussion

However, it could also be that the assembly was blocked and therefore the overexpressed α -tubulin monomers could no longer assemble the microtubule strand and therefore generated the background signal. In addition, *M. aquatica* essential oil had a stronger effect than menthofuran, which was expected because of the higher mortality rate of TuA3 cells. The effect caused by menthofuran was very weak, but the diffuse signal could be observed as well.

In general, it could be that the compound enters the cell via a transporter localized in the plasma membrane, such as an ATP-binding cassette (ABC) transporter. So far, however, no transporter has been identified for monoterpenes in trichomes (Tissier *et al.*, 2017), only for volatile organic compounds (VOCs) in *Petunia* flowers (Adebesin *et al.*, 2017). Subsequently, the compound could bind to an intracellular receptor, as previously shown for sesquiterpenes (Nagashima *et al.*, 2019), and trigger a signaling cascade, leading to the disruption of microtubules as a cellular target. If microtubules are not present in the cell, the spindle phase apparatus cannot be formed. As a result, mitosis is blocked and cells are unable to proliferate. This could be the explanation for the inhibition of germination and growth in cress and poppy. In addition, microtubules are needed for cell stability. If this is interrupted, the cell collapses, which explains the cytotoxicity.

Furthermore, very rapid and strong actin bundling was observed when GF11 cells were exposed to *M. spicata* var. *crispa* essential oil. In one study, it was found that changes in the cytoskeleton can trigger and regulate cell death in plants (Smertenko and Franklin-Tong, 2011), and actin bundling is one of these alterations. Based on the very high cytotoxicity in the GF11 cell line caused by *M. spicata* var. *crispa* essential oil, the hypothesis that actin bundling is a signal that mediates cell death is supported. Carvone also showed a rapid and strong bundling effect, followed by *M. aquatica* essential oil, where the effect was delayed, and menthofuran, where only a very slight effect was observed.

A rough model of the different cellular modes of action of the two monoterpenes causing cell death is presented in **Figure 40**.

5. Discussion

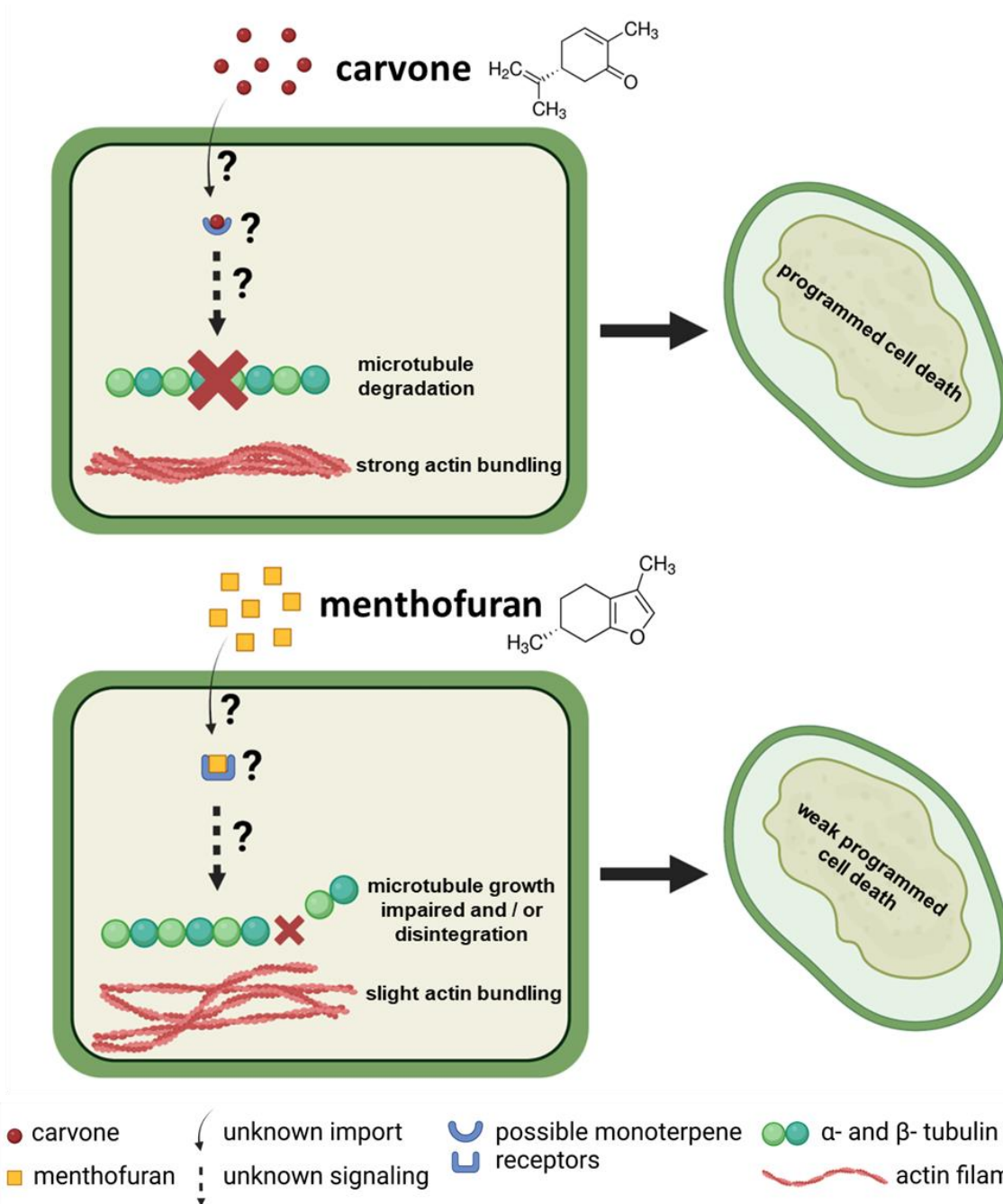


Figure 40: Model of the monoterpenes carvone and menthofuran as signals for different cellular effects leading to cell death. The import, perception, and signal transduction of monoterpenes have not yet been elucidated. Nevertheless, plasma membrane-localized transporters could facilitate the import of monoterpenes, as shown for the import of VOCs via an ABC transporter in the flowers of *Petunia* (Adebesin *et al.*, 2017). This could be followed by binding to an intracellular receptor to mediate the signal, as observed for sesquiterpenes (Nagashima *et al.*, 2019). In this study, it was proven that carvone and menthofuran act at the cellular level on microtubules and actin filaments. Carvone induces microtubule degradation and strong actin bundling, causing cell death. In contrast, menthofuran has a different cellular mode of action on microtubules, namely, to impair their growth and / or cause them to disintegrate. In addition, it induces slight actin bundling. Both effects of menthofuran on the cytoskeleton also result in cell death, albeit in an attenuated form. The graphic was created with BioRender.com.

5. Discussion

Taken together, microtubule disruption and strong actin bundling were significant cytoskeletal alterations that resulted in high programmed cell death and strong germination inhibition of cress and poppy, as demonstrated for carvone. Thus, carvone is a highly bioactive compound with herbicidal properties and could be valuable for the application of a sustainable specific bioherbicide for certain weeds.

6. Conclusion and Outlook

This study provided insight into the chemical diversity of closely related mints as well as into the regulation and phylogeny of their monoterpene synthases. It was shown that the hybrid *M. x piperita* has evolved a unique chemical profile that does not seem to be completely derived from the parents, *M. aquatica* and *M. spicata* var. *crispa*. However, a close phylogenetic relationship and similar protein structures of the important key enzymes PR and MFS were found for *M. x piperita* and *M. aquatica*, which contained the same main compound menthofuran but in different abundances. Additionally, it was demonstrated that monoterpene biosynthesis is regulated at the transcript level and correlates with the metabolite level. Here, the influence of evolution could be detected, as expression patterns of some enzymes were shifted between species in time, suggesting that the developmental program has changed, indicating heterochrony. Heterochrony combined with an interplay of regulatory mechanisms, such as transcript upregulation of L3H that directs the metabolic flux towards menthol and menthofuran and repression of the competing enzyme L6H, or a reduced negative feedback loop of the metabolite menthofuran leading to higher transcript levels of PR, may have contributed to the novel chemical profile of *M. x piperita*. Furthermore, *M. spicata* var. *crispa*, which was chemically very different from the other two *Mentha* species, was shown to have undergone lineage-specific independent evolution with respect to the key enzyme MFS, since the transcript was abundant but the expected metabolite was not. Compared to the other two species, numerous amino acid changes were detected, which might be sufficient to establish a new monoterpene synthase that differs in function, while the localization remained the same. Therefore, feeding studies have to be conducted to confirm this hypothesis. Promoter analyses revealed that abiotic factors as well as phytohormones also play an important role in the regulation of monoterpene biosynthesis. All this demonstrates that many factors contribute to the chemical diversity within the genus *Mentha*. Ultimately, the question remains why such chemical diversity within the genus is necessary at all. Plants are constantly adapting to their environment. They can achieve this with secondary compounds, which they use as an advantage for their survival, e.g., as a defense against pathogens or competitors in the neighborhood. Carvone was detected as the main compound of *M. spicata* var. *crispa*, which is not present in the other two species. In comparative assays with *M. aquatica*, carvone was shown to be a strongly bioactive substance with an herbicidal character.

6. Conclusion and Outlook

It led to strong cytotoxicity in tobacco cells and prevented the germination of various weeds such as cress or poppy by degrading the microtubules and causing actin bundling. Therefore, this compound could be used as a sustainable and specific bioherbicide against certain weeds based on the natural effect of allelopathy.

However, the path to application is quite long and complicated. One has to find ways to apply the highly volatile compound. One possibility would be to use slow-release carriers. However, this area of research is poorly explored, and studies are needed to determine what sustainable material and pore size would be most appropriate. In addition, many insights into regulation have been addressed in this study, but how the plant itself is resistant to its own signal or how only certain competitors are specifically affected remains elusive. Therefore, it would be very important to understand the signal pathway from monoterpene perception to programmed cell death. Belief in the existence of monoterpene receptors is growing with the discovery of an intracellular sesquiterpene receptor called TOPLESS, which physically interacts with an adaptor protein that in turn binds to a transcription factor that modulates gene expression. It appears to be a fairly conserved receptor, as it is also involved in phytohormone signal transduction and effector protein perception. Therefore, it is likely that it may also mediate monoterpene signaling through interaction with, e.g., another adaptor protein. One way to directly find a monoterpene receptor would be to use receptor-ligand technology, in which the monoterpene is bound to a stationary phase and submerged with the proteome. Subsequently, the bound compounds could be eluted and elucidated by GC-MS. Another option would be *in silico* analysis, in which various potential receptors are screened using computational modeling to see if the monoterpene fits in the binding pocket. If a receptor looks promising, the sequences of the mint and its non-resistant competitors can be cloned and compared. Sequence variations could indicate differences in terms of the binding pocket that might explain why the mint plant is resistant to its own compound and the weed is not. If a receptor is found, further analysis of upstream and downstream signaling pathways should be performed to elucidate the entire signaling cascade. This knowledge could be used to develop a specific bioherbicide, as interventions could be made at different points in the signaling pathway, allowing us to target only the unwanted weeds and not the worthy crops or cereal plants. Taken together, this study has laid the foundation for a bioherbicide, but much more research is needed for its application.

7. References

Adebesin, F., Widhalm, J.R., Boachon, B. et al. (2017). Emission of volatile organic compounds from petunia flowers is facilitated by an ABC transporter. *Science* **356** (6345), 1386-1388.

Ahkami, A., Johnson, S.R., Srividya, N. et al. (2015). Multiple levels of regulation determine monoterpenoid essential oil compositional variation in the mint family. *Mol Plant* **8**, 188-191.

Aktar, Md.W., Sengupta, D. and Chowdhury, A. (2009). Impact of pesticides use in agriculture: their benefits and hazards. *Interdiscip Toxicol* **2** (1), 1-12.

Alberch, P., Gould, S.J., Oster, G.F. et al. (1979). Size and shape in ontogeny and phylogeny. *Paleobiology* **5** (3), 296-317.

Alves, M.S., Dadalto, S.P., Gonçalves, A.B. et al. (2014). Transcription factor functional protein-protein interactions in plant defense responses. *Proteomes* **2** (1), 85-106.

Atwood, D. and Paisley-Jones, C. (2017). Pesticides industry sales and usage 2008-2012 market estimates. EPA's biological and economic analysis division, office of pesticide programs, and office of chemical safety and pollution prevention. Available online at: <https://www.epa.gov/pesticides> (accessed June 21st, 2023).

Azirak, S. and Karaman, S. (2008). Allelopathic effect of some essential oils and components on germination of weed species. *Acta Agric Scand - B Soil Plant Sci* **58** (1), 88-92.

Bertea, C.M., Schalk, M., Karp, F. et al. (2001). Demonstration that menthofuran synthase of mint (*Mentha*) is a cytochrome p450 monooxygenase: cloning, functional expression, and characterization of the responsible gene. *Arch Biochem Biophys* **390** (2), 279-286.

Blattner, F.R. (1999). Direct amplification of the entire ITS region from poorly preserved plant material using recombinant PCR. *BioTechniques* **27** (6), 1180-1186.

Boni, C.G., Busato de Feiria, S.N., Laet Santana, P. et al. (2016). Antifungal and cytotoxic activity of purified biocomponents as carvone, menthone, menthofuran and pulegone from *Mentha* spp. *Afr J Plant Sci* **10** (10), 203-210.

7. References

- Brach, A.R. and Song, H. (2006).** eFloras: new directions for online floras exemplified by the Flora of China project. *Taxon* **55** (1), 188-192.
- Bryson, A.E., Lanier, E.R., Lau, K.H. et al. (2023).** Uncovering a miltiradiene biosynthetic gene cluster in the Lamiaceae reveals a dynamic evolutionary trajectory. *Nat Commun* **14**, 343.
- Bunsawat, J., Elliott, N.E., Hertweck, K.L. et al. (2004).** Phylogenetics of *Mentha* (Lamiaceae): evidence from chloroplast DNA sequences. *Syst Bot* **29** (4), 959-964.
- Bühler, K. (1965).** Sprachtheorie: Die Darstellungsfunktion der Sprache. Stuttgart: Gustav Fischer.
- Cao, Y., Li, K., Li, Y. et al. (2020).** MYB transcription factors as regulators of secondary metabolism in plants. *Biology* **9** (3), 61.
- Chaimovitsh, D., Abu-Abied, M., Belausov, E. et al. (2010).** Microtubules are an intracellular target of the plant terpene citral. *Plant J* **61** (3), 399-408.
- Chaimovitsh, D., Rogovoy-Stelmakh, O., Altshuler, O. et al. (2012).** The relative effect of citral on mitotic microtubules in wheat roots and BY2 cells. *Plant Biol* **14**, 354-364.
- Chandel, N.S. (2021).** Glycolysis. *Cold Spring Harb Perspect Biol* **13** (5), a040535.
- Chapple, C. (1998).** Molecular-genetic analysis of plant cytochrome P450-dependent monooxygenases. *Annu Rev Plant Physiol Plant Mol Biol* **49**, 311-43.
- Choi, H.W., Lee, B.G., Kim, N.H. et al. (2008).** A Role for a menthone reductase in resistance against microbial pathogens in plants. *Plant Physiol* **148**, 383-401.
- Chung, K.P., Gonzalez-Duran, E., Ruf, S. et al. (2023).** Control of plastid inheritance by environmental and genetic factors. *Nat Plants* **9**, 68-80.
- Codina-Pascual, N., Torra, J., Baraibar, B. et al. (2022).** Weed suppression capacity of camelina (*Camelina sativa*) against winter weeds: The example of corn-poppy (*Papaver rhoeas*). *Ind Crops Prod* **184**, 115063.
- Croteau, R.B., Davis, E.M., Ringer, K.L. et al. (2005).** (-)-Menthol biosynthesis and molecular genetics. *Naturwissenschaften* **92** (12), 562-577.

7. References

- Dong, W., Xu, C., Li, C. et al. (2015).** *ycf1*, the most promising plastid DNA barcode of land plants. *Sci Rep* **5**, 8348.
- Dorman, H.J.D., Kosar, M., Kahlos, K. et al. (2003).** Antioxidant properties and composition of aqueous extracts from *Mentha* species, hybrids, varieties, and cultivars. *J Agric Food Chem* **51**, 4563-4569.
- Edgar, R.C. (2004).** MUSCLE: multiple sequence alignment with high accuracy and high throughput. *Nucleic Acids Res* **32** (5), 1792-1797.
- Einhellig, F.A. (1995).** Allelopathy: current status and future goals. *ACS Symp Ser* **582** (1), 1-24.
- Eisenreich, W., Sagner, S., Zenk, M.H. et al. (1997).** Monoterpenoid essential oils are not of mevalonoid origin. *Tetrahedron Lett* **38** (22), 3889-3892.
- Fahn, A. (1988).** Secretory tissues in vascular plants. *New Phytol* **108**, 229-257.
- Fang, X., Yang, C.Q., Wi, Y.K. et al. (2011).** Genomics grand for diversified plant secondary compounds. *Plant Divers* **33** (1), 53-64.
- Frank, L., Wenig, M., Ghirardo, A. et al. (2021).** Isoprene and β -caryophyllene confer plant resistance via different plant internal signalling pathways. *Plant Cell Environ* **44**, 1151-1164.
- Fuchs, L.K., Holland, A.H., Ludlow, R.A. et al. (2022).** Genetic manipulation of biosynthetic pathways in mint. *Front Plant Sci* **13**, 928178.
- Gaff, D.F. and Okong'o-Ogola, O. (1971).** The use of non-permeating pigments for testing the survival of cells. *Exp Bot* **22** (3), 756-758.
- Gaines, T.A., Duke, S.O., Morran, S. et al. (2020).** Mechanisms of evolved herbicide resistance. *J Biol Chem* **295** (30), 10307-10330.
- Gershenzon, J., Maffei, M. and Croteau, R. (1989).** Biochemical and histochemical localization of monoterpene biosynthesis in the glandular trichomes of spearmint (*Mentha spicata*). *Plant Physiol* **89** (4), 1351-1357.
- Gershenzon, J., McConkey, M.E. and Croteau, R.B. (2000).** Regulation of monoterpene accumulation in leaves of peppermint. *Plant Physiol* **122**, 205-213.

7. References

- Gershenzon, J. and Dudareva, N. (2007).** The function of terpene natural products in the natural world. *Nat Chem Biol* **3** (7), 408-14.
- Gobert, V., Moja, S., Taberlet P. et al. (2006).** Heterogeneity of three molecular data partition phylogenies of mints related to *M. x piperita* (*Mentha*; Lamiaceae). *Plant Biol* **8**, 470-485.
- Grand View Research. (2019).** Mint essential oils market size, share & trends analysis report by product (cornmint, peppermint, spearmint, dementholized peppermint), by application, by usage (direct, indirect), and segment forecasts, 2019-2025. Available online at: <https://www.grandviewresearch.com/industry-analysis/mint-essential-oils-market> (accessed June 7th, 2023).
- Hagemann, R. and Schröder, M.B. (1989).** The cytological basis of the plastid inheritance in angiosperms. *Protoplasma* **152**, 57-64.
- Hall, D.O., and Rao, K. (1999).** Photosynthesis. Cambridge: Cambridge University Press.
- Hambrock, A., Löffler-Walz, C. and Quast, U. (2002).** Glibenclamide binding to sulphonylurea receptor subtypes: dependence on adenine nucleotides. *Br J Pharmacol* **136**, 995-1004.
- Harley, K.M. and Brighton, C.A. (1977).** Chromosome numbers in the genus *Mentha* L. *Bot J Linn Soc, Bot* **74**, 71-96.
- Hartley, J.L., Temple, G.F. and Brasch, M.A. (2000).** DNA cloning using *in vitro* site-specific recombination. *Genome Res* **10** (11), 1788-1795.
- Hashimoto, T. (2015).** Microtubules in plants. *Arabidopsis Book* **13**, e0179.
- Heimes, K., Hauk, F. and Verspohl, E. J. (2011).** Mode of action of peppermint oil and (-)-menthol with respect to 5-HT₃ receptor subtypes: binding studies, cation uptake by receptor channels and contraction of isolated rat ileum. *Phytother Res* **25**, 702-708.
- Hendry, A.P. and Kinnison, M.T. (2001).** An introduction to microevolution: rate, pattern, process. *Genetica* **112-113**, 1-8.

7. References

- Hwang, H.S., Adhikari, P.B., Jo, H.J. et al. (2020).** Enhanced monoterpene emission in transgenic orange mint (*Mentha × piperita* f. *citrata*) overexpressing a tobacco lipid transfer protein (NtLTP1). *Planta* **252** (3), 44.
- Karimi, M., Inzé, D. and Depicker, A. (2002).** GATEWAY vectors for *Agrobacterium*-mediated plant transformation. *Trends Plant Sci* **7** (5), 193-195.
- Koselski, M., Wasko, P., Kupisz, K. et al. (2019).** Cold- and menthol-evoked membrane potential changes in the moss *Physcomitrella patens*: influence of ion channel inhibitors and phytohormones. *Physiol Plant* **167**, 433-446.
- Kress, W.J., Erickson, D.L., Jones, F.A. et al. (2009).** Plant DNA barcodes and a community phylogeny of a tropical forest dynamics plot in Panama. *Proc Natl Acad Sci USA* **106** (44), 18621-18626.
- Kumagai, F., Yoneda, A., Tomida, T. et al. (2001).** Fate of nascent microtubules organized at the M/G1 interface, as visualized by synchronized tobacco BY-2 cells stably expressing GFP-tubulin: time-sequence observations of the reorganization of cortical microtubules in living plant cells. *Plant Cell Physiol* **42** (7), 723-732.
- Kumar, P., Mishra, S., Malik, A. et al. (2011).** Insecticidal properties of *Mentha* species: A review. *Ind Crops and Prod* **34** (1), 802-817.
- Kumar, S., Stecher, G. and Tamura, K. (2016).** MEGA7: molecular evolutionary genetics analysis version 7.0 for bigger datasets. *Mol Biol Evol* **33** (7), 1870-1874.
- Lange, B.M., Wildung, M.R., Stauber, E.J. et al. (2000).** Probing essential oil biosynthesis and secretion by functional evaluation of expressed sequence tags from mint glandular trichomes. *Proc Natl Acad Sci USA* **97** (6), 2934-2939.
- Lange, B.M. and Srividya, N. (2019).** Enzymology of monoterpene functionalization in glandular trichomes. *J Exp Bot* **70** (4), 1095-1108.
- Lange Laboratory at Washington State University (WSU). (2014-2021).** Mint genomics resource - species directory. Available online at: <http://langelabtools.wsu.edu/mgr/species-directory> (accessed August 30th, 2023).
- Lee, G.W., Lee, S., Chung, M.S. et al. (2015).** Rice terpene synthase 20 (OsTPS20) plays an important role in producing terpene volatiles in response to abiotic stresses. *Protoplasma* **252**, 997-1007.

7. References

- Lescot, M., Déhais, P., Thijs, G. et al. (2002).** PlantCARE, a database of plant cis-acting regulatory elements and a portal to tools for in silico analysis of promoter sequences. *Nucleic Acids Res* **30** (1), 325-327.
- Liu, C., Gao, Q., Shang, Z. et al. (2021).** Functional characterization and structural insights into stereoselectivity of pulegone reductase in menthol biosynthesis. *Front Plant Sci* **12**, 780970.
- Livak, K.J. and Schmittgen, T.D. (2001).** Analysis of relative gene expression data using real-time quantitative PCR and the $2^{-\Delta\Delta Ct}$ method. *Methods* **25** (4), 402-408.
- Maffei, M., Camusso, W. and Sacco, S. (2001).** Effect of *Mentha x piperita* essential oil and monoterpenes on cucumber root membrane potential. *Phytochemistry* **58**, 703-707.
- Mahmoud, S.S. and Croteau, R.B. (2001).** Metabolic engineering of essential oil yield and composition in mint by altering expression of deoxyxylulose phosphate reductoisomerase and menthofuran synthase. *Proc Natl Acad Sci USA* **98** (15), 8915-8920.
- Mahmoud, S.S. and Croteau, R.B. (2003).** Menthofuran regulates essential oil biosynthesis in peppermint by controlling a downstream monoterpene reductase. *Proc Natl Acad Sci USA* **100** (24), 14481-14486.
- Maisch, J. and Nick, P. (2007).** Actin is involved in auxin-dependent patterning. *Plant Physiol* **143** (4), 1695-1704.
- McCaskill, D. and Croteau, R. (1995).** Monoterpene and sesquiterpene biosynthesis in glandular trichomes of peppermint (*Mentha x piperita*) rely exclusively on plastid-derived isopentenyl diphosphate. *Planta* **197**, 49-56.
- McConkey, M.E., Gershenzon, J. and Croteau, R.B. (2000).** Developmental regulation of monoterpene biosynthesis in the glandular trichomes of peppermint. *Plant Physiol* **122**, 215-223.
- Mimica-Dukić, N., Bozin, B., Soković, M. et al. (2003).** Antimicrobial and antioxidant activities of three *Mentha* species essential oils. *Planta Med* **69** (5), 413-419.

7. References

- Mint Evolutionary Genomics Consortium. (2018).** Phylogenomic mining of the mints reveals multiple mechanisms contributing to the evolution of chemical diversity in Lamiaceae. *Mol Plant* **11** (8), 1084-1096.
- Molisch, H. (1937).** Der Einfluß einer Pflanze auf die andere. Allelopathie. Jena: Gustav Fischer.
- Nagashima, A., Higaki, T., Koeduka, T. et al. (2019).** Transcriptional regulators involved in responses to volatile organic compounds in plants. *J Biol Chem* **294** (7), 2256-2266.
- Nagata, T., Nemoto, Y., and Hasezawa, S. (1992).** Tobacco BY-2 cell line as the “HeLa” cell in the cell biology of higher plants. *Int Rev Cytol* **132**, 1-30.
- Ninkovic, V., Markovic, D. and Rensing, M. (2021).** Plant volatiles as cues and signals in plant communication. *Plant Cell Environ* **44** (4), 1030-1043.
- Oberdorfer, E., Schwabe, A. and Müller, T. (2001).** Pflanzensoziologische Exkursionsflora: Für Deutschland und angrenzende Gebiete (8. revised edition). Stuttgart: Eugen Ulmer.
- Parolly, G. and Rohwer, J.G. (2019).** SCHMEIL-FITSCHEN Die Flora Deutschlands und angrenzender Länder: Ein Buch zum Bestimmen aller wildwachsenden und häufig kultivierten Gefäßpflanzen (97. revised and expanded edition). Wiebelsheim: Quelle & Meyer Verlag.
- Patra, B., Schluttenhofer, C., Wu, Y.M. et al. (2013).** Transcriptional regulation of secondary compound biosynthesis in plants. *BBA Gene Regul Mech* **1829** (11), 1236-1247.
- Pauwels, L., Barbero, G.F., Geerinck, J. et al. (2010).** NINJA connects the co-repressor TOPLESS to jasmonate signalling. *Nature* **464** (7289), 788-91.
- Peier, A.M., Moqrich, A., Hergarden, A.C. et al. (2002).** A TRP channel that senses cold stimuli and menthol. *Cell* **108** (5), 705-15.
- Petre, B., Saunders, D.G.O., Sklenar, J. et al. (2015).** Candidate effector proteins of the rust pathogen *Melampsora larici-populina* target diverse plant cell compartments. *MPMI* **28** (6), 689-700.

7. References

- Rasmann, S., Köllner, T., Degenhardt, J. et al. (2005).** Recruitment of entomopathogenic nematodes by insect-damaged maize roots. *Nature* **434**, 732-737.
- Reddy, V.A., Wang, Q., Dhar, N. et al. (2017).** Spearmint R2R3-MYB transcription factor MsMYB negatively regulates monoterpene production and suppresses the expression of geranyl diphosphate synthase large subunit (*MsGPPS.LSU*). *Plant Biotechnol J* **15** (9), 1105-1119.
- Riechmann, J.L., Heard, J., Martin, G. et al. (2000).** Arabidopsis transcription factors: genome-wide comparative analysis among eukaryotes. *Science* **290**, 2105-2110.
- Sánchez-Bayo, F. and Wyckhuys, K.A.G. (2019).** Worldwide decline of the entomofauna: A review of its drivers. *Biol Conserv* **232**, 8-27.
- Sang, T., Crawford, D. and Stuessy, T. (1997).** Chloroplast DNA phylogeny, reticulate evolution, and biogeography of *Paeonia* (Paeoniaceae). *Am J Bot* **84** (8), 1120.
- Sano, T., Higaki, T., Oda, Y. et al. (2005).** Appearance of actin microfilament 'twin peaks' in mitosis and their function in cell plate formation, as visualized in tobacco BY-2 cells expressing GFP-fimbrin. *Plant J* **44** (4), 595-605.
- Sarheed, M.M., Rajabi, F., Kunert, M. et al. (2020).** Cellular base of mint allelopathy: menthone affects plant microtubules. *Front Plant Sci* **11**, 546345.
- Schalk, M. and Croteau, R. (2000).** A single amino acid substitution (F363I) converts the regiochemistry of the spearmint (-)-limonene hydroxylase from a C6- to a C3-hydroxylase. *Proc Natl Acad Sci USA* **97** (22), 11948-11953.
- Schulz, M., Kussmann, P., Knop, M. et al. (2007).** Allelopathic monoterpenes interfere with *Arabidopsis thaliana* cuticular waxes and enhance transpiration. *Plant Signal Behav* **2** (4), 231-239.
- Shaiq Ali, M., Saleem, M., Ahmad, W. et al. (2002).** A chlorinated monoterpene ketone, acylated beta-sitosterol glycosides and a flavanone glycoside from *Mentha longifolia* (Lamiaceae). *Phytochemistry* **59** (8), 889-95.
- Sharkey, T.D. and Singas, E.L. (1995).** Why plants emit isoprene. *Nature* **374**, 769.
- Sharkey, T.D., Wiberley, A.E. and Donohue, A.R. (2008).** Isoprene emission from plants: why and how. *Ann Bot* **101** (1), 5-18.

7. References

- Singh, D. and Laxmi, A. (2015).** Transcriptional regulation of drought response: a tortuous network of transcriptional factors. *Front Plant Sci* **6**, 895.
- Smertenko, A. and Franklin-Tong, V.E. (2011).** Organisation and regulation of the cytoskeleton in plant programmed cell death. *Cell Death Differ* **18**, 1263-1270.
- Smith, K.K. (2001).** Heterochrony revisited: the evolution of developmental sequences. *Biol J Linn Soc* **73**, 169-186.
- Soleymani, F., Taheri, H. and Shafeinia, A.R. (2017).** Relative expression of genes of menthol biosynthesis pathway in peppermint (*Mentha piperita* L.) after chitosan, gibberellic acid and methyl jasmonate treatments. *Russ J Plant Physiol* **64** (1), 59-66.
- Tamura, K. and Nei, M. (1993).** Estimation of the number of nucleotide substitutions in the control region of mitochondrial DNA in humans and chimpanzees. *Mol Biol Evol* **10** (3), 512-526.
- Tate, J.A. and Simpson, B.B. (2003).** Paraphyly of *Tarasa* (Malvaceae) and diverse origins of the polyploid species. *Syst Bot* **28** (4), 723-737.
- Tate, J.A., Soltis, D.E. and Soltis, P.S. (2005).** Polyploidy in plants. In T.R. Gregory [ed.], *The evolution of the genome*, 371-426. San Diego: Elsevier Academic Press.
- Tissier, A., Morgan, J.A. and Dudareva, N. (2017).** Plant volatiles: going 'in' but not 'out' of trichome cavities. *Trends Plant Sci* **22** (11), 930-938.
- Torra, J., Rojano-Delgado, A.M., Menéndez, J. et al. (2021).** Cytochrome P450 metabolism-based herbicide resistance to imazamox and 2,4-D in *Papaver rhoeas*. *Plant Physiol Biochem* **160**, 51-61.
- Trethewey, R.N. (2004).** Metabolite profiling as an aid to metabolic engineering in plants. *Curr Opin Plant Biol* **7** (2), 196-201.
- Turner, G.W., Gershenzon, J. and Croteau, R.B. (2000).** Development of peltate glandular trichomes of peppermint. *Plant Physiol* **124**, 665-679.
- Turner, G.W. and Croteau, R. (2004).** Organization of monoterpene biosynthesis in *Mentha*. Immunocytochemical localizations of geranyl diphosphate synthase, limonene-6-hydroxylase, isopiperitenol dehydrogenase, and pulegone reductase. *Plant Physiol* **136** (4), 4215-27.

7. References

Wang, Q., Reddy, V.A., Panicker, D. et al. (2016). Metabolic engineering of terpene biosynthesis in plants using a trichome-specific transcription factor MsYABBY5 from spearmint (*Mentha spicata*). *Plant Biotechnol J* **14** (7), 1619-1632.

Wink, M. (1988). Plant breeding: importance of plant secondary compounds for protection against pathogens and herbivores. *Theoret Appl Genetics* **75**, 225-233.

Wu, X., Liu, Y., Zhang, Y. et al. (2021). Advances in research on the mechanism of heterosis in plants. *Front Plant Sci* **12**, 745726.

Zhang, H., Lang, Z. and Zhu, J.K. (2018). Dynamics and function of DNA methylation in plants. *Nat Rev Mol Cell Biol* **19**, 489-506.

Zhang, Z., Liu, Y., Yuan, L. et al. (2021). Effect of allelopathy on plant performance: a meta-analysis. *Ecol Lett* **24** (2), 348-362.

Appendix

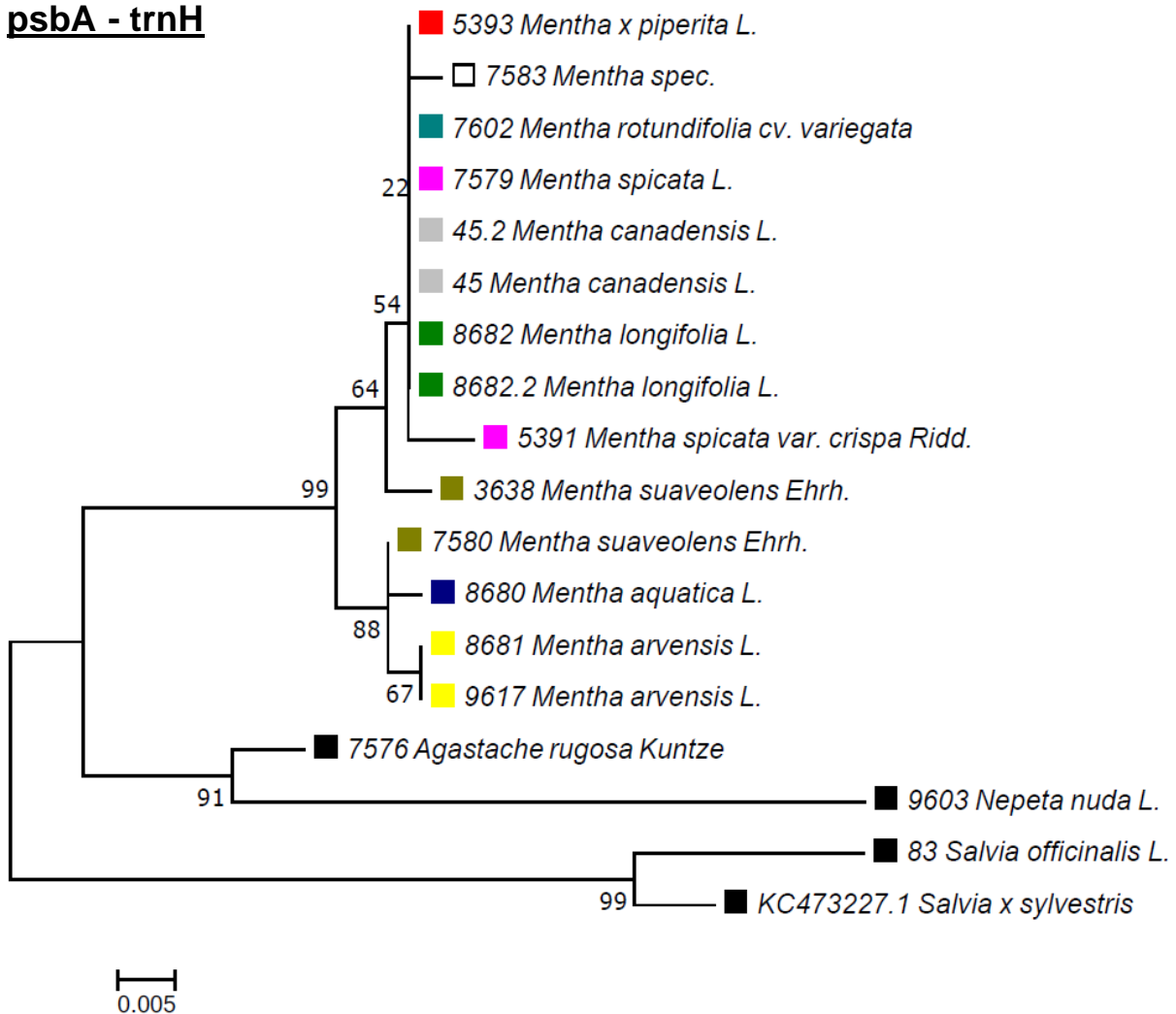
psbA - trnH

Figure 41: Phylogenetic tree based on the plastidic *psbA* - *trnH* intergenic spacer region. Neighbor-joining was used to infer the evolutionary history. Bootstrap values are given in percent next to the branches. The tree is drawn to scale, with branch lengths in the same units as the evolutionary distances used for phylogenetic inference. Evolutionary distances were calculated using the Tamura-Nei method in units of the number of base substitutions per site. Analyses were performed in MEGA7. Individuals of one *Mentha* species are represented by the same color, other genera are indicated by black squares. One sequence from NCBI (<https://www.ncbi.nlm.nih.gov/>) was included and can be remarked by its accession ID.

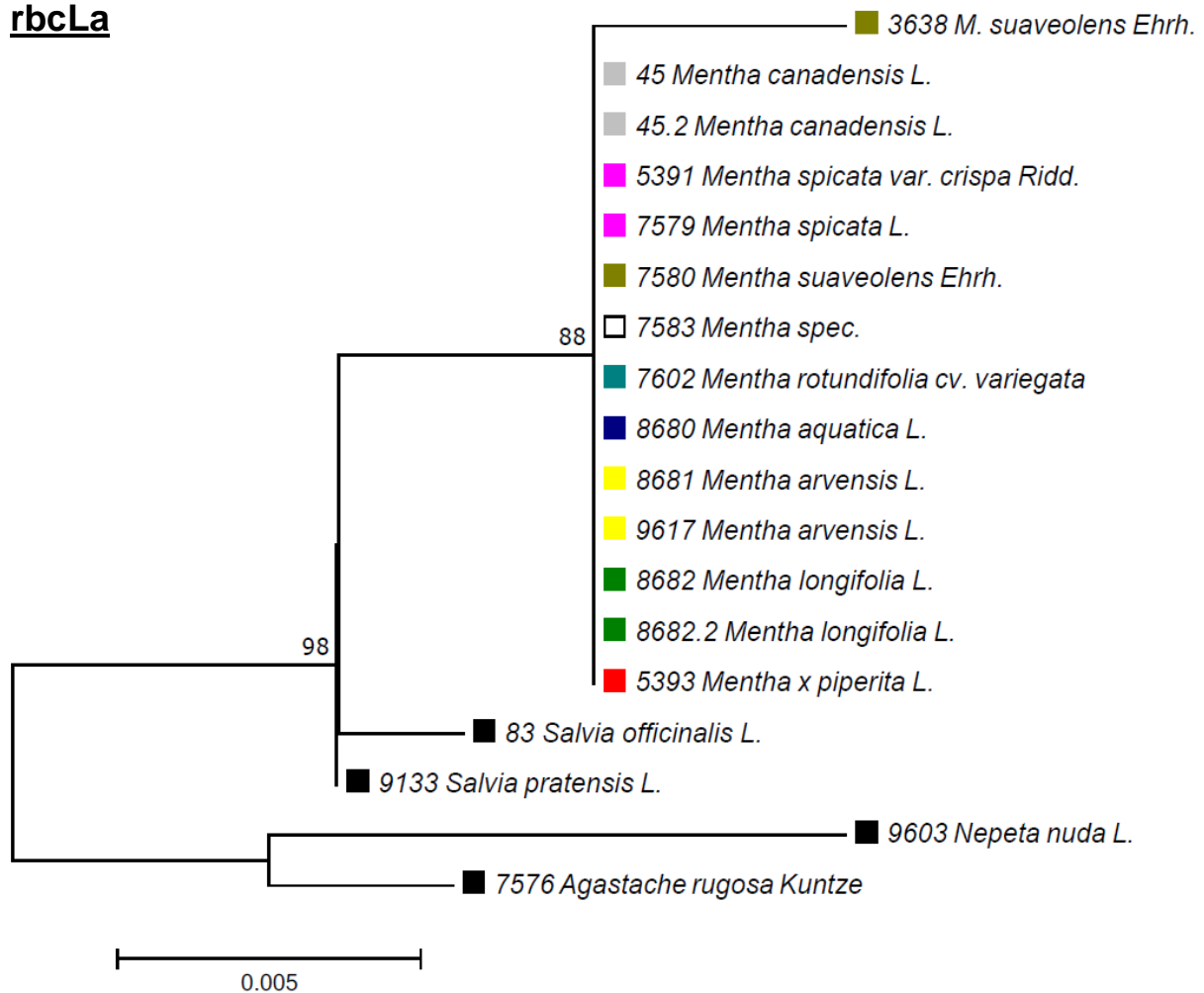
rbcLa

Figure 42: Phylogenetic tree based on the plastidic barcoding marker *rbcLa*. Neighbor-joining was used to infer the evolutionary history. Bootstrap values are given in percent next to the branches. The tree is drawn to scale, with branch lengths in the same units as the evolutionary distances used for phylogenetic inference. Evolutionary distances were calculated using the Tamura-Nei method in units of the number of base substitutions per site. Analyses were performed in MEGA7. Individuals of one *Mentha* species are represented by the same color, other genera are indicated by black squares.

Appendix

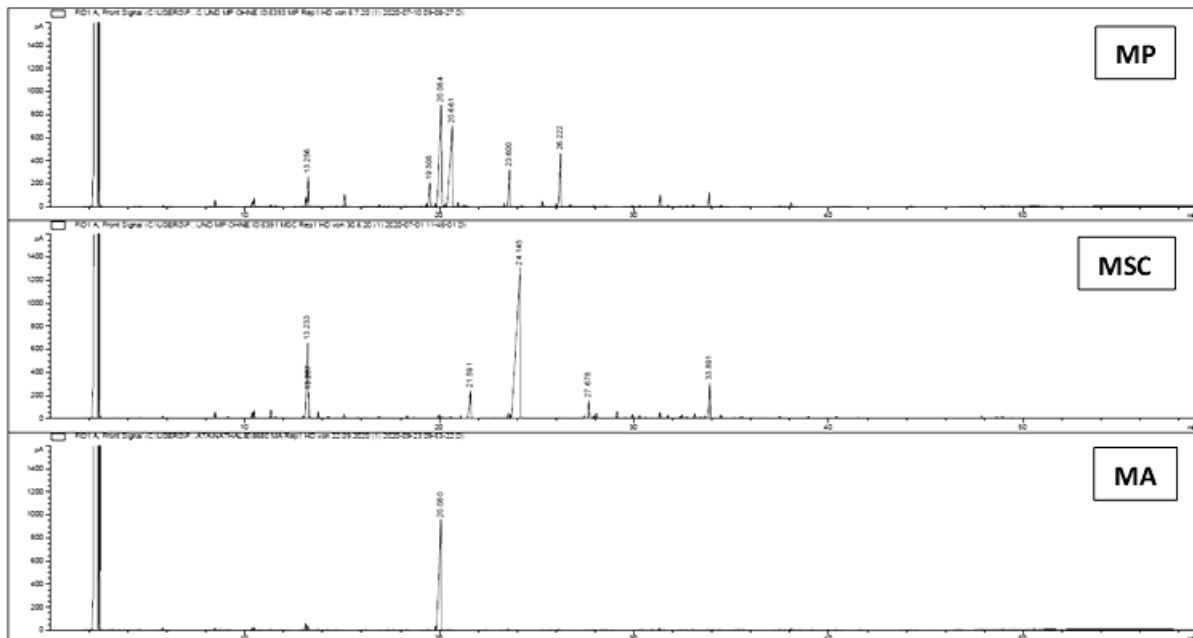


Figure 43: Exemplary GC chromatograms of the essential oils of the three *Mentha* species. Only relevant peaks are shown with their retention times. MP = *M. x piperita*; MSC = *M. spicata* var. *crispa*; MA = *M. aquatica*.

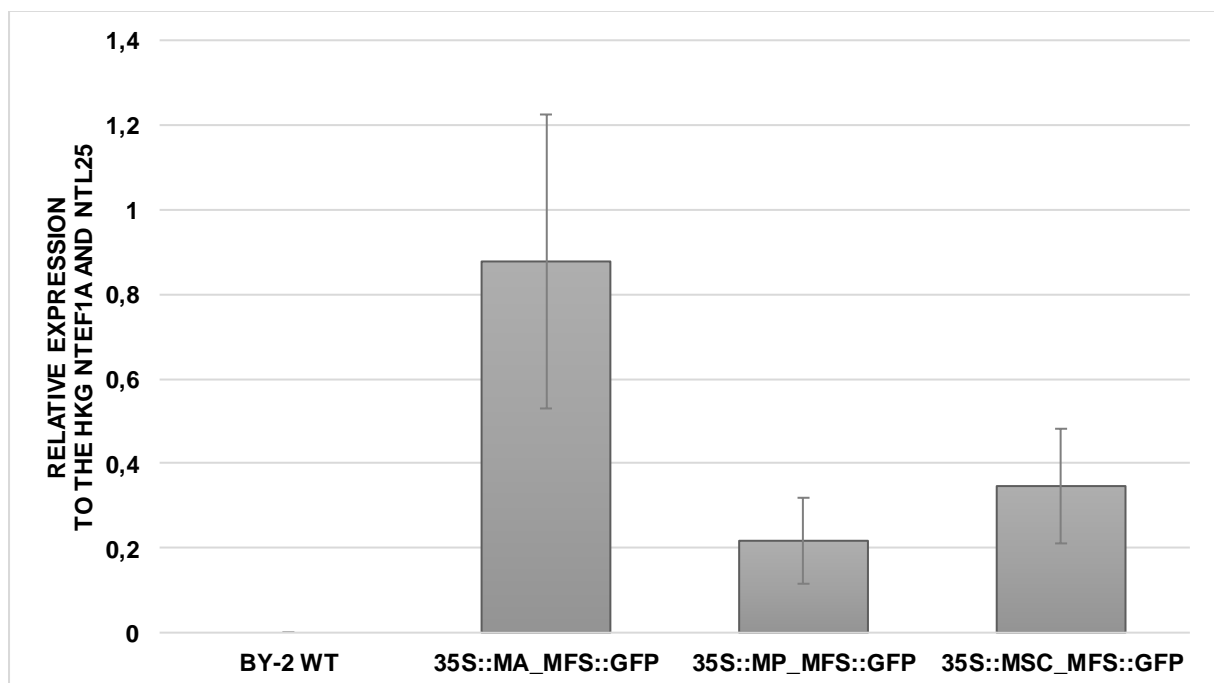


Figure 44: Relative expression of MFS to the housekeeping genes NtEF1 α and NtL25 in a BY-2 tobacco WT cell line and in the three established transgenic ones. Ct values were determined using qPCR. Relative expression values were calculated using the $2^{-\Delta Ct}$ method according to Livak and Schmittgen (2001). Standard error is based on three biological replicates.